Conclusions to Part 2

1. The analysis of forces acting on the bearing structure of the flat wagon in operation is carried out; the method applied is also given. It is also used for determining the forces acting on the bearing structure of a flat wagon mod. 13-401 manufactured by the Dnipro VahonMash company (Ukraine) for calculating the main strength characteristics of the flat wagon.

2. The stress-strain state of the bearing structure of the flat wagon is investigated. The calculation is carried out in SolidWorks Simulation using the finite element method. The main strength indicators of the bearing structure of the flat wagon are determined. It is found that the maximum equivalent stresses occur at design mode I (impact); they are close to the yield strength of the structural material of the flat wagon, however do not exceed the permissible values. The maximum equivalent stresses are concentrated in the interaction areas between the centre sill and the bolster beams.

The calculation is also carried out for other design loading diagrams.

PART 3
IMPROVED BEARING STRUCTURES OF FLAT WAGONS WITH HIGHER OPERATIONAL EFFICIENCY

3.1 Improvements for the bearing structure of a flat wagon carrying containers, steel coils, timber bundles, and industrial woodchips

Due to the increase in containers transported between Europe and Asia, the projects to upgrade existing flat wagon designs for carrying containers have been developed and are being implemented. Figure 3.1 shows a modernized large-capacity flat wagon mod. 13-401M2 [23] [TU 3182-020-4429774-00].

The modernization of the flat wagon mod. 13-401M2 for carrying large capacity containers includes the installation

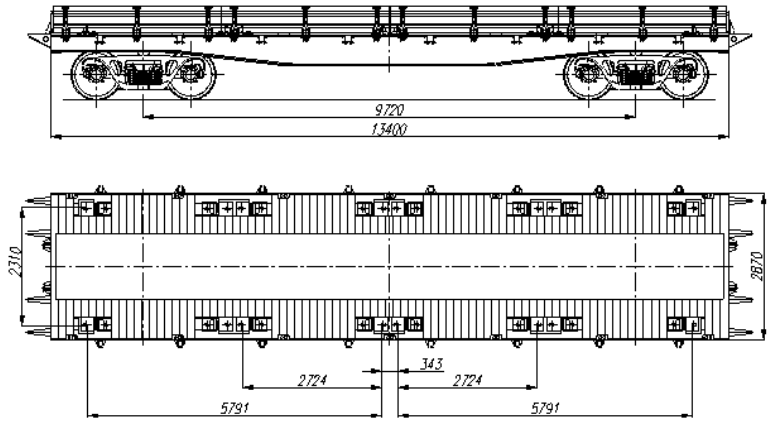

Figure 3.1 – Flat wagon mod. 13-401M2 for large-capacity containers

of 16 folding stops (Figure 3.2) for securing containers. These folding stops can be used for accommodating one container 1A, 1AA, 1B, 1BB, two containers 1C, 1CC or four containers 1D, 1DX. All of them must have wooden or wooden/metal flooring.

There are three loading diagrams.

Loading diagram 1 includes the installation of four stationary and four folding stops for containers, it is suitable for one container 1A or 1AA, or two containers 1C or 1CC. The side walls can be removed as optional order.

Loading diagram 2 (for flat wagons with wooden flooring) includes the dismantling of wooden flooring and the installation of a metal sheet in the cantilever part of the flat wagon for accessing by forklift trucks.

Loading diagram 3 (for flat wagons with wooden-and-metal flooring) includes the dismantling of wooden flooring and the installation of a metal sheet in the cantilever part of the flat wagon for accessing by forklift trucks. A container placed on the flat wagon is shown in Figure 3.3 [24].

The tests were conducted by the innovation and research company 'Wagons'. The fitting stops were produced by the NPTB-Vagon Company. The modernization was conducted at the wagon depot. The flat wagons were in accordance with

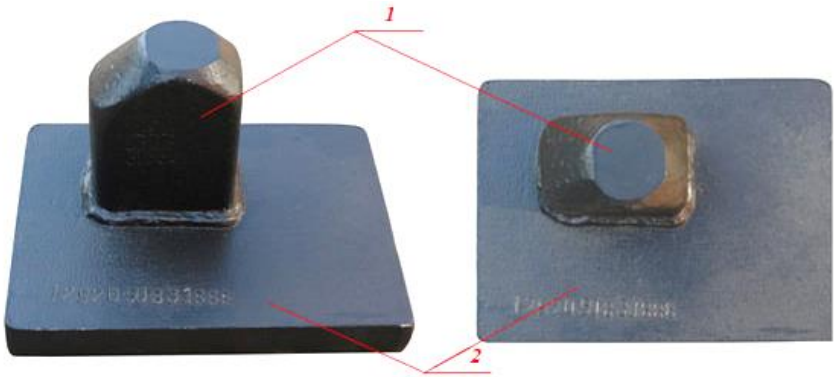

Figure 3.2 – Fitting stops of flat wagons
1 – stopper; 2 – baseplate

Figure 3.3 – A container on the flat wagon

TU 3182-020-4429774-00, validity period – from 14.08.2000, payload – 70 tonnes, tare weight – 21 tonnes.

The re-equipment of the flat wagon for carrying large-capacity containers 1A or 1AA, 1C or 1CC includes the installation of four stationary and four folding (as optional order) fitting stops for securing containers, which provides carrying one container 1A or 1AA, or two containers. Containers can be loaded/unloaded on/from the flat wagon with a special loader, the stops provide a shift of 600 mm relative to the transverse axis of the wagon (the maximum permissible shift of the centre of gravity of the container 1A or 1AA relative to the centre of gravity of the wagon is 1,970 mm). Since the floor of the flat wagon mod. 13-H004 (Figure 3.4) is inappropriate to access by a loader, the end part was fitted with metal flooring.

The tests were conducted by the innovation and research centre 'Wagons'. The flat wagons were manufactured in accordance with TU 3182-035-4429774-02, validity period – from 12.02.2002, payload – 66 tonnes, tare weight – 20.6 tonnes.

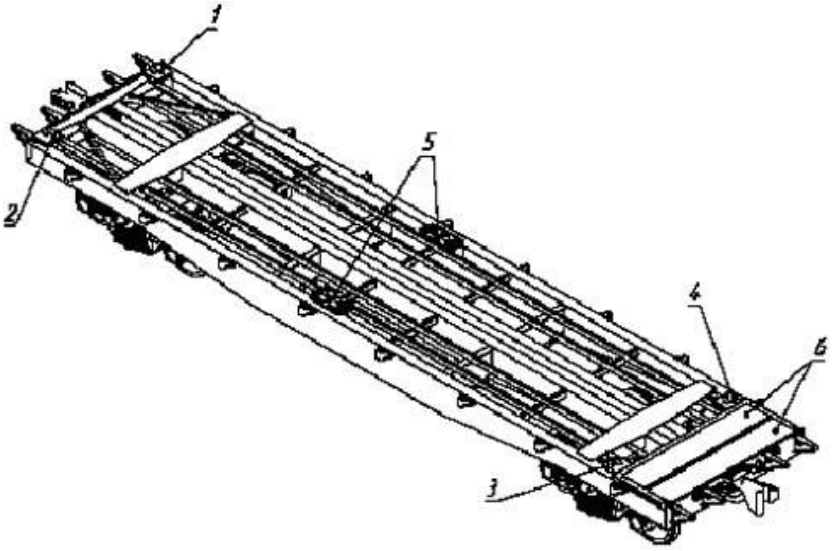

Figure 3.4 – Flat wagon mod. 13-H004
1, 2, 3, 4 – stationary stops; 5 – folding stops;
6 – metal flooring for a loader

The flat wagon mod. 13-401 was fitted with supports on the bearing structure for carrying and securing steel coils (Figure 3.5).

The geometric parameters of the supports were selected identical to those used on flat wagons for carrying steel coils.

The strength of the improved bearing structure of the flat wagon was calculated using the finite element method in SolidWorks Simulation.

The FEM of the bearing structure of the flat wagon is shown in Figure 3.6.

The optimal number of mesh elements was determined with the graphical analytical method [25–29]. The number of mesh elements is 468,470, the number of nodes is 149,709. The maximum size of the mesh element is 200 mm, the minimum size is 40 mm, the maximum aspect ratio of the elements is 9113.9, the percentage of elements with an aspect ratio of less than three is 9.59, and more than ten – 40.

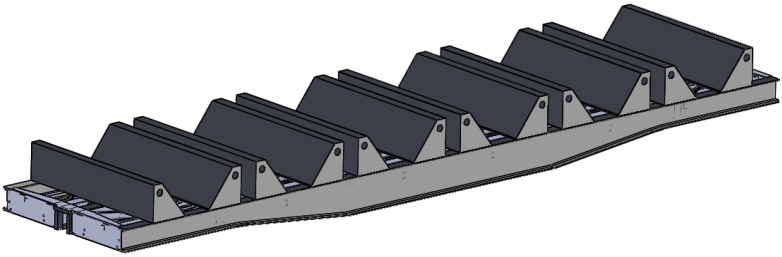

Figure 3.5 – Spatial model of an improved bearing structure of the flat wagon for carrying steel coils

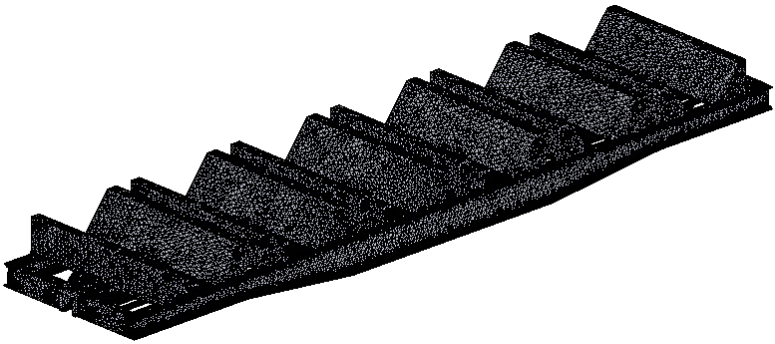

Figure 3.6 – FEM of the improved bearing structure of the flat wagon for carrying steel coils

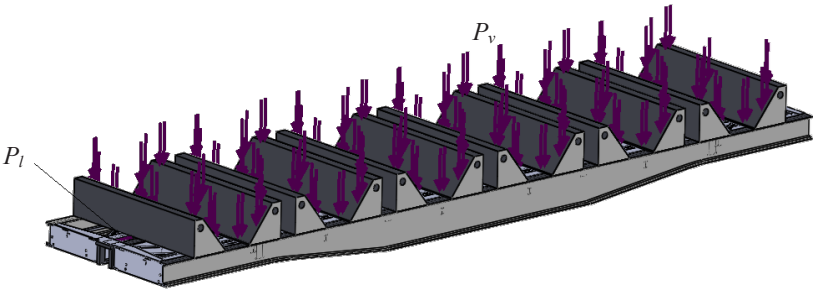

Figure 3.7 – Design diagram of the improved bearing structure of the flat wagon for carrying steel coils at design mode I

The design diagram of the bearing structure of the flat wagon (Figure 3.7) includes six steel coils ten tonnes each. The calculation results are given below.

The results of the strength calculation are given in Table 3.1. The maximum equivalent stresses occur at design mode I and are concentrated in the interaction area between the centre sill and the bolster beam; they do not exceed permissible values (Figure 3.8) [21, 22].

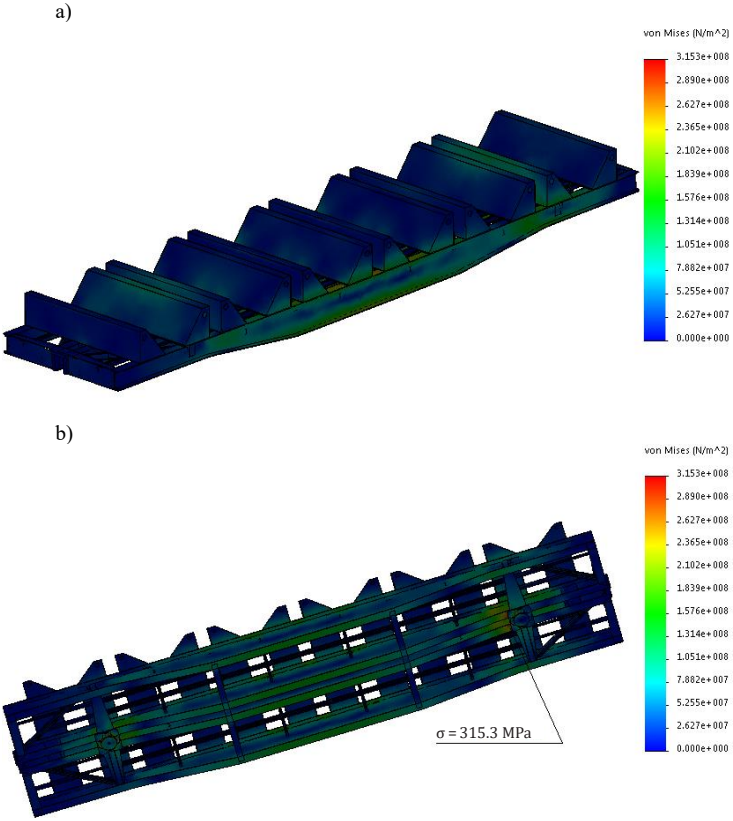

Figure 3.8 – Stress state of the improved bearing structure of the flat wagon for carrying steel coils at design mode I
a) side view; b) bottom view

a)

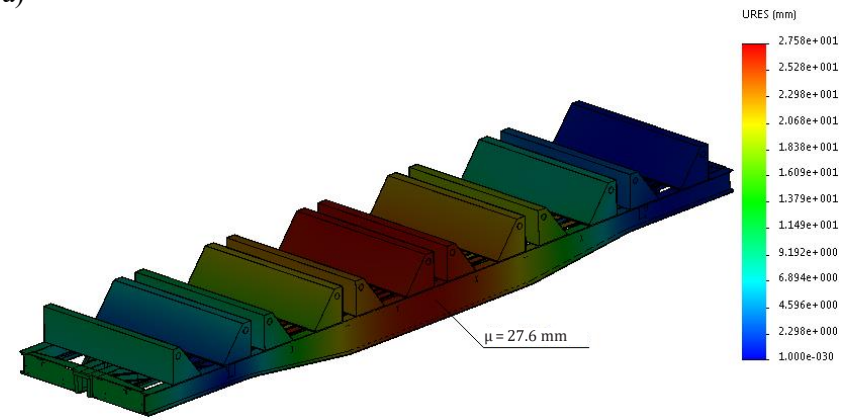

b)

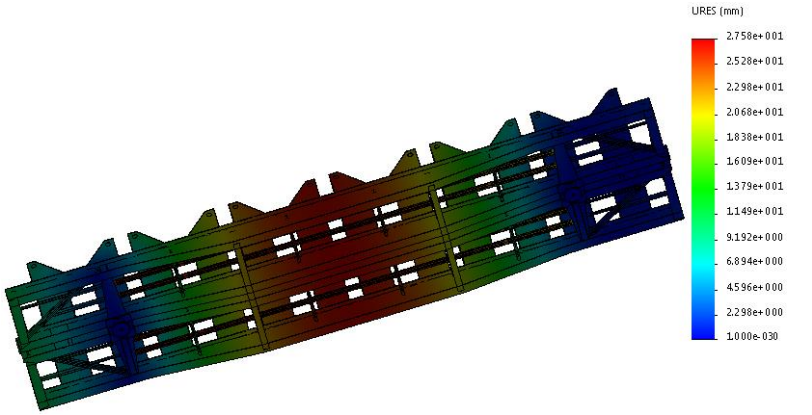

Figure 3.9 – Displacements in the units of the improved bearing structure of the flat wagon for carrying steel coils at design mode I

a) side view; b) bottom view

a)

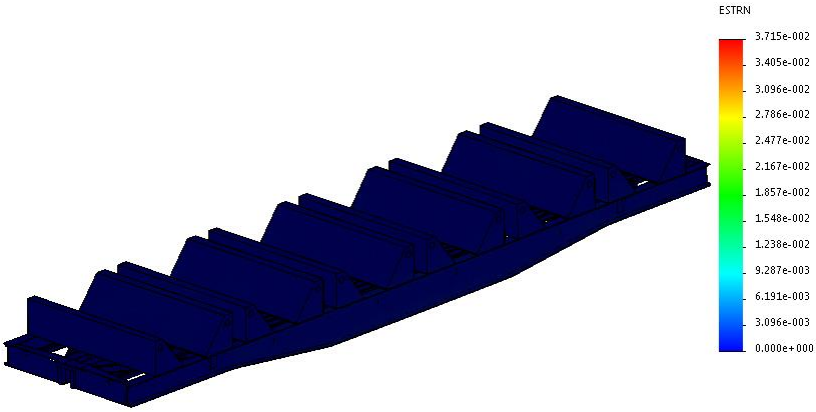

b)

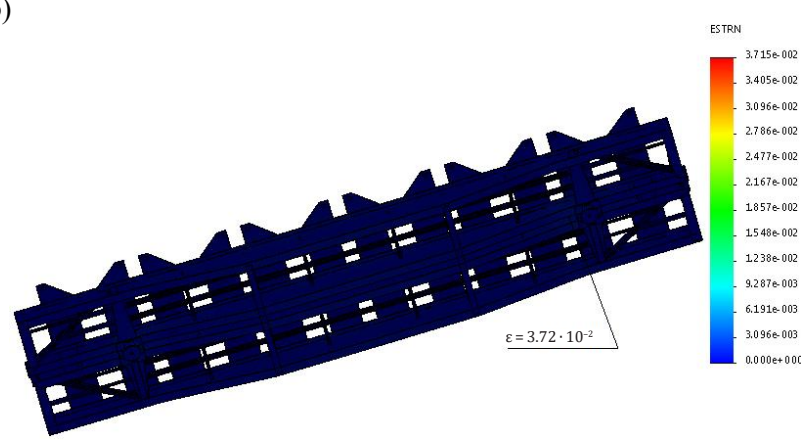

Figure 3.10 – Deformations in the improved bearing structure of the flat wagon for carrying steel coils at design mode I
a) side view; b) bottom view

Table 3.1 – Strength indices of the improved bearing structure of the flat wagon for carrying steel coils at loading modes

Strength index	Loading mode					
	I				III	
	Impact	Compression	Jerk	Tension	Impact/ Compression	Jerk/ Tension
Stress, MPa	315.3	308.5	312.6	278.5	271.3	277.1
Displacement in units, mm	27.6	23.2	24.8	24.6	23.4	22.3
Deformations	$3.7 \cdot 10^{-2}$	$3.8 \cdot 10^{-2}$	$4.1 \cdot 10^{-2}$	$3.96 \cdot 10^{-2}$	$3.7 \cdot 10^{-2}$	$3.8 \cdot 10^{-2}$

For carrying timber bundles, bearing structure of the flat wagon mod. 13-401 is equipped with rotating supports for securing freight (Figure 3.11).

The geometrical parameters of the supports are identical to those used on flat wagons for carrying timber bundles.

The strength of the improved bearing structure of the flat wagon was calculated using the finite element method in SolidWorks Simulation.

The FEM of the bearing structure of the flat wagon is shown in Figure 3.12.

The optimal number of mesh elements was determined with the graphical analytical method. The number of mesh elements is 392,015, the number of nodes is 126,835. The maximum size of the mesh element is 200 mm, the minimum – 40 mm, the maximum aspect ratio of the elements is 16,448, the percentage of elements with an aspect ratio of less than three is 15.9, and more than ten – 27.6.

The design diagram of the bearing structure of the flat wagon is shown in Figure 3.13. The model includes the following loads: the impact load on the vertical wall of the rear draft lug P_l, the

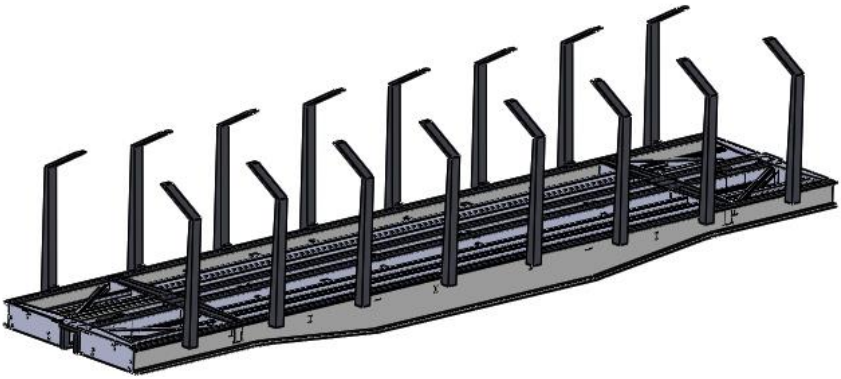

Figure 3.11 – Spatial model of the improved bearing structure of the flat wagon for carrying timber bundles

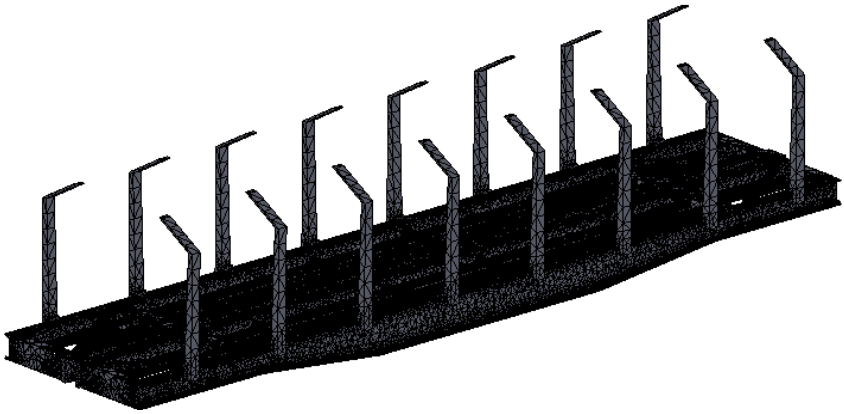

Figure 3.12 – FEM of the improved bearing structure of the flat wagon for carrying timber bundles

vertical load from the gross weight of the bearing structure of the flat wagon P_v, and the pressure from timber bundles on the vertical supports P_b.

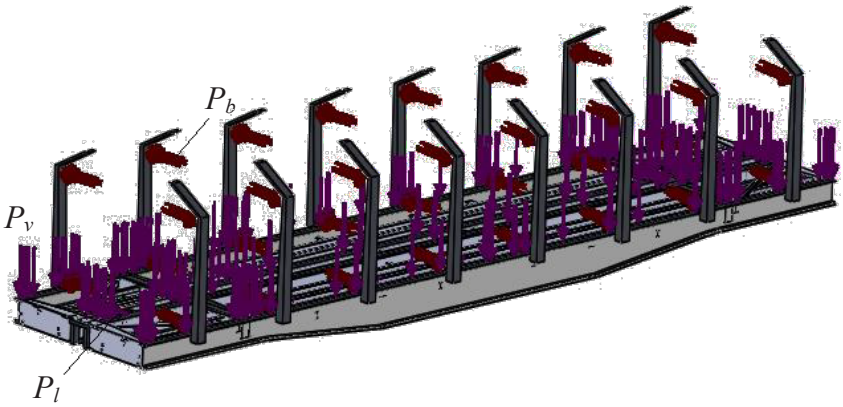

Figure 3.13 – Design diagram of the improved bearing structure of the flat wagon for carrying timber bundles at design mode I

The results of strength calculation are given in Table 3.2. The maximum equivalent stresses occur at design mode I and are concentrated in the interaction area between the centre sill and the bolster beam; they do not exceed the permissible values (Figure 3.14) [21, 22]. Other strength indices of the bearing structure of the flat wagon were also calculated (Figures 3.15, 3.16).

The bearing structure can also be fitted with composite poles installed in metal boots on the sectors rotating relative to the vertical axis, which facilitates the loading of the flat wagon [66].

This solution can reduce the tare weight of the improved flat wagon by 4.6 % compared to that with steel poles.

The main strength indices of the improved bearing structure of the flat wagon were calculated using the finite element method implemented in the SolidWorks Simulation.

The FEM consists of isoparametric tetrahedra. The optimal number of model elements was calculated using the graphical analytical method. The number of nodes in the model is 263,362, the number of elements is 768,396. The maximum element size is 100 mm, the minimum – 20 mm.

a)

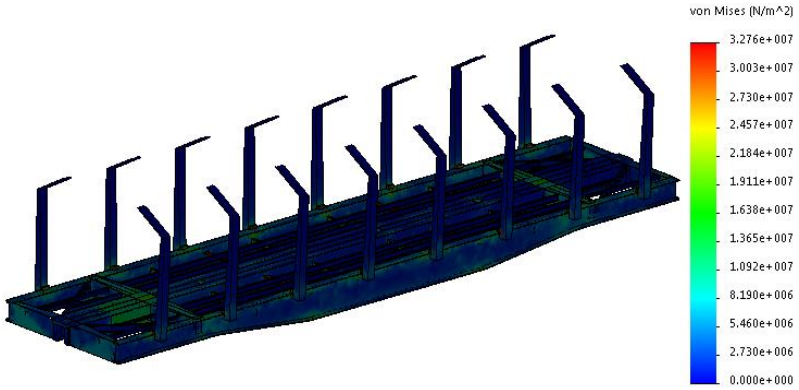

b)

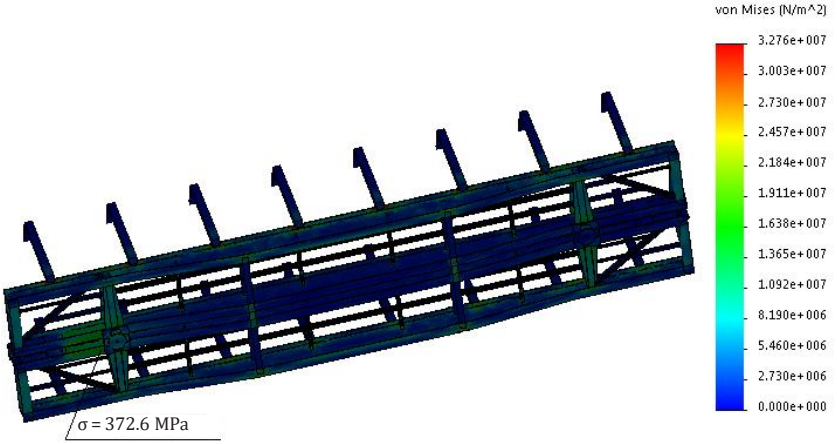

Figure 3.14 – Stress state of the improved bearing structure of the flat wagon for carrying timber bundles at design mode I
a) side view; b) bottom view

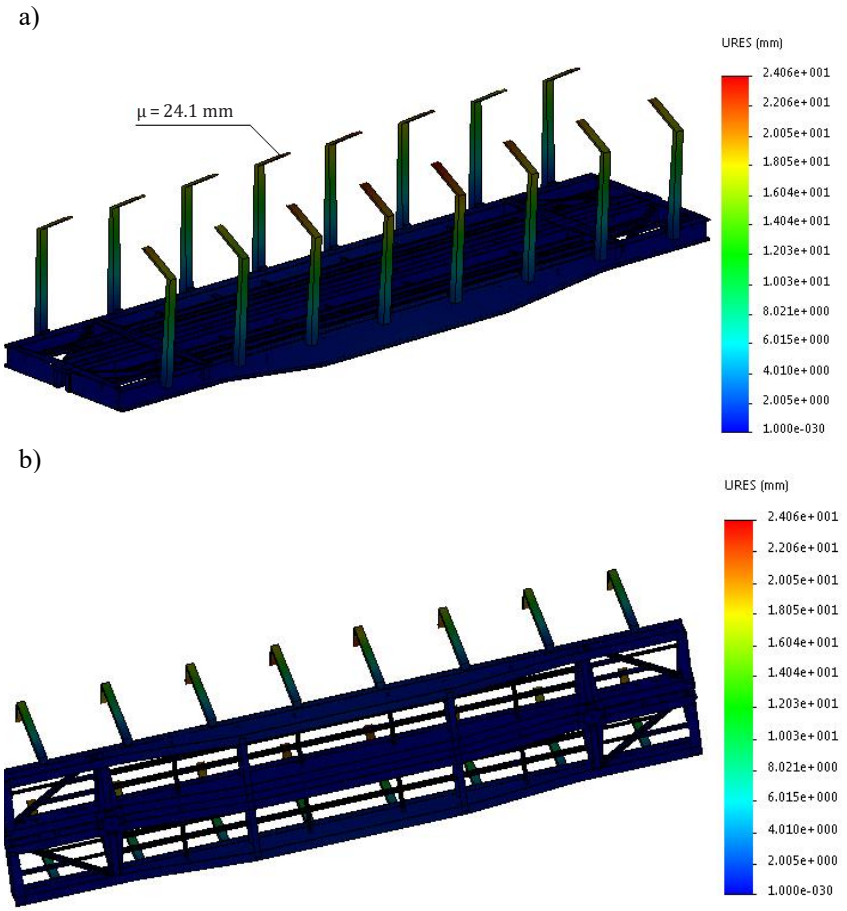

Figure 3.15 – Displacements in the units of the improved bearing structure of the flat wagon for carrying timber bundles at design mode I
a) side view; b) bottom view

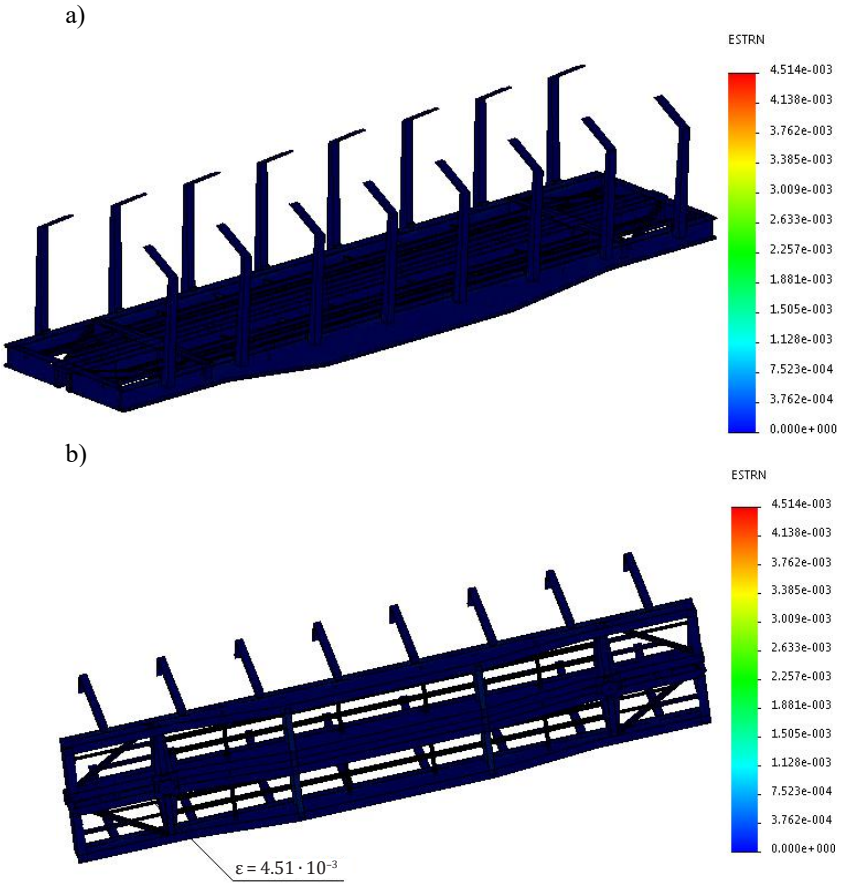

Figure 3.16 – Deformations in the improved bearing structure of the flat wagon for carrying timber bundles at design mode I
a) side view; b) bottom view

Table 3.2 – Strength indices of the improved bearing structure of the flat wagon for carrying timber bundles at loading modes

Strength index	Loading mode					
	I				III	
	Impact	Compression	Jerk	Tension	Impact/ Compression	Jerk/Tension
Stress, MPa	327.6	312.7	323.2	284.7	286.7	294.6
Displacements in units, mm	24.1	23.6	24.3	23.1	23.5	23.8
Deformations	$4.51 \cdot 10^{-3}$	$4.6 \cdot 10^{-3}$	$4.13 \cdot 10^{-3}$	$4.62 \cdot 10^{-3}$	$4.55 \cdot 10^{-3}$	$4.45 \cdot 10^{-3}$

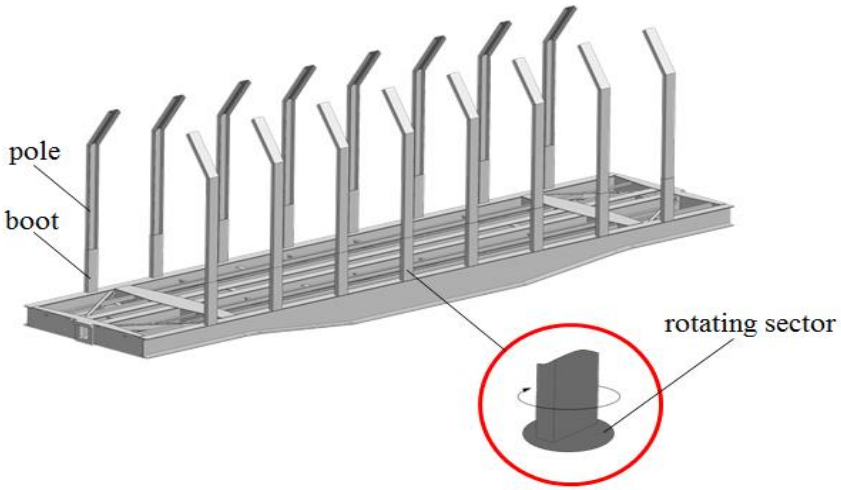

Figure 3.17 – Bearing structure of the flat wagon

The percentage of elements with an aspect ratio of more than ten – 13.5, less than three – 13.5. The minimum number of elements in the circle is 9, the ratio of element size increase is 1.7. The model is fixed in the areas where it rests on the bogies. The bearing structure of the flat wagon is made of Steel 09G2S, the poles are composite with a tensile strength of 1,500 MPa and a density of 2,200 kg/m^3.

The design diagram of the bearing structure of the flat wagon is shown in Figure 3.18.

The first stage included the calculation of the bearing structure of the flat wagon at design mode I. It was taken into account that the bearing structure of the flat wagon is under the vertical load P_v distributed over the centre sill and longitudinal beams in the proportions 5/8 and 3/8, respectively. The bearing structure of the flat wagon is under the longitudinal load P_l applied to the rear draft lug of the coupler and is equal to 3.5 MN, as well as transverse loads on the poles P_p. It was assumed that the height of the poles is 3.169 m [30].

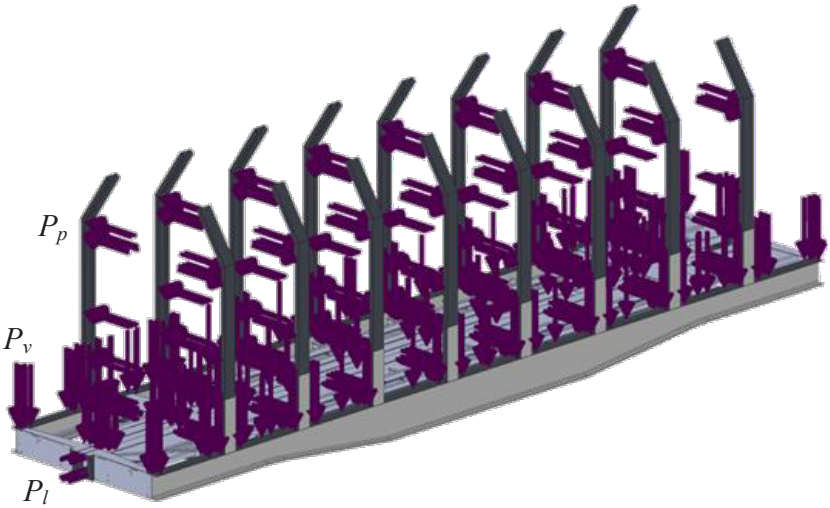

Fig. 3.18 – Design diagram of the bearing structure of the flat wagon

The value of the uniformly distributed transverse load over the height of the pole for each stack was determined as [30]:

$$P_c = \frac{\Delta F_t}{L_r}, \tag{3.1}$$

where ΔF_t is the transverse inertial force from the stack mass according to the placement along the wagon length, kN.

Herewith,

$$\Delta F_t = n \cdot (F_t + W) - F_{fr}^a, \tag{3.2}$$

where n is the coefficient calculated when developing specifications for the flat wagon; F_t is the transverse inertial load from the stacked cargo according to its placement along the wagon length and the action of the centrifugal force; W is the wind load on the cargo; F_{fr}^a is the frictional force acting on the stacked cargo according to its placement along the wagon length in the transverse direction.

The calculations included that the flat wagon was loaded with a 6-m stack. Since steel is an isotropic material and composite is anisotropic, the calculation was carried out according to the Mises criterion and the maximum normal stresses criterion [18, 19].

It was established that the maximum equivalent stresses in the bearing structure of the flat wagon occur in the interaction areas between the bolster beams and the centre sill and are about 342 MPa, which do not exceed permissible values [21, 22] (Figure 3.19).

The results of the calculation with the criterion of maximum normal stresses reveal that the maximum normal stresses in the longitudinal direction are 237.5 MPa, in the transverse direction are 151.7 MPa, and in the vertical direction they are 174.8 MPa. Therefore, the resulting stress do not exceed permissible values [21, 22].

The strength of the improved bearing structure of the flat wagon at other design diagrams was also calculated. The results show that the strength of the bearing structure is ensured.

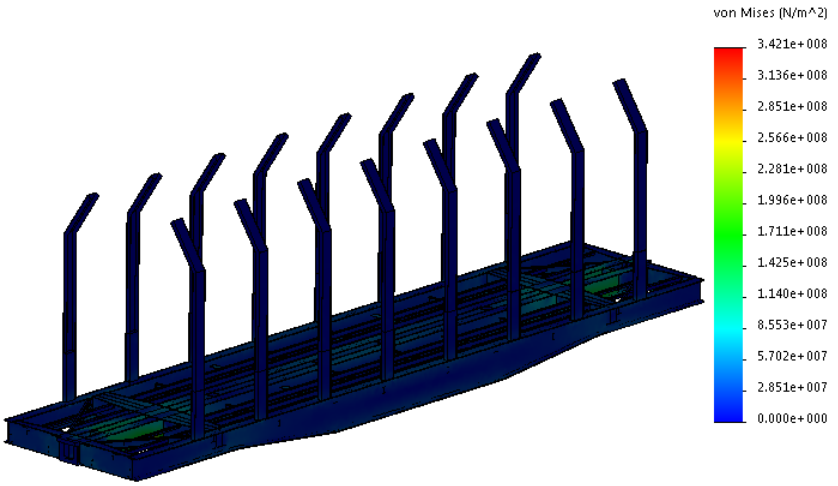

Figure 3.19 – Stress state of the bearing structure of the flat wagon

The main indicators of the dynamics of the bearing structure of the flat wagon with composite poles for carrying timber bundle were determined using mathematical modelling. The model included the bouncing and galloping oscillations. The first stage of the study delt with the movement of the unloaded flat wagon on a rail irregularity given that the track is elastic-viscous [31, 32, 66].

The flat wagon was considered as a three-solid-body system: a frame and two bogies mod. 18-100 with spring groups with some stiffness and a coefficient of relative friction (Figure 3.20).

It is assumed that the system had the following limitations:

– wheelsets move without slipping;

– without elastic elements in the axle-box suspension, the bouncing of bogies is determined though the bouncing of wheelsets.

The motion equations of the design model are as follows [21]:

$$M_1 \cdot \frac{d^2}{dt^2} z + C_{1,1} \cdot z + C_{1,3} \cdot z_{T_1} + C_{1,5} \cdot z_{T_2} = -F_{FR} \cdot \Delta, \qquad (3.3)$$

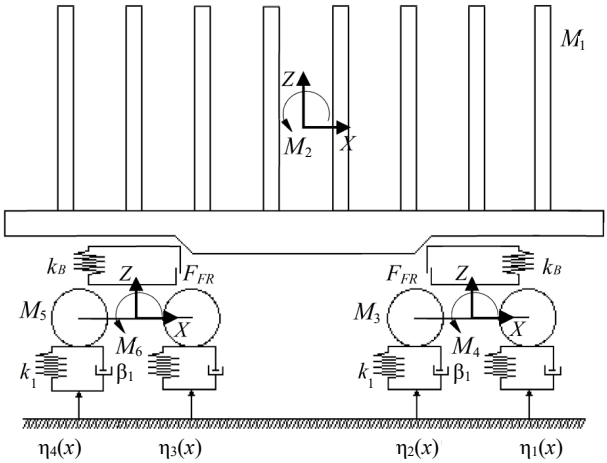

Figure 3.20 – Design diagram of the flat wagon

$$M_2 \cdot \frac{d^2}{dt^2}\varphi + C_{2,2}\cdot\varphi + C_{2,3}\cdot\varphi_{T_1} + C_{2,5}\cdot\varphi_{T_2} = F_{FR}\cdot l\cdot\Delta, \tag{3.4}$$

$$M_3 \cdot \frac{d^2}{dt^2} z_{T_1} + C_{3,1}\cdot z + C_{3,2}\cdot\varphi + C_{3,3}\cdot z_{T_1} + B_{3,3}\cdot\frac{d}{dt} z_{T_1} = \\ = F_{FR}\cdot\Delta_1 + k_1\left(\eta_1 + \eta_2\right) + \beta_1\left(\frac{d}{dt}\eta_1 + \frac{d}{dt}\eta_2\right), \tag{3.5}$$

$$M_4 \cdot \frac{d^2}{dt^2}\varphi_{T_1} + C_{4,4}\cdot\varphi_{T_1} + B_{4,4}\cdot\frac{d}{dt}\varphi_{T_1} = -k_1\left(\eta_1 - \eta_2\right) - \\ -\beta_1\cdot a\cdot\left(\frac{d}{dt}\eta_1 - \frac{d}{dt}\eta_2\right), \tag{3.6}$$

$$M_5 \cdot \frac{d^2}{dt^2} z_{T_2} + C_{5,1}\cdot z + C_{5,2}\cdot\varphi + C_{5,5}\cdot z_{T_2} + B_{5,5}\cdot\frac{d}{dt} z_{T_2} = \\ = F_{FR}\cdot\Delta_2 + k_1\left(\eta_3 + \eta_4\right) + \beta_1\left(\frac{d}{dt}\eta_3 + \frac{d}{dt}\eta_4\right), \tag{3.7}$$

$$M_6 \cdot \frac{d^2}{dt^2}\varphi_{T_2} + C_{6,6} \cdot \varphi_{T_2} + B_{6,6} \cdot \frac{d}{dt}\varphi_{T_2} = \\ = -k_1 \cdot a \cdot (\eta_3 - \eta_4) - \beta_1 \cdot a \cdot \left(\frac{d}{dt}\eta_3 - \frac{d}{dt}\eta_4 \right), \tag{3.8}$$

$$\Delta = \Delta_1 + \Delta_2 = \left(sign\left(\frac{d}{dt}\delta_1 \right) + sign\left(\frac{d}{dt}\delta_2 \right) \right), \tag{3.9}$$

where M_1 and M_2 are the mass and moment of inertia of the bearing structure of the flat wagon, respectively, under the bouncing and galloping oscillations; M_3 and M_4 are the mass and the moment of inertia of the first bogie facing the engine, respectively, under the bouncing and galloping oscillations; M_5 and M_6 are the mass and the moment of inertia of the second bogie facing the engine, respectively, under bouncing and galloping oscillations; C_{ij} is the elasticity characteristics of the oscillating system elements; B_{ij} is the scattering function; a is half the bogie base; z, φ are the generalized coordinates corresponding to the translational displacement relative to the vertical axis and the angular displacement around the vertical axis of the bearing structure of the flat wagon; z_{T1}, φ_{T1} are the generalised coordinates corresponding to the translational movement relative to the vertical axis and the angular displacement around the vertical axis of the first bogie facing the engine; z_{T2}, φ_{T2} are the generalised coordinates corresponding to the translational displacement around the vertical axis and the angular displacement around the vertical axis of the second bogie facing the engine; k_i is the spring suspension stiffness; β_i is the damping coefficient; F_{FR} is the absolute frictional force in the spring group; η_i is the track irregularity; δ_i is the deformations of the elastic elements in the spring suspension.

The calculation of the inertial coefficients used in the system of differential equations included the nominal geometric parameters of the bearing structure of the flat wagon. These coefficients were determined by means of a spatial model of the bearing structure in SolidWorks using the relevant application options.

It was assumed that the amplitude of the joint irregularity was 0.01 m, the length was 3 m, the distance between the irregularities was 25 m. The coefficients of relative friction were taken equal to 0.1.

The track stiffness was taken as 100,000 kN/m, and the damping coefficient as 200 kN·s/m. The dynamic indicators of the flat wagon were calculated for a speed of 27.8 m/s.

The transport delay was determined according to the distance between the wheelsets and the wagon speed. For the first wheelset it is 0, for the second one – 0.067 sec, for the third one – 0.31 sec, and for the fourth one – 0.38 sec.

Differential equations (3.3)–(3.8) were solved in MathCad, the following initial conditions were included: the initial movement of the bearing structure of the flat wagon – 0.004 m, and that of the bogie – 0.003 m. The initial rate was assumed to be 0. The Runge-Kutta method was used.

Figures 3.21–3.24 show the main indicators of dynamics for the flat wagon. The graphical dependence shown in Figure 3.21 was determined by double differentiation of the displacement z of the bearing structure of the flat wagon.

The acceleration of the bearing structure of the flat wagon in the areas of resting on the bogies was determined as $ddz - ldd\varphi$.

The forces in the spring suspension of the flat wagon were determined with the following dependence: $k_B\ (z - l\cdot\varphi - z_{T1}) + + F_{FR}\ sign(dz - l\cdot d\varphi - dz_{T1})$.

The coefficient of dynamics was calculated as the ratio of the force in the spring suspension to the static load on the bogie.

The maximum acceleration acting on the bearing structure of the flat wagon in the centre of gravity is about 0.54 g (Figure 3.21), which corresponds to the 'good' motion of the unloaded wagon. The acceleration in the areas on which the bearing structure of the flat wagon rests is about 0.65 g (Figure 3.22). The maximum force arising in the spring suspension of the flat wagon is almost 60 kN (Figure 3.23). The coefficient of dynamics is about 0.6 (Figure 3.24).

The analysis of the graphical dependencies shown in Figures 3.21–3.24 demonstrates that all the indicators of dynamics under study do not exceed permissible values [21, 22], (Figure 3.25).

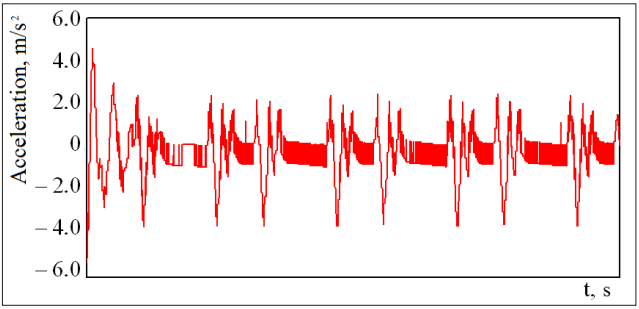

Figure 3.21 – Acceleration of the bearing structure of the unloaded flat wagon in the centre of mass

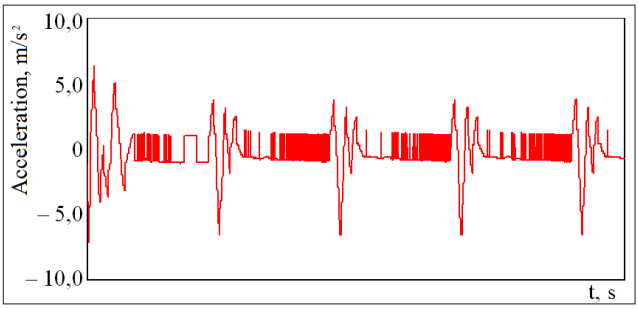

Figure 3.22 – Acceleration of the bearing structure of the unloaded flat wagon in the areas of resting on bogies

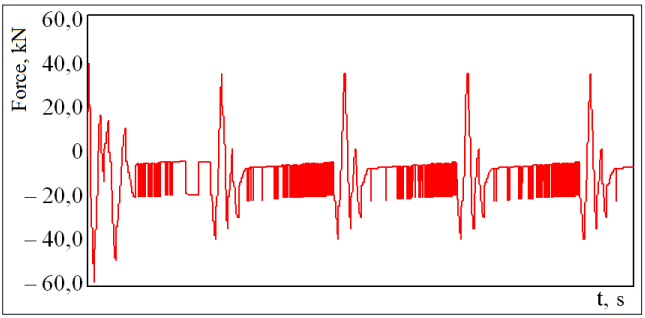

Figure 3.23 – Forces arising in the spring suspension of the unloaded flat wagon moving

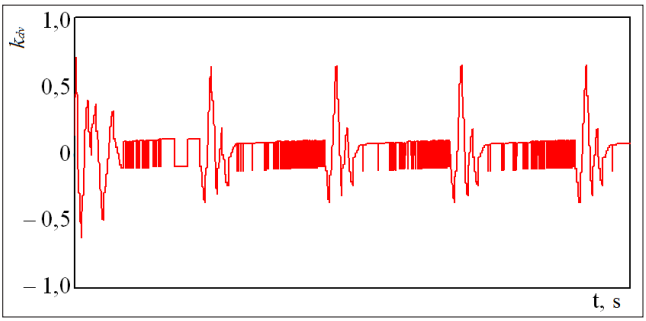

Figure 3.24 – Coefficient of dynamics of the spring-suspended structure of the unloaded flat wagon moving

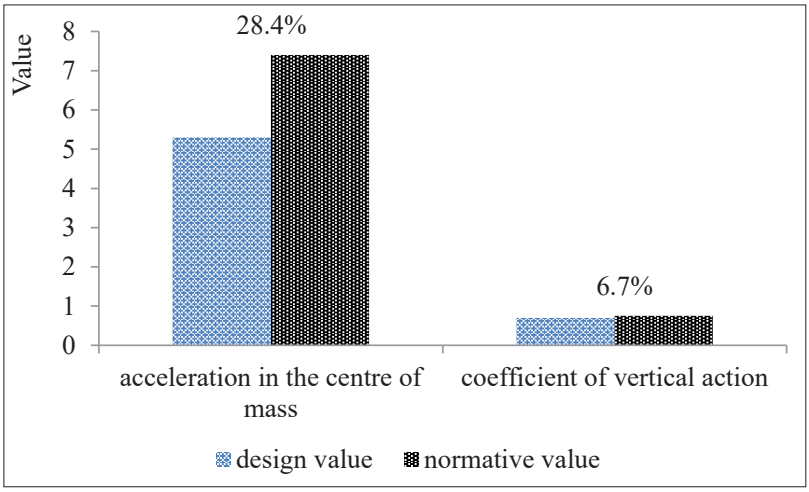

Figure 3.25 – Comparative analysis of the indicators of dynamics of the flat wagon

The next stage included the determination of the indicators of dynamics of the loaded flat wagon moving. The calculation included the payload capacity of the flat wagon. The results are given in Table 3.3.

Table 3.3. – Main indicators of dynamics of the loaded flat wagon moving

Indicator	Value
Acceleration of the bearing structure of the flat wagon in the centre of mass, m/s^2	1.7
Acceleration of the bearing structure of the flat wagon in the areas of resting on the bogies, m/s^2	1.9
Forces arising in the spring suspension, kN	80.2
Coefficient of dynamics of the sprung-suspended structure of the flat wagon	0.2

The data given in Table 3.3 show that the indicators of dynamics of the loaded flat when moving do not exceed permissible values (Figure 3.26). The motion of the wagon is assessed as 'excellent'.

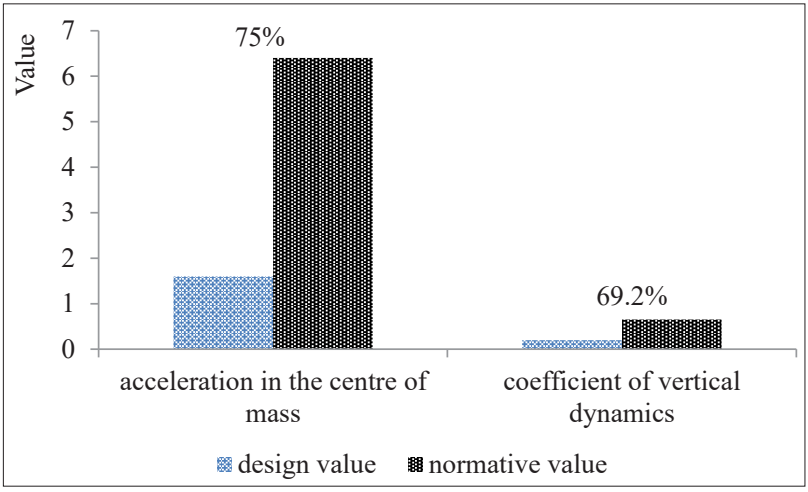

Figure 3.26 – Comparative analysis of the indicators of dynamics of the flat wagon

The results of the study will contribute to the database of developments of innovative rolling stock designs with enhanced operational efficiency characteristics.

It is proposed to install a metal frame sheathed with steel sheets on the bearing structure of the flat wagon mod. 13-401 to use it for carrying industrial woodchips (Figure 3.27).

The profile of vertical poles was determined by means of the cross-section method. The pole was considered as a rod under the action of the transverse load with a triangular distribution. The load intensity was determined as described in [16].

The vertical pole perceives the bend deformation from the pressure forces of the bulk freight, then $\sigma = \frac{M_x}{W}$, hence $[W] = \frac{M_x}{[\sigma]}$, while $[\sigma] = 345$ MPa, then at $M_x = 3512{,}1$ kN·cm, $[W] = 101{,}8$ cm^3. The resulting resistance moment is close to the resistance moment of the vertical poles of the open wagon, therefore, it is proposed to make the frame poles using Ω-shaped profile with a value of $W_x = 118{,}2$ cm^3 and $W_y = 119{,}3$ cm^3. The geometric parameters of the body siding were taken identical to those of the prototype wagon.

The strength of the improved bearing structure of the flat wagon was studied by means of the finite element method in SolidWorks Simulation.

The FEM of the bearing structure of the flat wagon is shown in Figure 3.28.

The optimal number of mesh elements was determined using the graphical analytical method. The number of mesh elements is 990,154, the number of nodes is 322,866. The maximum size of the mesh element is 100 mm, the minimum size is 20 mm, the maximum aspect ratio of the elements is 4,426.8, the percentage of elements with an aspect ratio of less than three is 30.6, and more than ten is 23.4.

The design diagram of the bearing structure of the flat wagon is shown in Figure 3.29. The model includes the following loads: the impact on the vertical wall of the rear draft lug P_l, the vertical load from the gross weight of the bearing structure of the flat wagon P_v, and the pressure from the bulk freight P_p.

a)

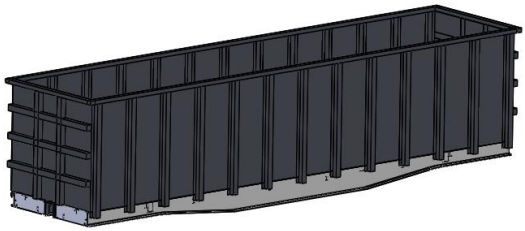

b)

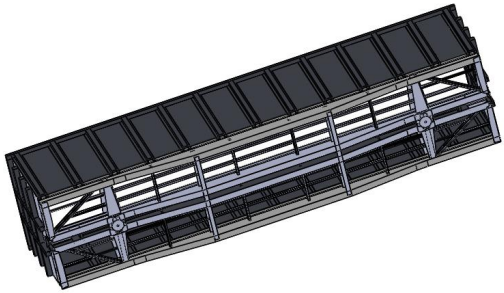

Figure 3.27 – Spatial model of the improved bearing structure of the flat wagon for carrying industrial woodchips
a) side view; b) bottom view

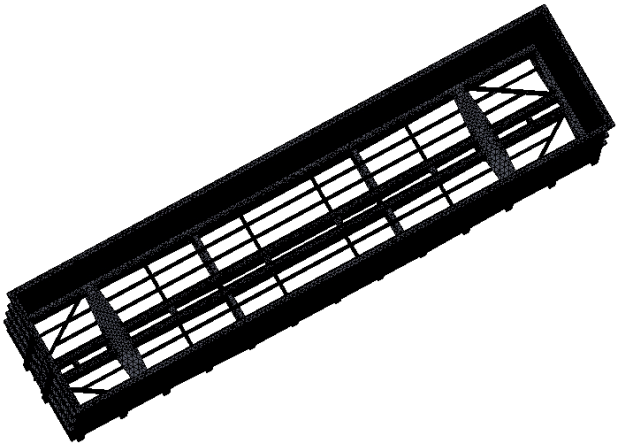

Figure 3.28 – FEM of the improved bearing structure of the flat wagon for carrying industrial woodchips

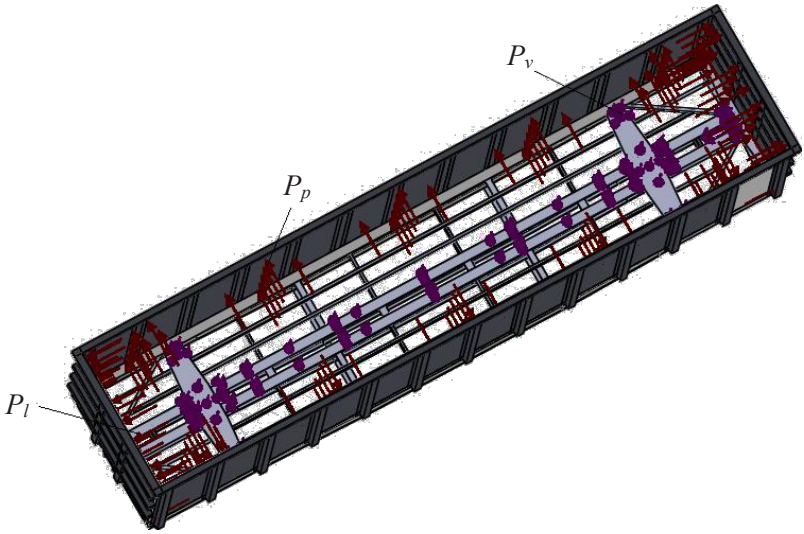

Figure 3.29 – Design diagram of the improved bearing structure of the flat wagon for carrying industrial woodchips at design mode I

Table 3.4 – Strength indices of the improved bearing structure of the flat wagon for carrying industrial woodchips at loading conditions

Strength index	Loading mode					
	I				III	
	Impact	Compression	Jerk	Tension	Impact/ Compression	Jerk/Tension
Stresses, MPa	332.6	309.2	324.5	293.5	291.7	297.8
Displacements in units, mm	36.2	27.4	29.3	25.1	24.5	25.3
Deformations	$3.01 \cdot 10^{-2}$	$3.2 \cdot 10^{-2}$	$2.89 \cdot 10^{-2}$	$3.1 \cdot 10^{-2}$	$3.05 \cdot 10^{-2}$	$3.02 \cdot 10^{-2}$

a)

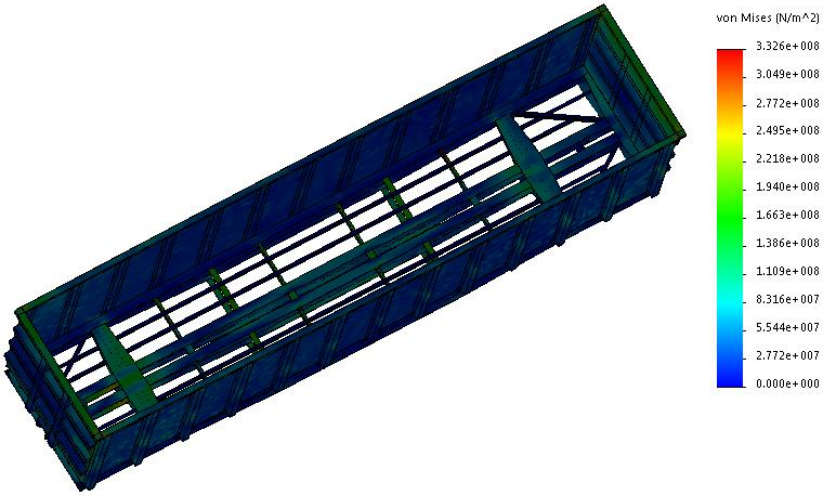

b)

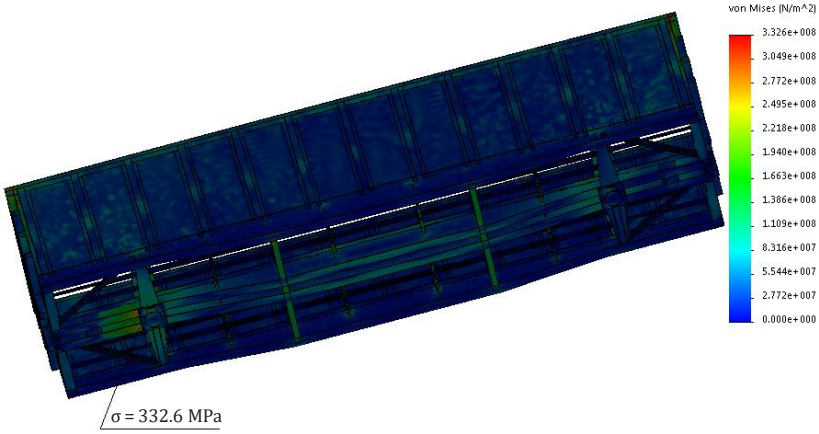

Figure 3.30 – Stress state of the improved bearing structure of flat wagon for carrying industrial woodchips at design mode I
a) side view; b) bottom view

The results of the strength calculation are given in Table 3.4. The maximum equivalent stresses occur at design mode I and are concentrated in the interaction area between the centre sill and the bolster beam; they do not exceed permissible values (Figure 3.30) [21, 22]. Other strength indicators of the bearing structure of the flat wagon were also calculated (Figures 3.31, 3.32).

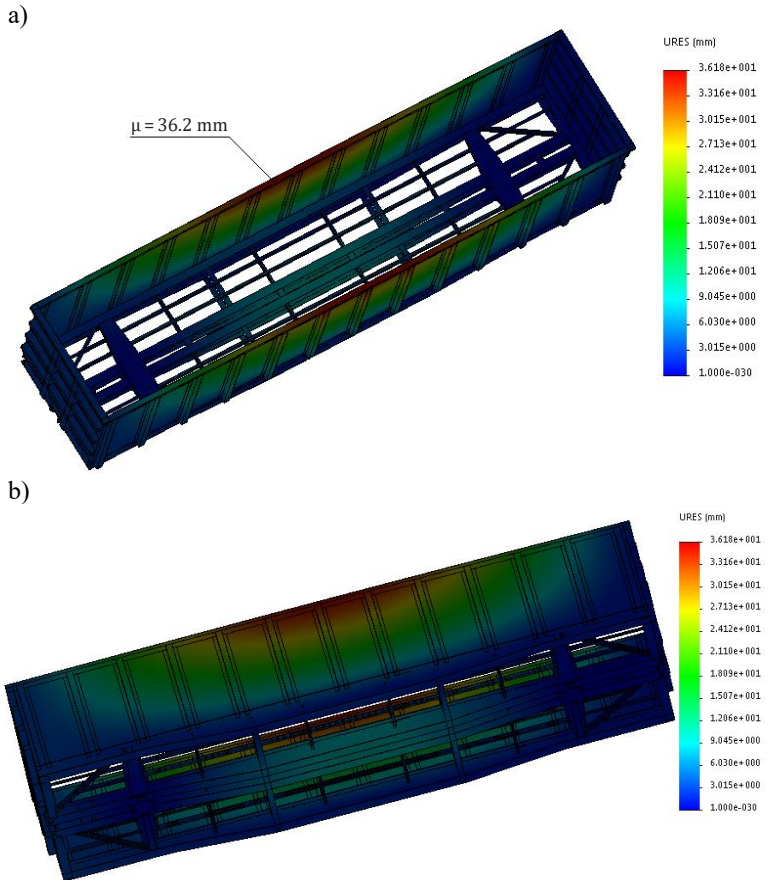

Figure 3.31 – Displacements in the units of the improved bearing structure of the flat wagon for carrying industrial woodchips at design mode I
a) side view; b) bottom view

a)

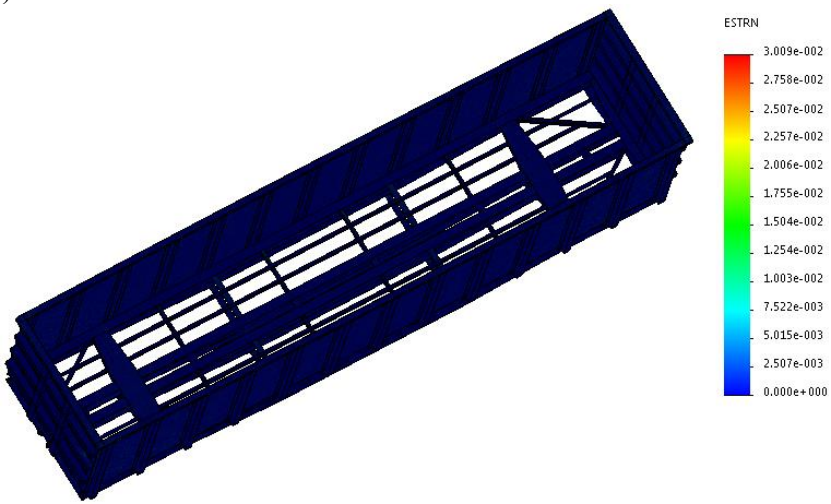

b)

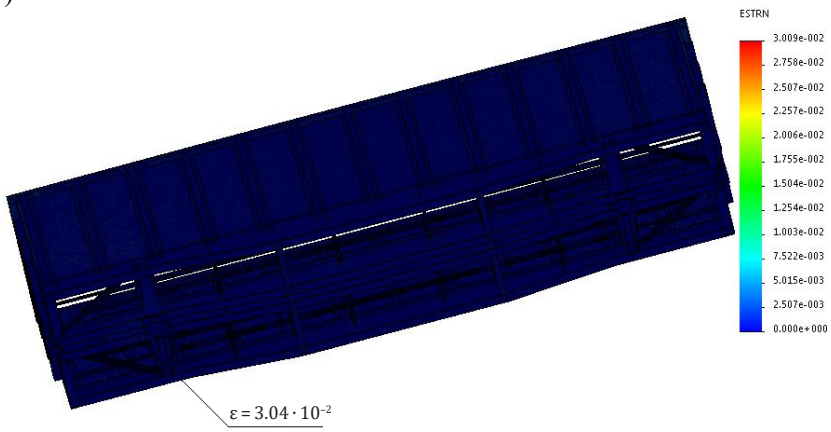

Figure 3.32 – Deformations in the improved bearing structure of the flat wagon for carrying industrial woodchips at design mode I
a) side view; b) bottom view

The results demonstrate that the strength indices are within the permissible limits. Therefore, the solutions to improve the bearing structure of the flat wagon are appropriate.

This wagon can also be equipped with a removable roof for protecting the freight against atmospheric agents. Similar studies conducted by the author are described in [43]. Their sequence was as follows:

– determination of the strength reserve of a typical removable roof;

– calculation of the strength of the improved removable roof; and

– determination of the strength of the bolted attachment of the roof to the upper side rail the wagon body.

The strength reserve of a typical removable roof was determined in SolidWorks using the spatial model (Figure 3.33).

According to regulatory documents, the roof is designed for the strength under the action of two forces of 1 kN each, distributed on the area 0.25 × 0.25 m and applied at 0.5 m from each other in any part of the roof. The roof was additionally calculated for design mode III (most dangerous) and for the mode when it is craned [21, 22].

The following loads acting on the roof are taken at design mode III:

– roof weight; and

– vertical dynamic force determined by multiplying the weight force of the roof by the coefficient of vertical dynamics.

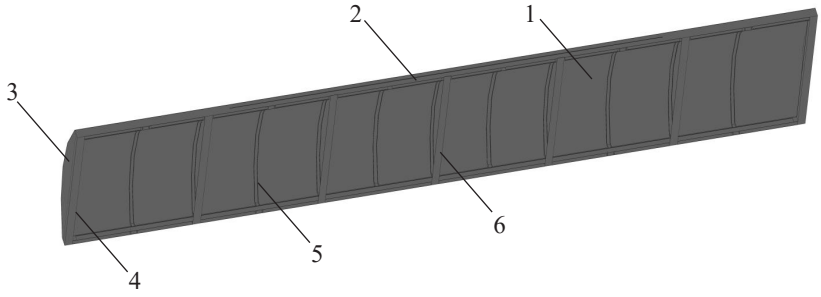

Figure 3.33 – Spatial model of the removable roof
1 – coating; 2 – side longitudinal beam; 3 – end plate of coating; 4 – end cross bearer; 5 – crossbow; 6 – intermediate cross bearer

The impact of snow load on the roof should also be taken into account.

The strength indices of the roof were calculated using the finite element method implemented in SolidWorks Simulation. The design diagram of the roof under the action of two forces of 1 kN each, distributed on the area 0.25 × 0.25 m and applied at 0.5 m from each other is shown in Figure 3.34.

The FEM consisted of isoparametric tetrahedra. The optimal number of model elements was determined using the graphical analytical method. The number of nodes in the model is 263,362, and the number of elements is 768,396. The maximum element size is 100 mm, and the minimum is 20 mm. The percentage of elements with an aspect ratio of less than three is 0.122 and more than ten is 63.3. The minimum number of elements in the circle is 22, the ratio of element size increase is 1.8.

The model is fixed along the roof perimeter in the area of interaction with the top side rail of the wagon body. The maximum equivalent stresses occur in the middle crossbow of the roof and are about 80 MPa (Figure 3.35). Thus, they do not exceed the permissible limits. The maximum displacements in the structural units occur in the middle part of the roof and are 1.3 mm. The results of the strength calculation for the removable roof of the open wagon reveal that the bearing structural elements have a significant safety factor.

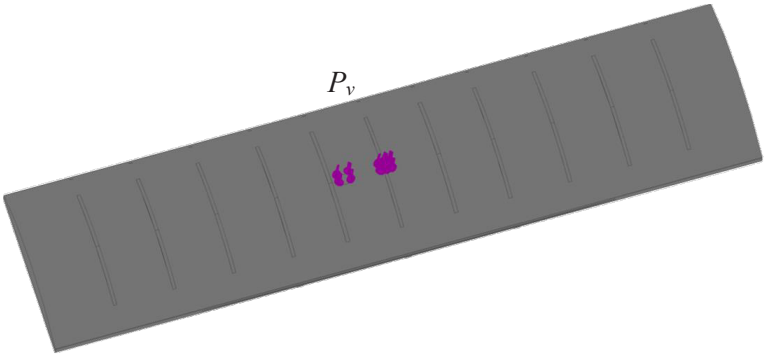

Figure 3.34 – Design diagram of the removable roof

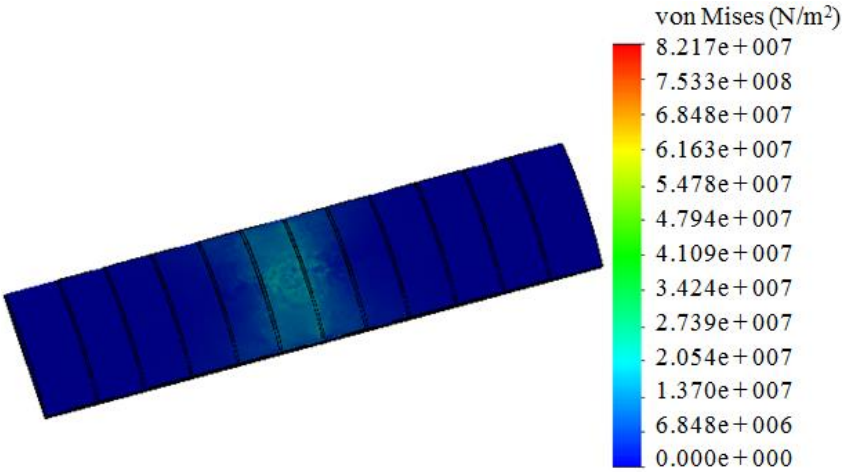

Figure 3.35 – Stress state of the removable roof

The weight of the removable roof was reduced by the optimization according to the safety factor of the bearing elements. The results of the calculations are given in Table 3.5.

The objective function is as follows:

$$m_r \rightarrow \min, \tag{3.10}$$

where m_r is the roof weight, kg.

The limitations of this optimized model are:

1. Geometric dimensions of the wagon.
2. Design stresses must be less than permissible:

$$\sigma_{eq} < [\sigma], \tag{3.11}$$

where σ_{eq} is the equivalent stresses in the structure, MPa;

$[\sigma]$ is the permissible stresses, MPa.

An advanced research area can be the application of pipes as bearing elements of the roof, which will decrease the total metal consumption of the structure given that the strength conditions are fulfilled (Figure 3.36).

Table 3.5 – Optimal parameters of the sections of removable roof elements

Roof frame element	n	σ_{eq}, MPa	I_x, cm^4	I_y, cm^4	W_x, cm^3	W_y, cm^3	$[W_x]$, cm^3	$[W_y]$, cm^3	Optimal parameters of the pipe			Weight of 1 m of pipe, kg
									W, cm^3	h, mm	S, mm	
Crossbow	2.6	92.6	10.2	10.2	5.1	5.1	1.96	1.96	2.18	30	2.5	2.07
Lateral longitudinal beam	3.1	78.3	97.26	621.29	12.16	155.32	3.93	50.1	4.17	35	4.0	3.67
End cross bearer	3.2	75.4	97.26	621.29	12.16	155.32	3.93	50.1	4.17	35	4.0	3.67
Intermediate cross bearer	2.8	87.3	10.2	10.2	5.1	5.1	1.96	1.96	2.18	30	2.5	2.07

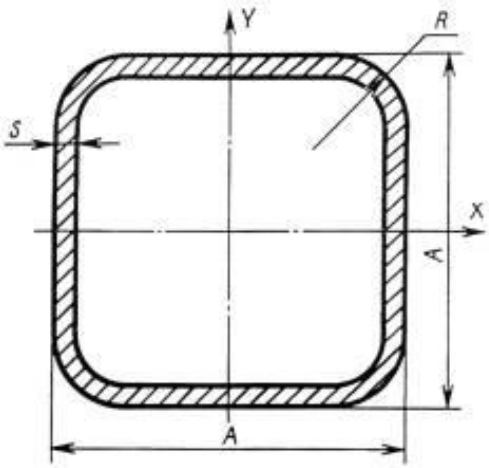

Figure 3.36 – Square section of the pipe

Based on the calculations, a spatial model of the removable roof was built (Figure 3.37).

Taking into account the proposed measures, it becomes possible to reduce the weight of the removable roof frame of the wagon by almost 15 % compared to that of a typical design.

Because the cantilever parts can be extended in the longitudinal direction, the roof can be used for different wagon types (Figure 3.38).

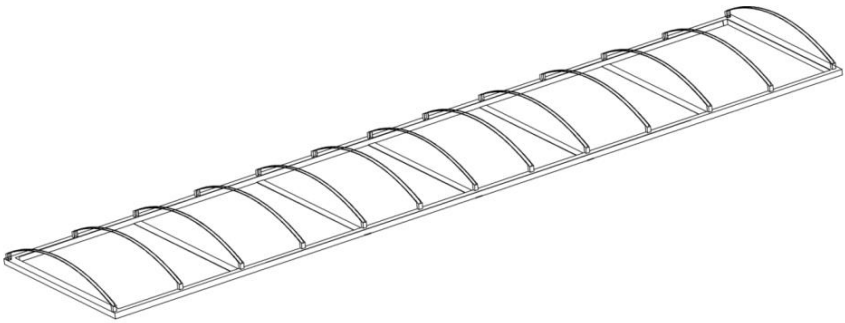

Figure 3.37 – Frame of the optimized removable roof

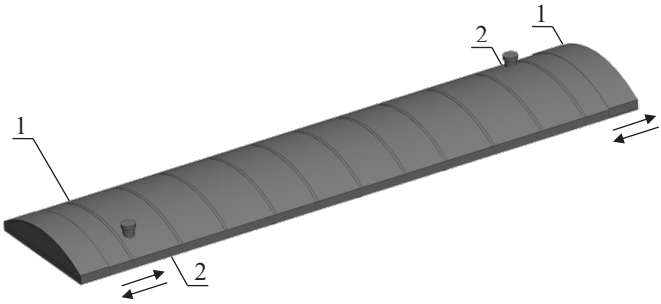

Figure 3.38 – Improved removable roof
1 – roof extension; 2 – deflectors

The deflectors are placed on stationary parts of the roof. The roof can be attached to the body either in a standard way or using pull-type fasteners.

The strength of the improved bearing structure of the removable roof was calculated. The FEM included isoparametric tetrahedra. The optimal number of model elements was determined using the graphical analytical method. The number of nodes is 42,534, and the number of elements was 137,547. The maximum element size is 100 mm, and the minimum is 20 mm. The percentage of elements with an aspect ratio of less than three is 0.138, and more than ten is 65.6. The minimum number of elements in the circle is 22, the ratio of element size increase is 1.8. The model is fixed along the roof perimeter in the area of interaction with the upper side rail of the wagon body.

The calculation results are shown in Figures 3.39–3.40. The maximum equivalent stresses occur in the middle part of the roof and amount to about 230 MPa, thus they do not exceed the permissible values. The maximum displacements in the structural units occur in the middle part of the roof and amount to 1.8 mm.

The results of strength calculation of the removable roof at design mode III show that the maximum equivalent stresses occur in the middle part of the roof and amount to about 230 MPa, thus they do not exceed the permissible limits. The maximum displacements in the structural components occurs in the middle part of the roof and amount to 1.8 mm.

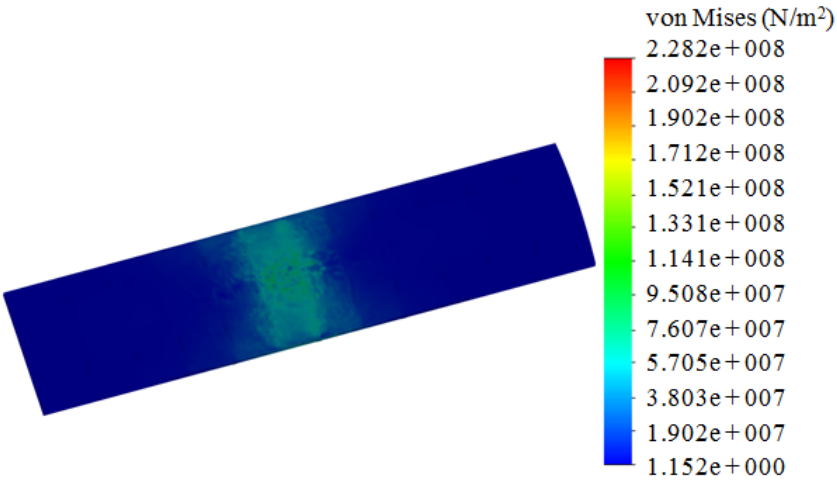

Figure 3.39 – Stress state of the removable roof

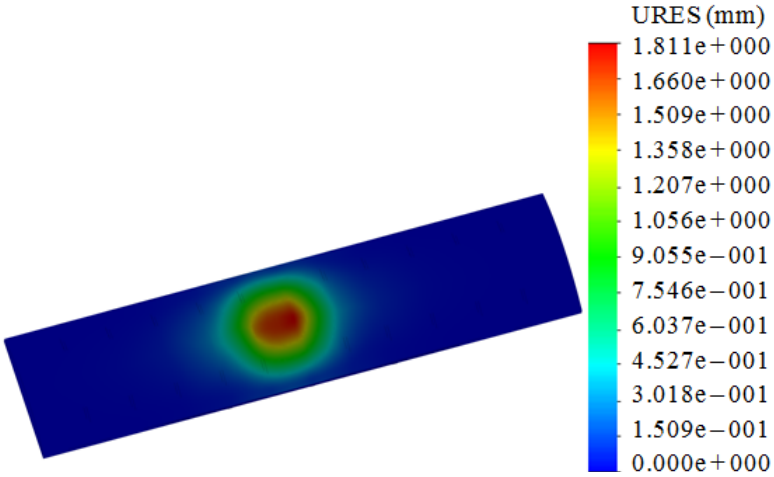

Figure 3.40 – Displacements in the units of the removable roof

When the removable roof is lifted with slings, the maximum equivalent stresses occur in the attachment areas and amount to about 120 MPa, but they do not exceed the permissible values. The maximum displacements in the structural units occur in the fixing areas of the roof and amount to 1.65 mm.

The removable roof can also withstand snow loads. The maximum equivalent stresses occur in the middle part of the roof and amount to about 104.1 MPa, i.e., they do not exceed the permissible values. The maximum displacements in the structural units occurs in the middle part of the roof and amount to 1,31 mm.

Thus, based on the calculations, it can be concluded that the measures proposed are reasonable and appropriate.

The strength with which the roof is attached to the wagon body using the bolted connection was also calculated. The roof is attached to the upper side rail with M12×90 bolts and to the end wall with M12×65 bolts. After tightening the bolted assembly, the nut is welded to prevent from self-unscrewing.

The case of loading the roof with a longitudinal force arising from a wagon collision was also taken into account as the case of the highest load in operation. The bolted assembly is affected by the longitudinal force Q, due to the longitudinal inertia force of the wagon body during collision, and the vertical force N, due to the self-weight of the roof (Figure 3.41).

Since the bolts are welded after screwing, the longitudinal force is subject to torsional forces in addition to the above-mentioned forces.

Then, the strength condition is as follows [44]:

$$N_{red} = \sqrt{\left(N_N + N_{M,\max}\right)^2 + N_Q^2} \le N_{b,\min}, \qquad (3.12)$$

where N_N is the longitudinal force acting on the bolted joint; $N_{M,\,max}$ is the largest possible load in the bolted joint; N_Q is the lateral force acting on the bolted joint; $N_{b,\,min}$ is the bearing capacity of the bolt.

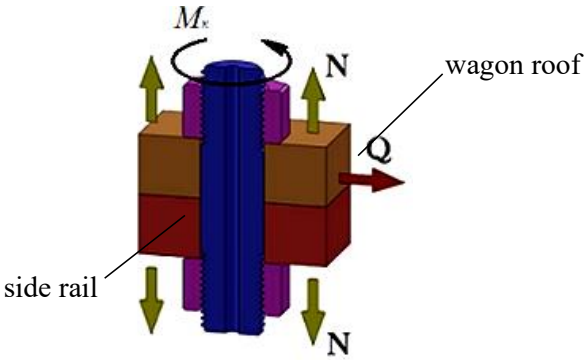

Figure 3.41 – Design diagram of the roof bolted to the upper side rail of the wagon body

Under the action of the shear force Q, it is assumed, for simplicity, that the forces in the bolts are evenly distributed. Thus, the force acting on one bolt is determined as:

$$N_Q = \frac{Q}{n}, \tag{3.13}$$

where n is the number of bolts in the joint.

The force N_N is calculated similarly to N_Q:

$$N_N = \frac{N}{n}. \tag{3.14}$$

The maximum load $N_{M,\max}$ due to the action of the torque M on the bolted joint is determined as follows:

$$N_{M,\max} = \frac{M \cdot l_{\max}}{m\sum_{i=1}^{k} l_i^2}, \tag{3.15}$$

where l_i is the distances between two bolts placed symmetrically relative to the centre of gravity of the joint; l_{max} is the maximum distance between the pairs of bolts; m is the number of pairs of bolts.

Assume that the maximum longitudinal inertia force is 4.0 g.

The vertical load N_N acting on the bolted joint includes a weight of the roof (1.2 tonnes) and a force of 210.21 N from 54 bolts with a diameter of 12 mm used for attaching the roof to the upper rail of the open wagon.

The transverse load N_Q on the bolts connecting the end part of the roof with the upper rail (the roof bolts are most stressed during shunting impacts) is 8,857.14 N.

Given that the distance between the roof bolts is 0.375 m, then $N_{M,max}$ = 3,489.8 N.

Taking into account the cross-sectional area of the bolt (S = 113,04 mm^2), N_{red} = 138,75 N/mm^2 at $N_{b,\min}$ = 122 N/mm^2. Thus, the strength condition is not fulfilled. Therefore, the use of typical bolts to secure the roof to the wagon body is not efficient.

Therefore, it is proposed to use bolts with greater bearing capacity, for example, M12×95 with the thread pitch 1.75 and the strength class 5.8, which will ensure the reliable fastening.

3.2 Improvements for the bearing structure of a flat wagon used for military strategic purposes

The technical and economic development of European countries, as well as the strengthening of their national security and defence require higher efficiency of railway transport, which is a leading branch of the entire transport system. Therefore, the introduction of a highly efficient interoperable rolling stock into operation is relevant. The defence capability of European countries requires addressing the issue of creating a specialized rolling stock for carrying military equipment [35].

As known, one of the most common types of wagons used for carrying military equipment is flat wagons (Figure 3.42).

The military equipment can drive onto the flat wagon through the inclined ramp (Figure 3.43).

Figure 3.42 – Flat wagons loaded with military equipment

Figure 3.43 – Loading of military equipment on the flat wagon

Military equipment can be secured on flat wagons by using the following lashing devices [36, 37]:

- universal reusable fasteners (method 1);
- metal spurs (method 2);
- wooden thrust bars and wire (standard) stretch rods (method 3);
- metal thrust shoes and wooden liners (method 4);
- wooden thrust bars and liners (method 5); and
- clamps-stretch bars and clamps (method 6).

Methods 1–4 are used for transporting equipment as part of military echelons, and if accompanied by the guards.

Reusable fasteners are shown in Figure 3.44. The diagram of fastening military tanks on the flat wagon is shown in Figure 3.45 [38, 39].

All fasteners are removable and can be used to secure military equipment of various dimensions on the bearing structure of a flat wagon. Brake shoes can be made of metal or wood. Wooden blocks or liners can also be used. Brake shoes can be rotating or folding.

The relevant calculations regarding the transportation of military equipment on flat wagons were carried out.

The stress state of the bearing structure of the flat wagon carrying military equipment was investigated through the strength calculations in CosmosWorks.

The design diagram of the bearing structure of the flat wagon is shown in Figure 3.46.

The design diagram includes the following loads: the vertical static load P_v, due to gross weight, longitudinal load on the coupler lugs P_l, load on the stanchion pockets P_b from the lashing devices of the tank.

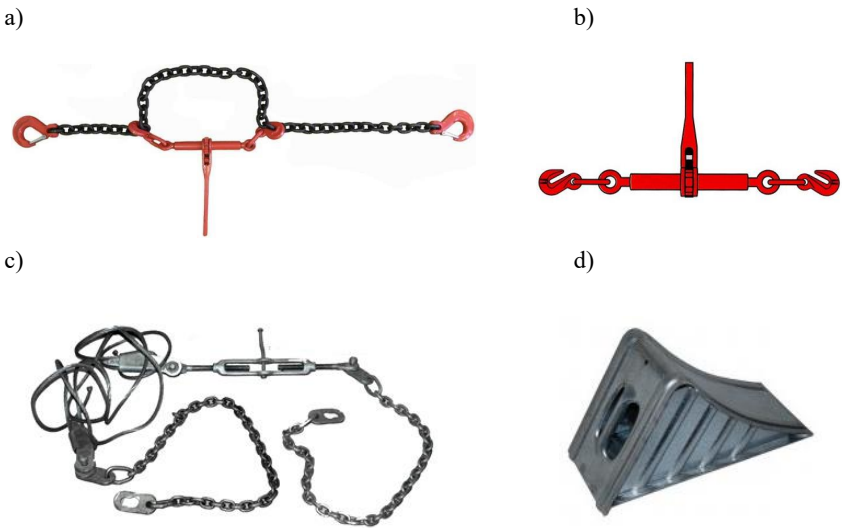

Figure 3.44 – Reusable fasteners
a) chain binder; b) metal brace; c) wire brace; d) metal shoe

Figure 3.45 – Tanks secured on flat wagons

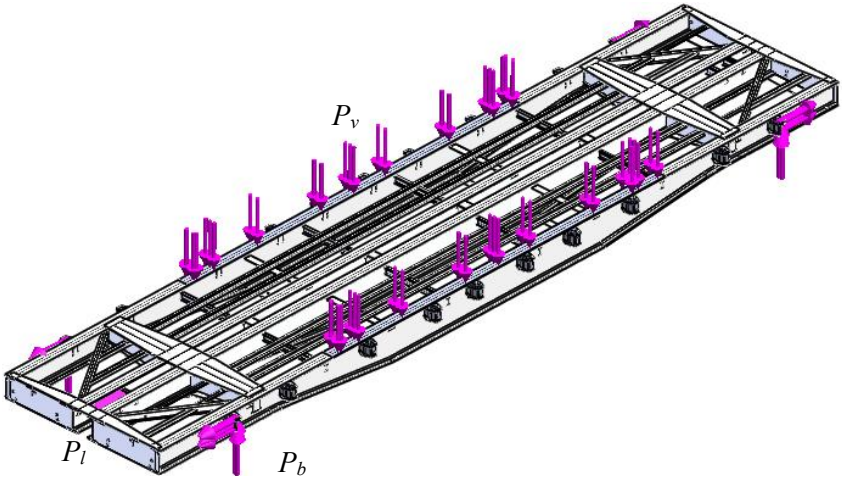

Figure 3.46 – Design diagram of the bearing structure of the flat wagon

Due to the spatial arrangement of the lashing devices, the load acting on the stanchion pockets break down into components. The inclination angle of the lashing devices is assumed to be 45°. The numerical values of loads on the stanchion pockets were calculated with the maximum longitudinal accelerations acting on the bearing structure of the flat wagon in operation; they amount to 40 m/s^2. The results of the calculation are shown below.

The results of the calculations indicate that the maximum equivalent stresses occur in the stanchion pockets and are about 350 MPa. The maximum displacements are concentrated in the middle parts of the main longitudinal beams and amount to about 6.0 mm. Thus, reusable lashing devices must not be fixed to stanchion pockets.

It is proposed to install special D-rings for securing chain binders on the bearing structure of the flat wagon for reliable fastening of military equipment (Figure 3.49).

D-rings are installed on the main longitudinal beams of the flat wagon (Figure 3.50). The stress state of the bearing structure of the flat wagon was determined with strength calculations in SolidWorks Simulation. The design diagram of the bearing structure of the flat wagon is shown in Figure 3.51.

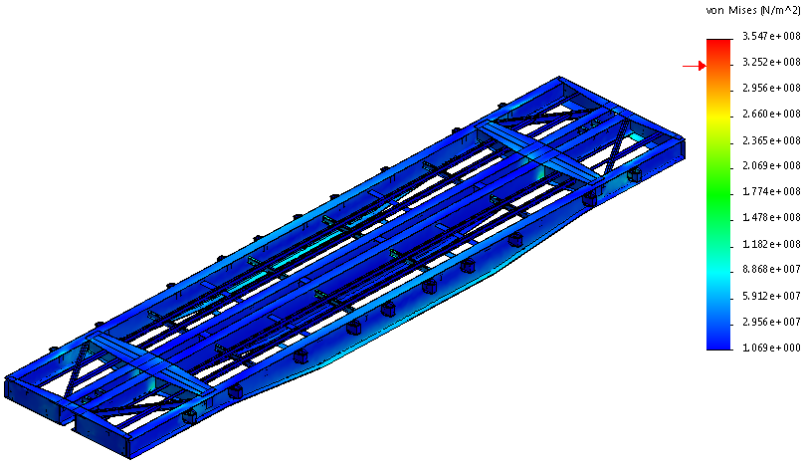

Figure 3.47 – Stress state of the bearing structure of the flat wagon

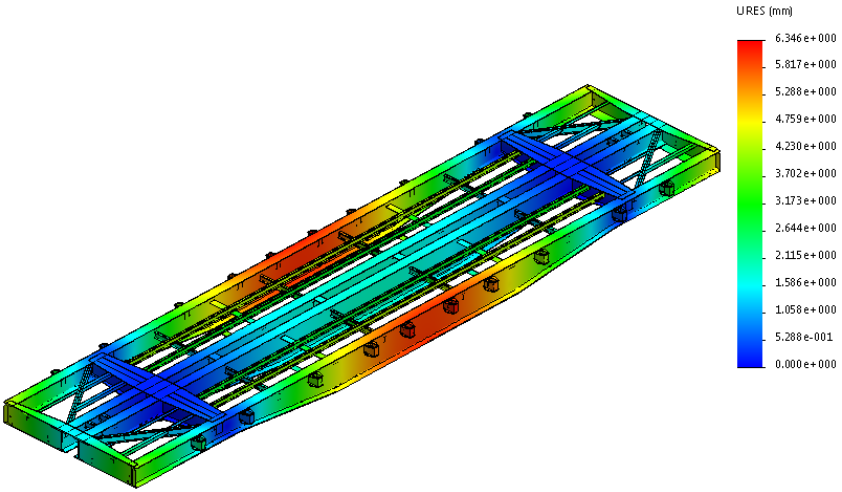

Figure 3.48 – Displacements in the units of the bearing structure of the flat wagon

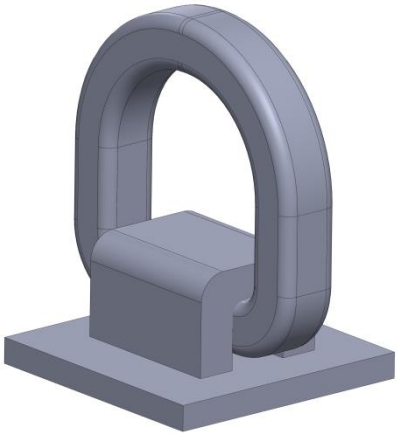

Figure 3.49 – D-ring for securing a tank on the flat wagon

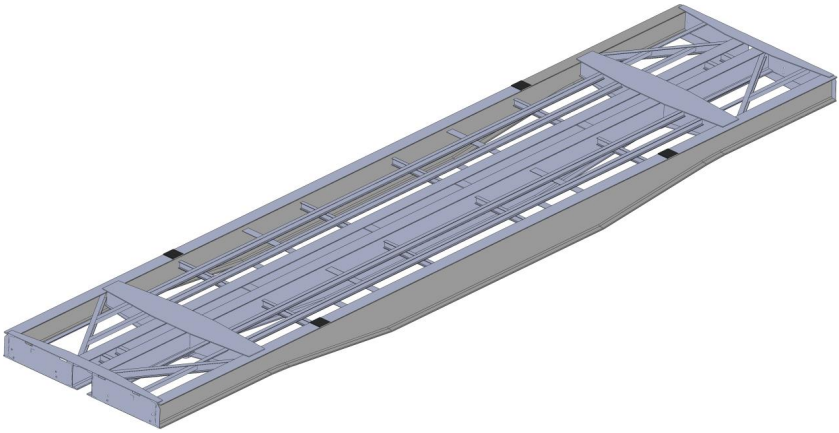

Figure 3.50 – D-rings on the bearing structure of the flat wagon

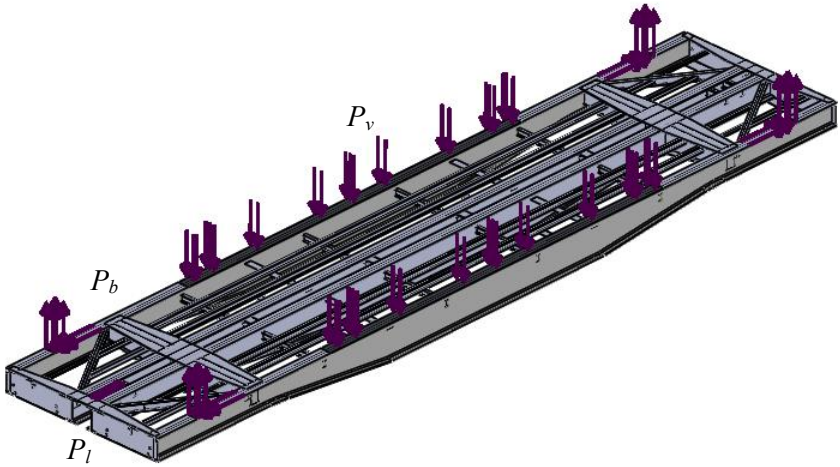

Figure 3.51 – Design diagram of the bearing structure of the flat wagon

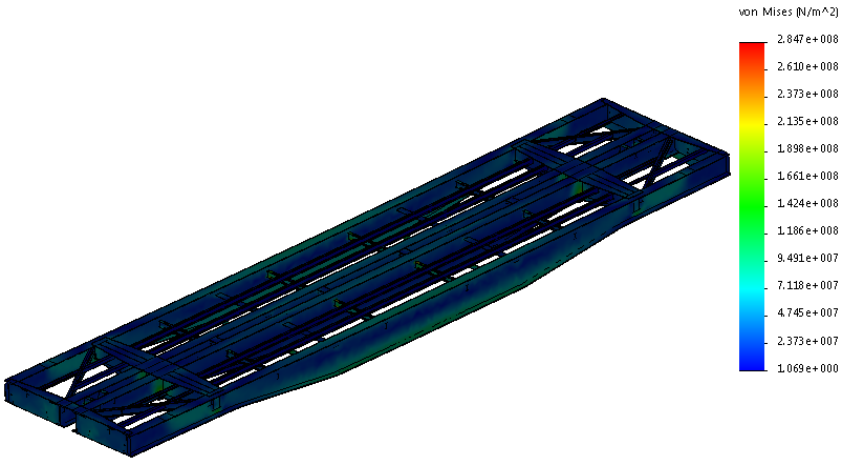

Figure 3.52 – Stress state of the bearing structure of the flat wagon

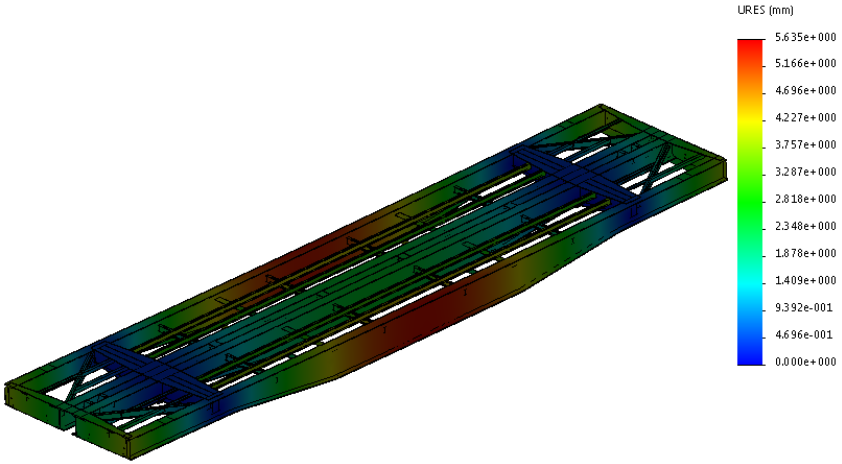

Figure 3.53 – Displacements in the bearing structure of the flat wagon

The results of the calculation are shown in Figures 3.52 and 3.53.

The results of the calculations indicate that the maximum equivalent stresses occur in the main longitudinal beams of the frame and are about 280 MPa. The maximum displacements are concentrated in the middle parts of the main longitudinal frame beams and amount to 5.6 mm. Thus, the strength of the bearing structure of the flat wagon is ensured [21, 22].

3.3 Improvements in the bearing structure of a flat wagon carrying trailers

It was proposed to improve a universal flat wagon for carrying trailers by optimising its longitudinal beams so that to reduce the amount of metal used for the bearing structure.

The objective function is as follows:

$$M_{FW} \rightarrow \min . \tag{3.16}$$

The limitations of the optimized model are:

1. The maximum equivalent stresses σ_{eq} must be less than the permissible ones (material fluidity σ_m was taken as permissible values):

$$\sigma_{eq} \leq \sigma_m . \tag{3.17}$$

2. The profile of the longitudinal beam of the flat wagon must provide the place for fitting stops for containers.

The optimal parameters of the structural elements of the flat wagon were obtained by the optimisation method according to the strength reserve at the following stages [20]:

1. Determination of the design capacity reserve of the bearing structure of the flat wagon based on the analysis of complex theoretical and calculation studies of its operating loads.

2. Determination of permissible strength characteristics of the structural elements of the flat wagon.

3. Determination of optimal cross-sections including structural and strength constraints.

4. Selection of the existing versions of rolled profiles on the basis of the optimal parameters.

5. Development of a new flat wagon design using the selected profiles.

6. Comprehensive theoretical and computational verification of the improved flat wagon design.

7. Analysis of the research results.

The 13-401 flat wagon can be used for carrying trailers if they fit within the prescribed dimensions when loaded. For this purpose, it is proposed to lower the side beams of the frame relative to the centre sill.

After carrying out the relevant calculations, the side beam profile was chosen according to the axial moment of resistance 121 cm^3. Thus, for the side beam profile, the most optimal is channel No. 18 reinforced with a stiffener 8 mm thick (Figure 3.54), with a weight of 16.3 kg per linear metre. The weight of one linear metre of I-beam No. 36 of the standard design is 48.6 kg. Consequently, the selected profile is almost three times less in terms of metal consumption than a typical one.

The 3D model of the improved bearing structure of the flat wagon is shown in Figure 3.55.

The stress-strain state of the improved flat wagon structure was determined using the finite element method. The number of mesh elements is 325,987, and the number of nodes is 108,870 (Figure 3.56). The maximum element size is 200 mm, the minimum is 40 mm, the maximum aspect ratio is 814.76, and the percentage of elements with an aspect ratio of less than three was 14.5 and more than ten was 27.

The design model of the bearing structure of the flat wagon included two 1CC containers.

The design diagram of the bearing structure of the flat wagon at design mode I is shown in Figure 3.57. The following loads were taken into account: P_l = 3.5 MN is the longitudinal impact force; R = 583.333 kN is the reaction to the action of longitudinal force in the fitting stops; P_v = 48 t is the vertical static force from containers placed on the flat wagon.

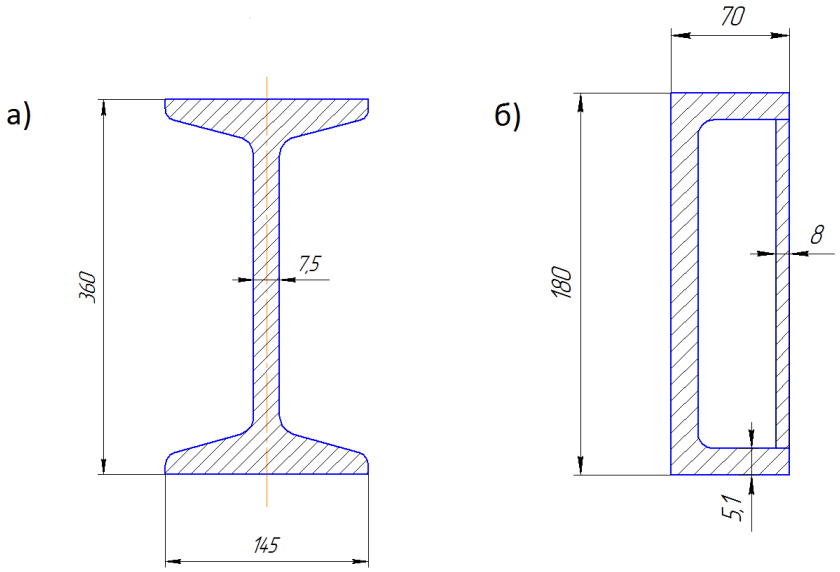

Figure 3.54 – Side beam profile
a) before improvement – I-beam No. 36;
b) after improvement – channel No. 18

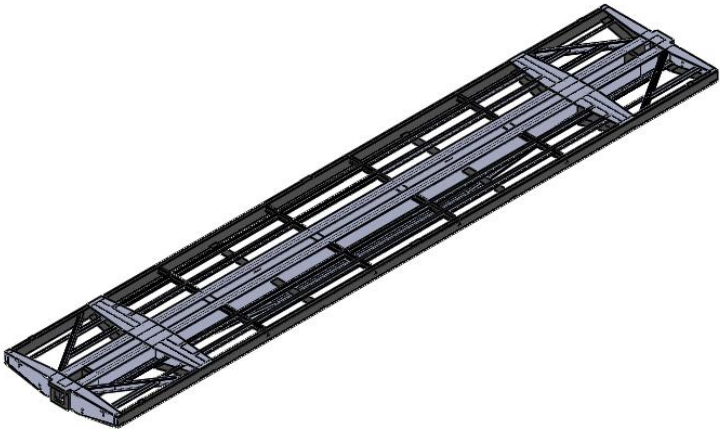

Figure 3.55 – Spatial model of the bearing structure of the flat wagon

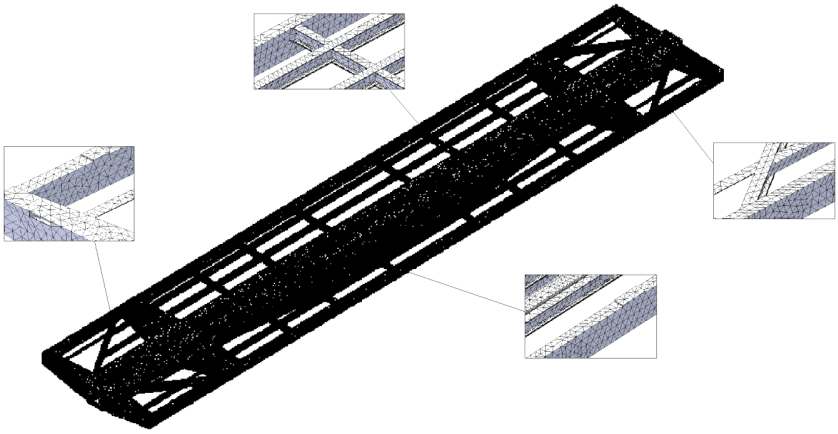

Figure 3.56 – FEM of the bearing structure of the flat wagon

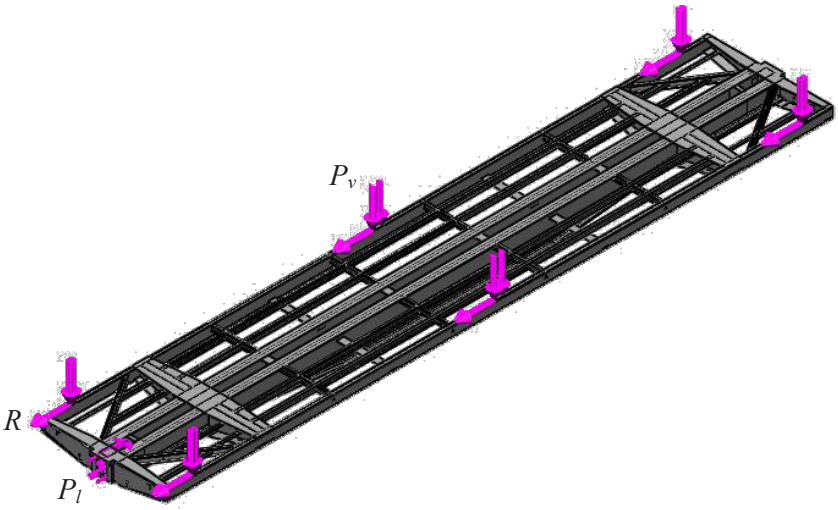

Figure 3.57 – Design diagram of the bearing structure of the flat wagon at design mode I

The results of the strength calculation of the bearing structure of the flat wagon at design mode I (impact) are shown in Figures 3.58 and 3.60. The highest stresses are concentrated in the area of interaction between the bolster beam and the centre sill and amount to about 274.7 MPa. The largest displacements are 18.59 mm, and the deformations are $2.909 \cdot 10^{-3}$.

As seen, the maximum equivalent stresses do not exceed the yield strength of the material, and therefore the strength of the bearing structure of the flat wagon is ensured in accordance with [21, 22].

The results of the strength calculation of the bearing structure of the flat wagon at design mode I (jerk) are shown in Figures 3.61–3.63. The highest stresses are concentrated in the area of interaction between the bolster beam and the centre sill and amount to about 265.3 MPa. The largest displacements are 15.43 mm, and the deformations are $2.822 \cdot 10^{-3}$.

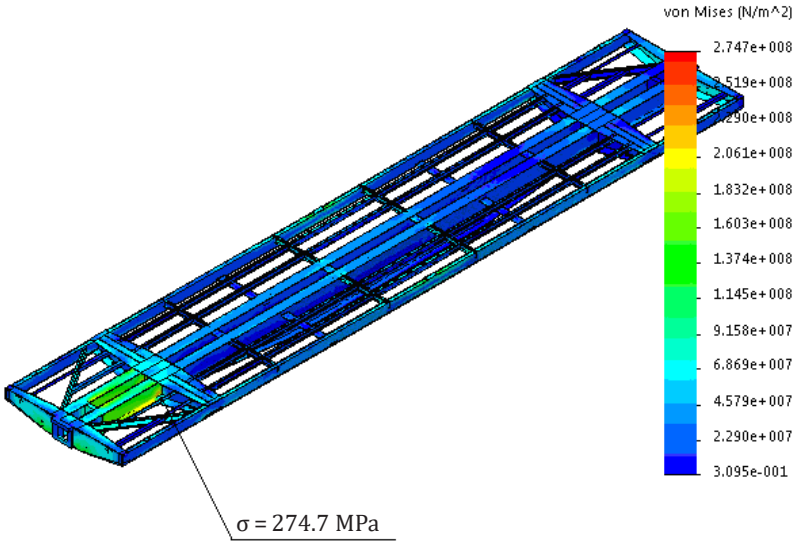

Figure 3.58 – Stress state of the bearing structure of a flat wagon at design module I (impact)

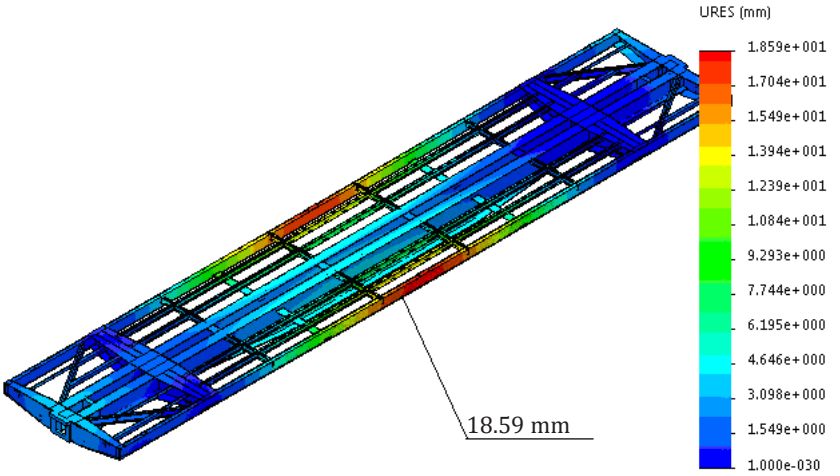

Figure 3.59 – Displacements in the bearing structure units of the flat wagon at design mode I (impact)

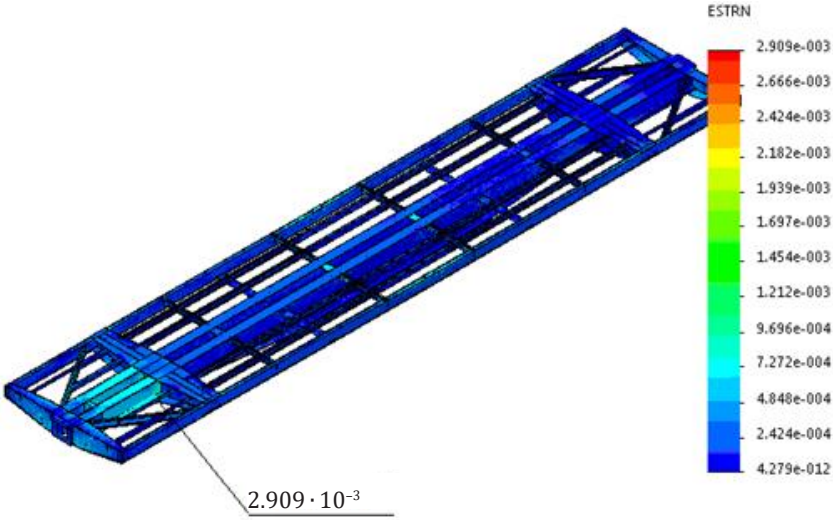

Figure 3.60 – Deformations in the bearing structure of the flat wagon at design mode I (impact)

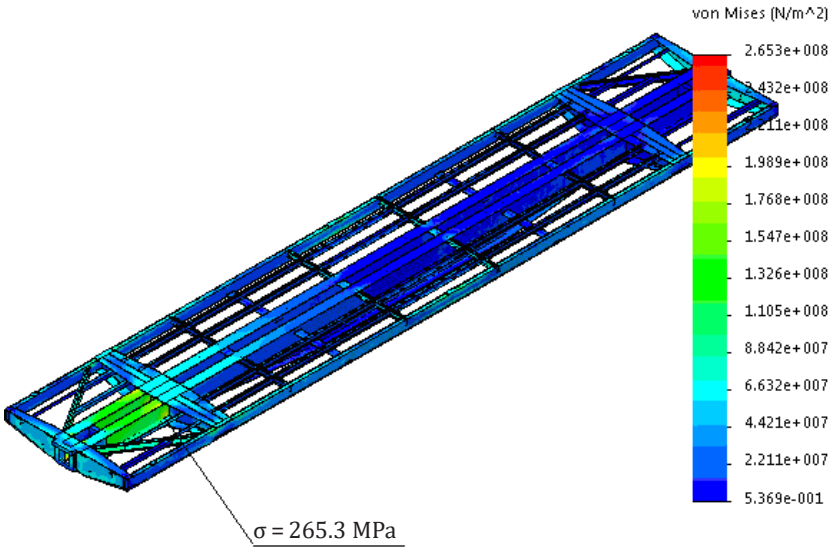

Figure 3.61 – Stress state of the bearing structure of the flat wagon at design mode I (jerk)

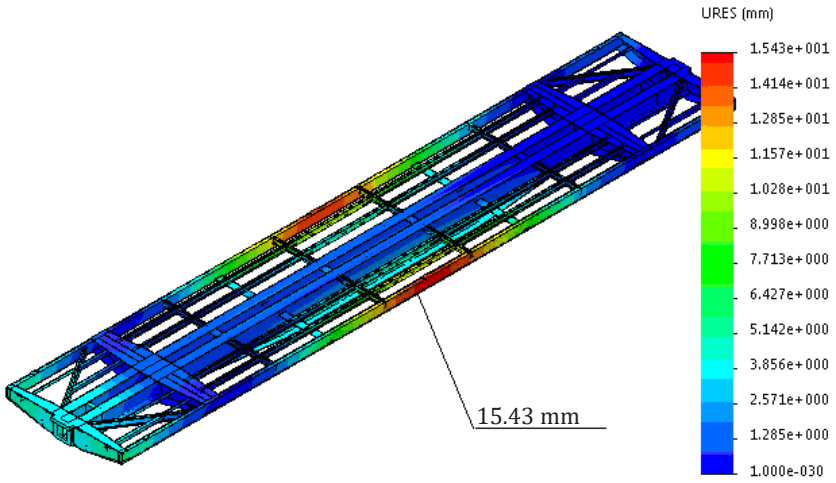

Figure 3.62 – Displacements in the bearing structure units of the flat wagon at design mode I (jerk)

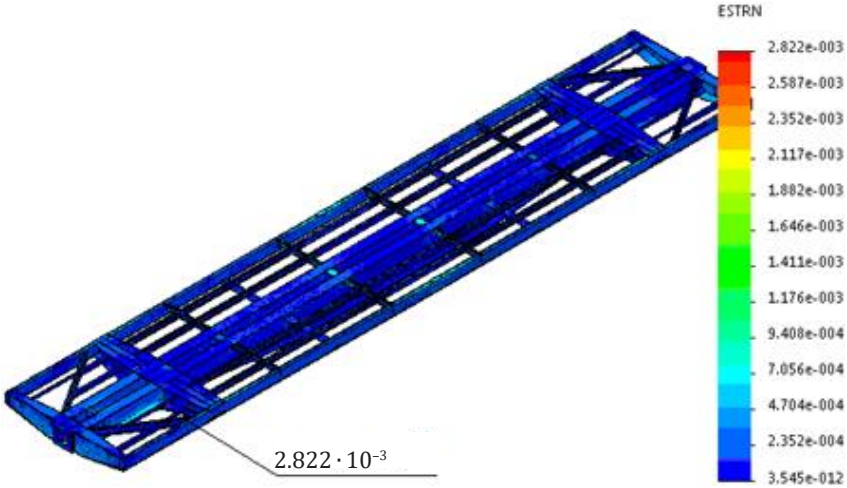

Figure 3.63 – Deformations in the bearing structure of the flat wagon at design mode I (jerk)

The results of the strength calculation of the bearing structure of the flat wagon at design mode III (impact) are shown in Figures 3.64–3.66. The highest stresses are concentrated in the area of interaction between the bolster beam and the centre sill and amount to about 180.2 MPa. The largest displacements are 17.26 mm, and the deformations are equal to $2.822 \cdot 10^{-3}$.

The results of the strength calculation of the bearing structure of the flat wagon at design mode III (jerk) are shown in Figures 3.67–3.69. The highest stresses are concentrated in the area of interaction between the bolster beam and the centre sill and amount to about 199.4 MPa. The largest displacements are 16.37 mm, and the deformations are $2.456 \cdot 10^{-3}$.

The bearing structure of the flat wagon can be equipped with folding fitting stops for fastening containers (Figure 3.70), [5], with removable stops for attaching piggyback loading units, or a removable or foldable beam for securing the front part of a semi-trailer to the kingpin of the fifth-wheel coupling.

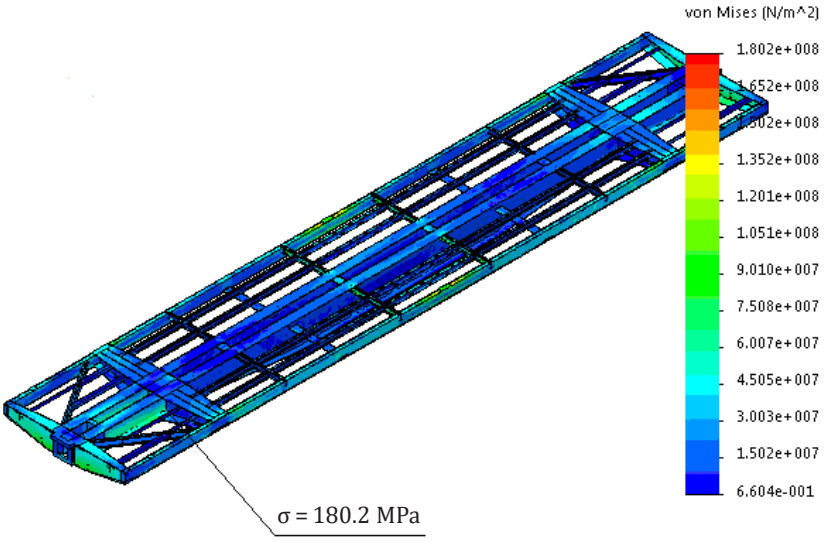

Figure 3.64 – Stress state of the bearing structure of the flat wagon at design mode III (impact)

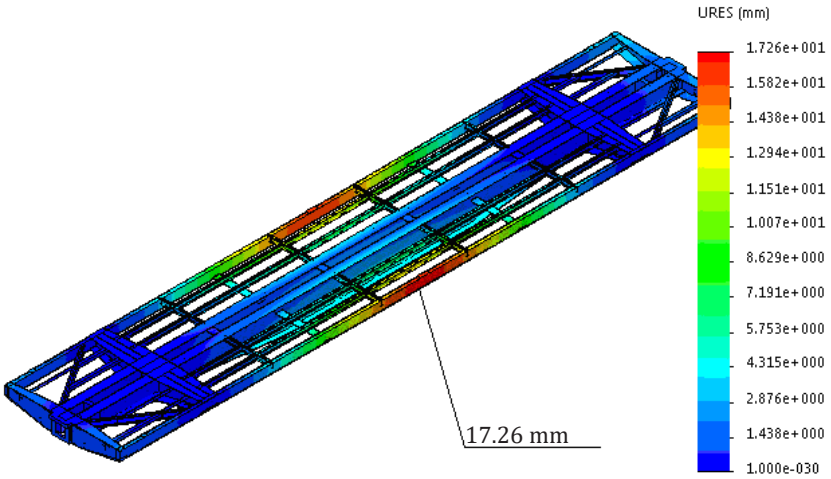

Figure 3.65 – Displacements in the bearing structure units of the flat wagon at design mode III (impact)

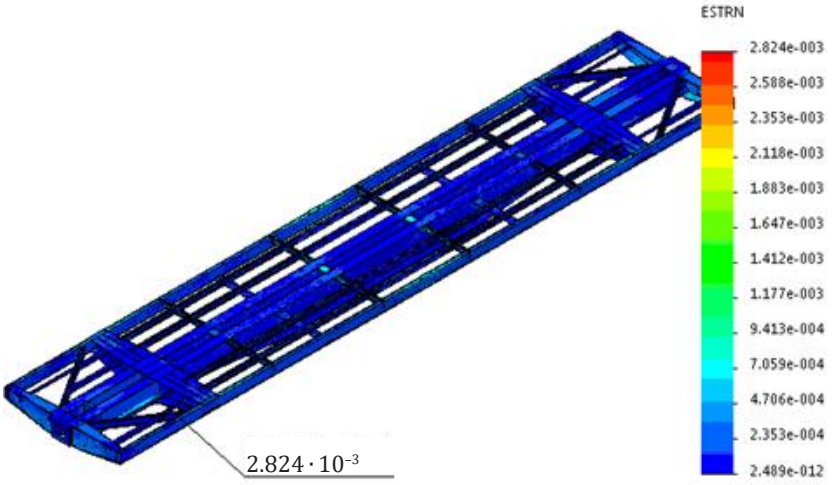

Figure 3.66 – Deformations in the bearing structure of the flat wagon at design mode III (impact)

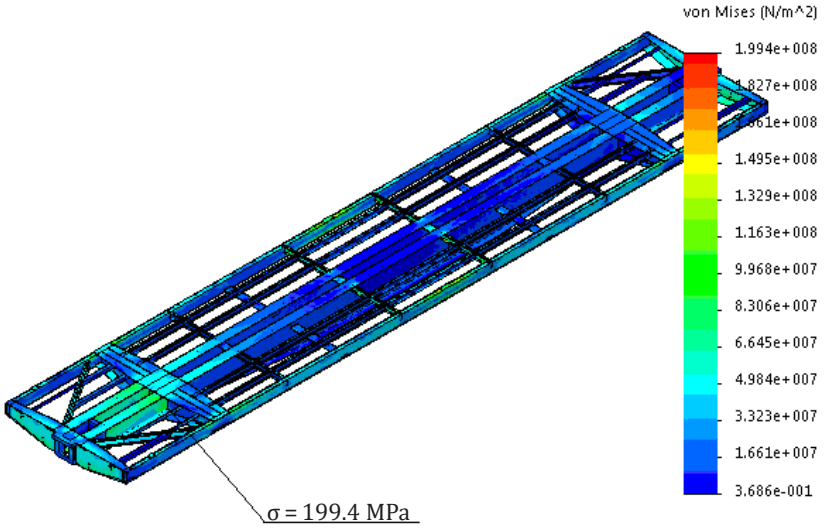

Figure 3.67 – Stress state of the bearing structure of the flat wagon at design module III (jerk)

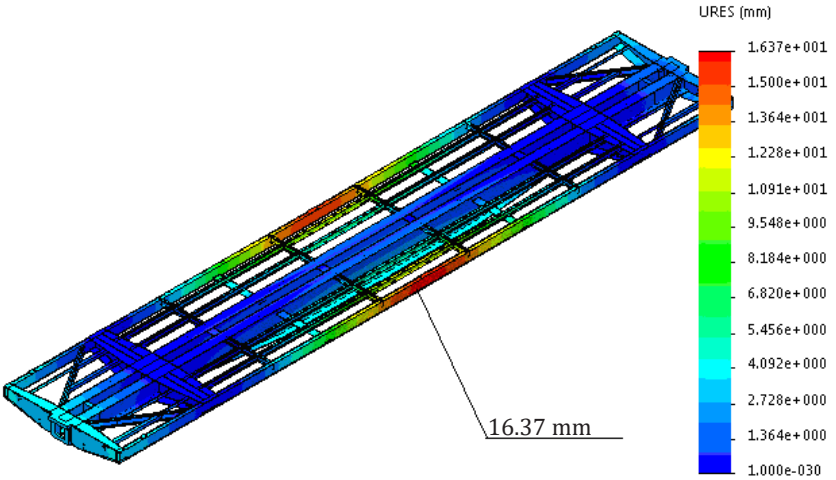

Figure 3.68 – Displacements in the bearing structure units of the flat wagon at design mode III (jerk)

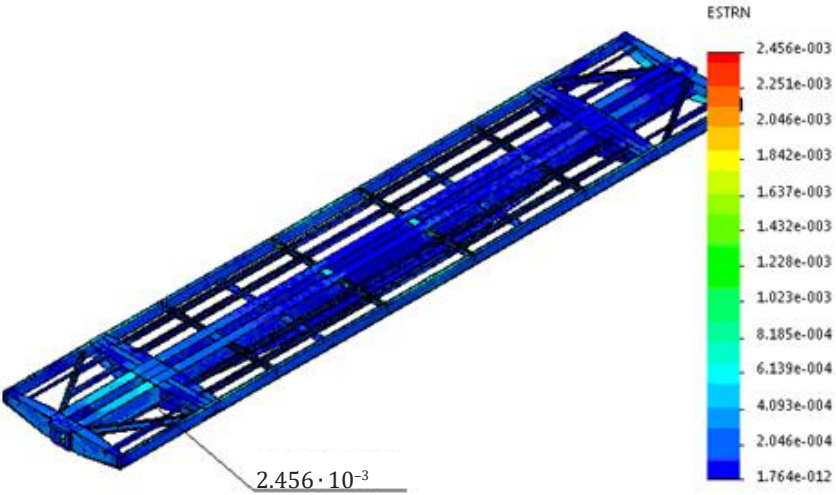

Figure 3.69 – Deformations in the bearing structure of the flat wagon at design mode III (jerk)

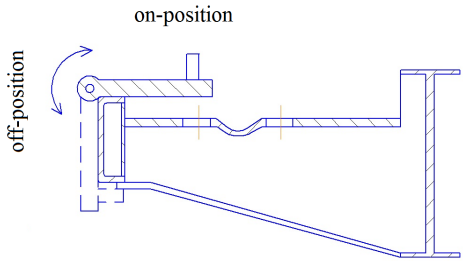

Figure 3.70 – Foldable fitting stop

Reusable stops are used to secure trailer trains on flat wagons. The Dnipro VahonMash company has developed two types of wheel stoppers [5]. The first model is a folding stop with a screw drive. When not in use, it folds up compactly and does not obstruct the passage of trailer trains. It has metal pads with a screw clamping mechanism and is fixed with special pins that fit into the oval holes in the floor panels of the flat wagon.

The second variant (Figure 3.71) is made in the form of a rigid prism based on a plate with pins inserted into the holes in the flat wagon floor. These stops are usually installed with gaps between the wheels and the structural elements. The results of studies of the transient motion modes of trailer trains show that these gaps can affect the dynamic load of trailer trains on flat wagons. Moreover, the maximum longitudinal accelerations of trailer trains and flat wagons are within the limits established by the standards and technical conditions for loading and securing freight [5].

The flat wagon under study can be fully loaded with a car, trailer, tractor or two 1CC containers (Figure 3.72).

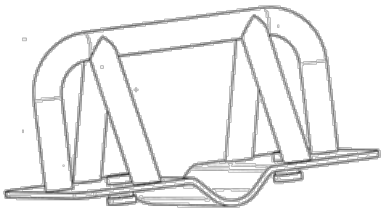

Figure 3.71 – General view of the wheel stopper on the flat wagon

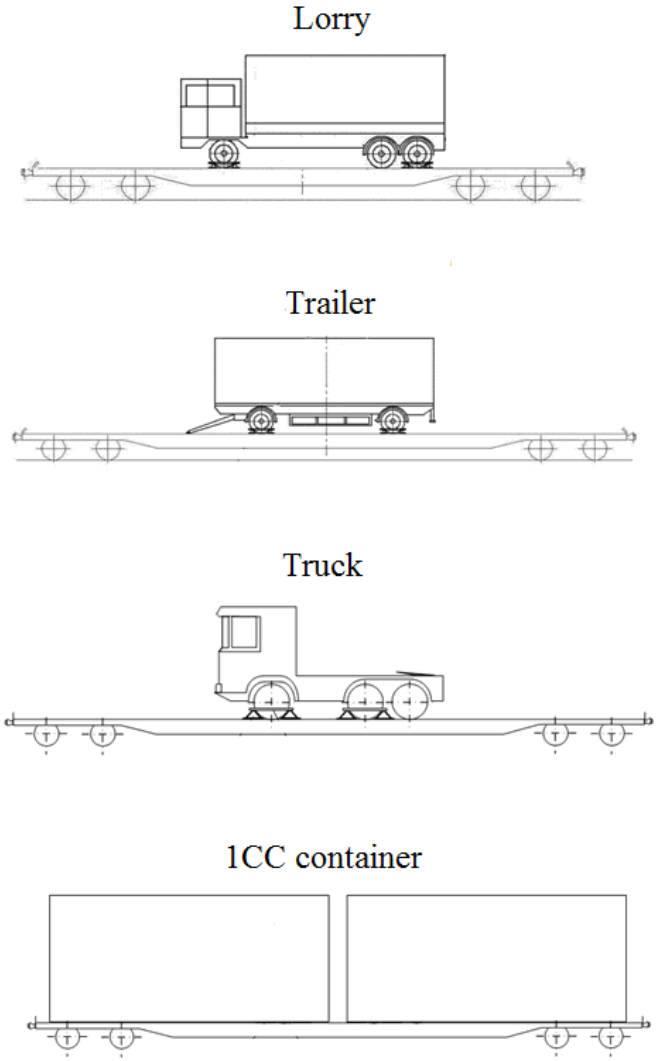

Figure 3.72 – Placement of freight on the flat wagon used for combined transportations

3.4 Development of an articulated long-wheelbase flat wagon for carrying containers

The first stage of the development of an articulated flat wagon on the basis of the existing structure included the strength calculation.

The strength of the bearing structure of the flat wagon was studied with a spatial model (Figure 3.73) built in SolidWorks.

The strength calculation was carried out using the finite element method in SolidWorks Simulation.

The number of mesh elements was determined with graphical analytical method. Ten-node isoparametric tetrahedra were used as finite elements. The FEM of the flat wagon is shown in Figure 3.74. The number of mesh elements is 464,673, the number of nodes is 152,074. The maximum size of the element is 160 mm, the minimum size is 32 mm, the maximum aspect ratio is 2,103.8, the percentage of elements with an aspect ratio of less than three is 13.3, and more than ten – 25.2. The minimum number of elements in the circle is 9, and the ratio of element size increase in the mesh is 1.7.

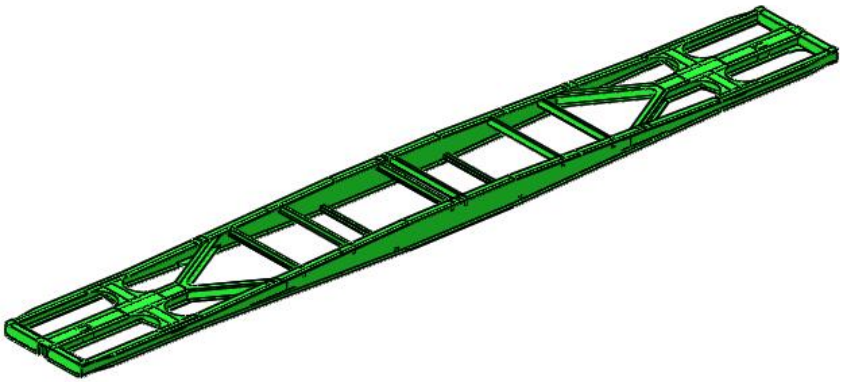

Figure 3.73 – Spatial model of the bearing structure of the flat wagon mod. 13-7024

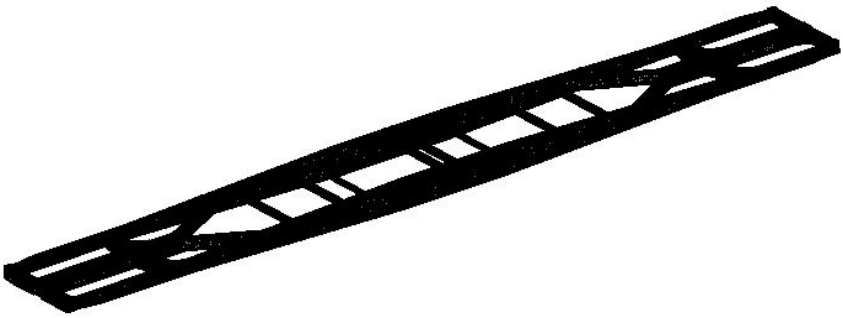

Figure 3.74 – FEM of the bearing structure of the flat wagon

The model does not include the welds in the areas of interaction between individual structural elements.

The bearing structure of the flat wagon is made of Steel 09G2S.

The design diagram of the bearing structure of the flat wagon includes the loads acting from 1CC containers at design mode I (Figure 3.75). The impact load P_l is applied to the vertical surface of the rear draft lug and is equal to 3.5 MN. In the vertical plane, the fitting stop is affected by the load P_c from the gross weight of the container.

The results of the strength calculation for design mode I (impact) are shown in Figures 3.76–3.78.

The results of the strength calculations at design mode I (jerk) are shown in Figures 3.79–3.81.

The results of the strength calculations for design mode I (compression) are shown in Figures 3.82–3.84.

The results of the strength calculations for design mode I (tension) are shown in Figures 3.85–3.87.

The results of the strength calculations for design mode III (impact, compression) are shown in Figures 3.88–3.90.

The results of the strength calculations for design mode III (tensile, jerk) are shown in Figures 3.91–3.93.

The strength indices of the bearing structure of the flat wagon were analysed with the histograms shown in Figures 3.94–3.96.

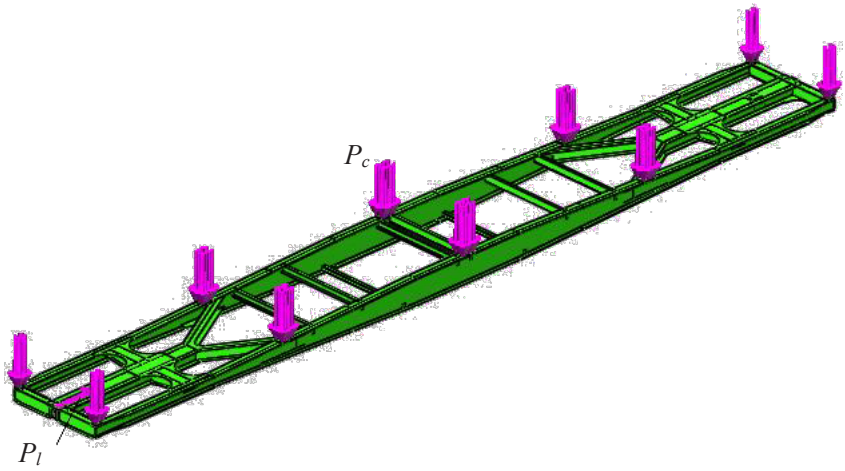

Figure 3.75 – Design diagram of the bearing structure of the flat wagon with containers at design mode I

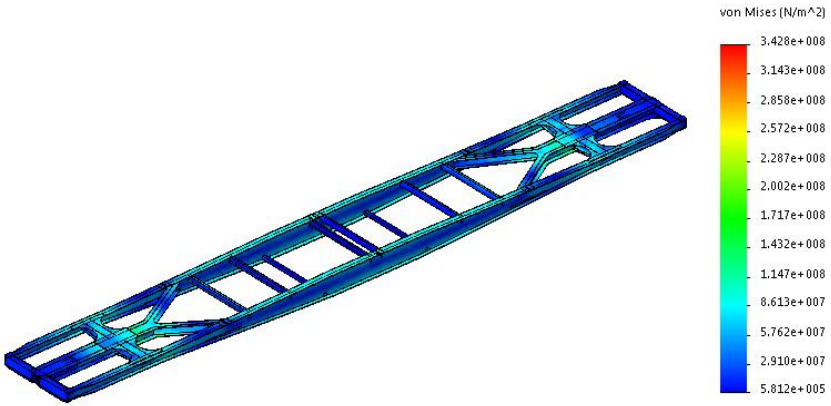

Figure 3.76 – Stress state of the bearing structure of the flat wagon at design mode I (impact)

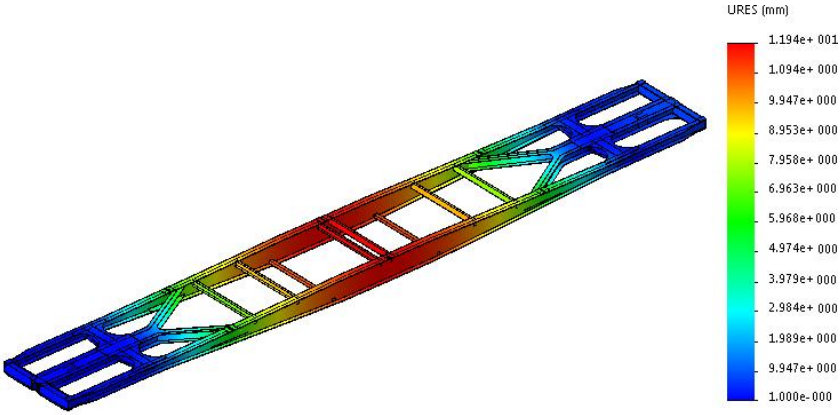

Figure 3.77 – Displacements in the bearing structure of the flat wagon at design mode I (impact)

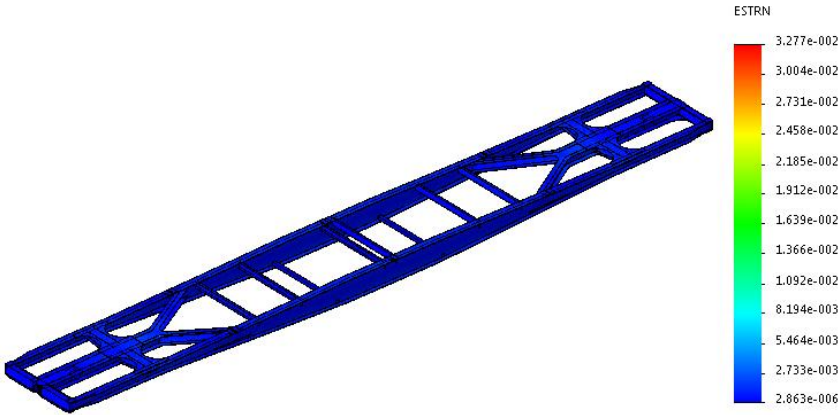

Figure 3.78 – Deformations of the bearing structure of the flat wagon at design mode I (impact)

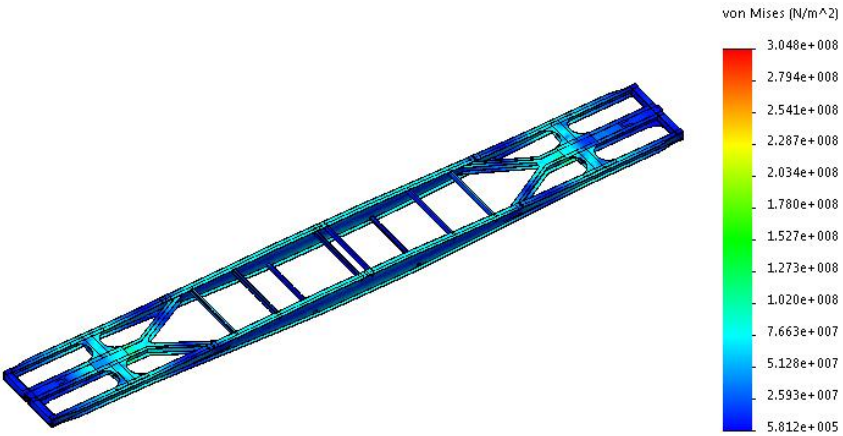

Figure 3.79 – Stress state of the bearing structure of the flat wagon at design mode I (jerk)

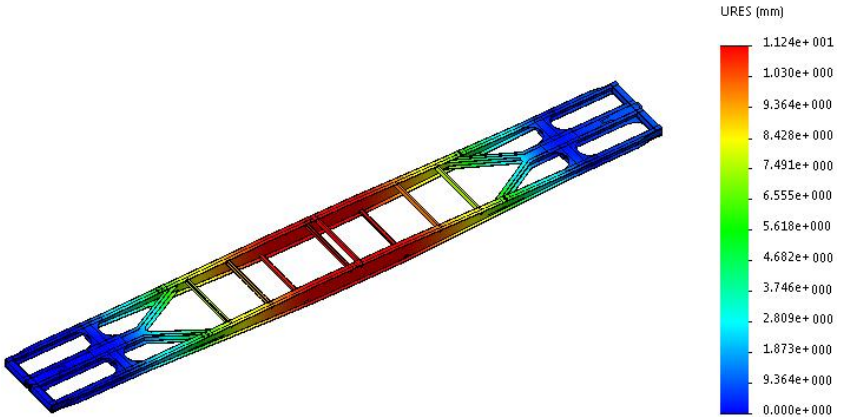

Figure 3.80 – Displacements in the bearing structure of the flat wagon at design module I (jerk)

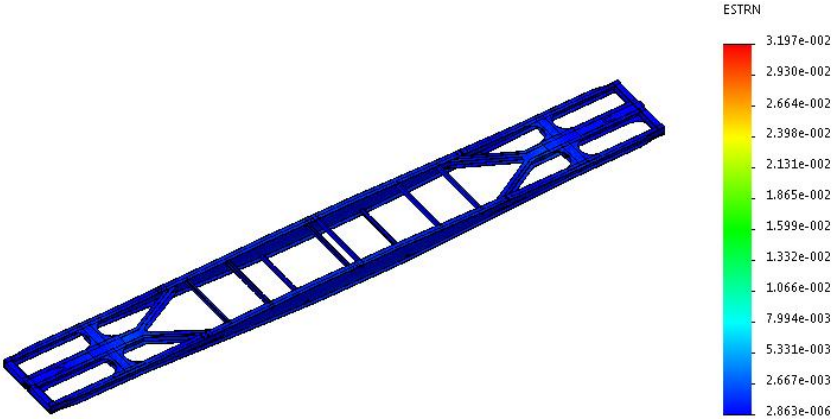

Figure 3.81 – Deformations of the bearing structure of the flat wagon at design mode I (jerk)

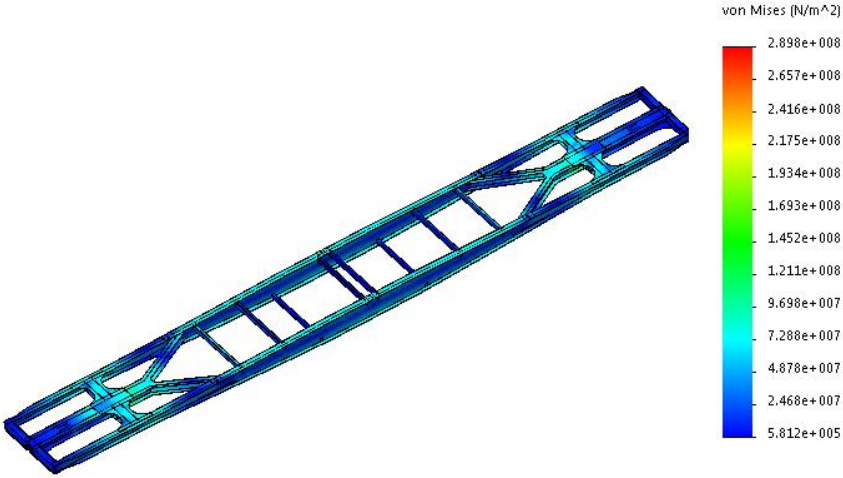

Figure 3.82 – Stress state of the bearing structure of the flat wagon at design mode I (compression)

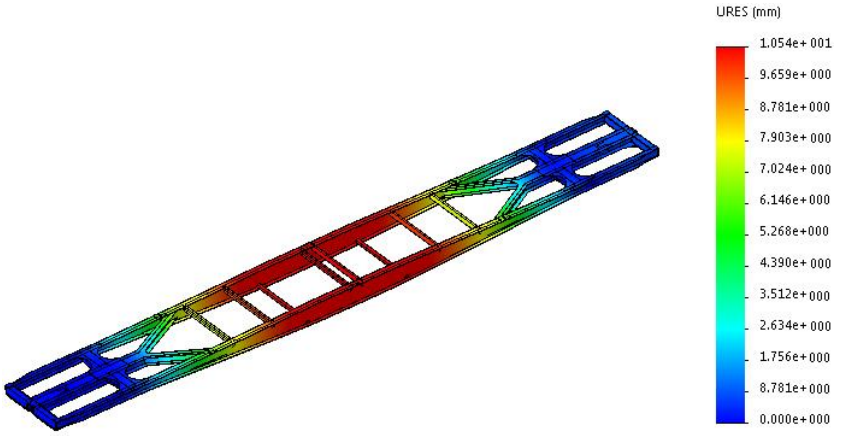

Figure 3.83 – Displacements in the bearing structure units of the flat wagon at design mode I (compression)

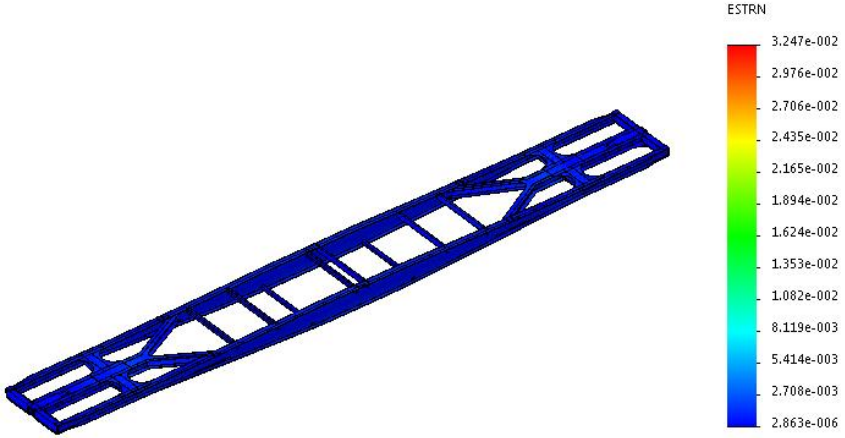

Figure 3.84 – Deformations of the bearing structure of the flat wagon at design mode I (compression)

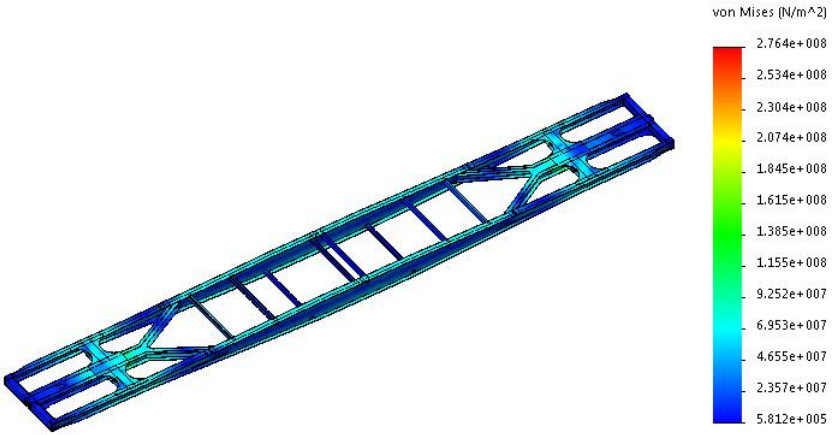

Figure 3.85 – Stress state of the bearing structure of the flat wagon at design mode I (tension)

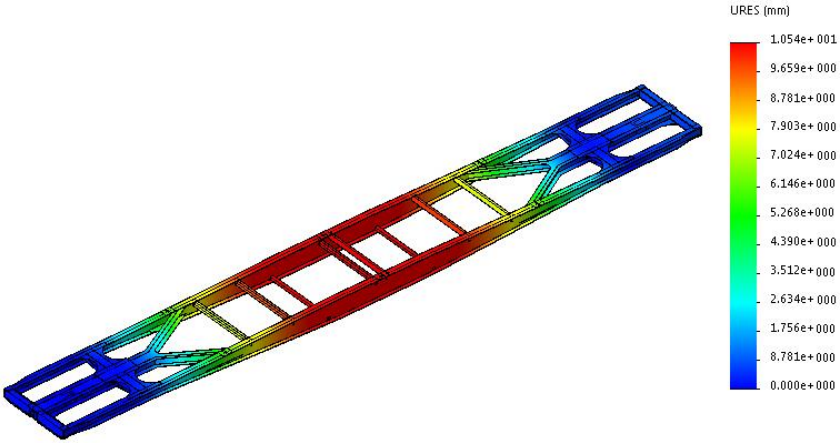

Figure 3.86 – Displacements in the bearing structure units of the flat wagon at design mode I (tension)

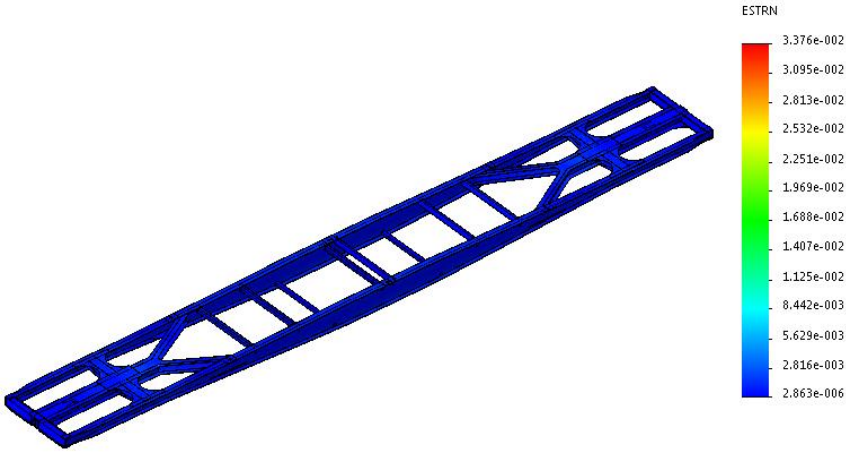

Figure 3.87 – Deformations of the bearing structure of the flat wagon at design mode I (tension)

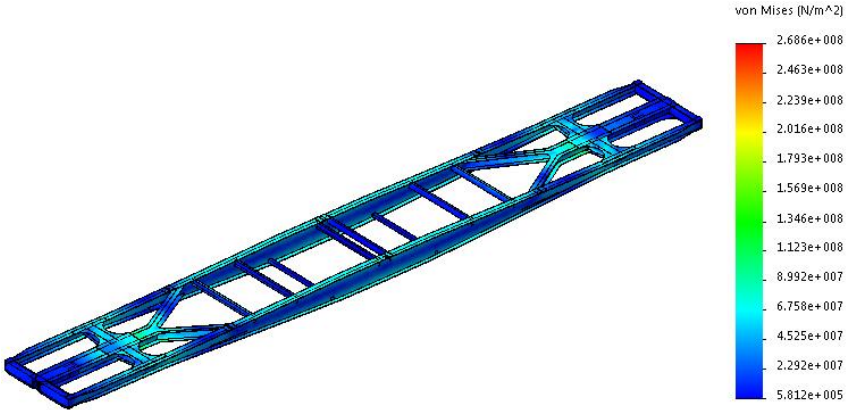

Figure 3.88 – Stress state of the bearing structure of the flat wagon at design mode III (impact, compression)

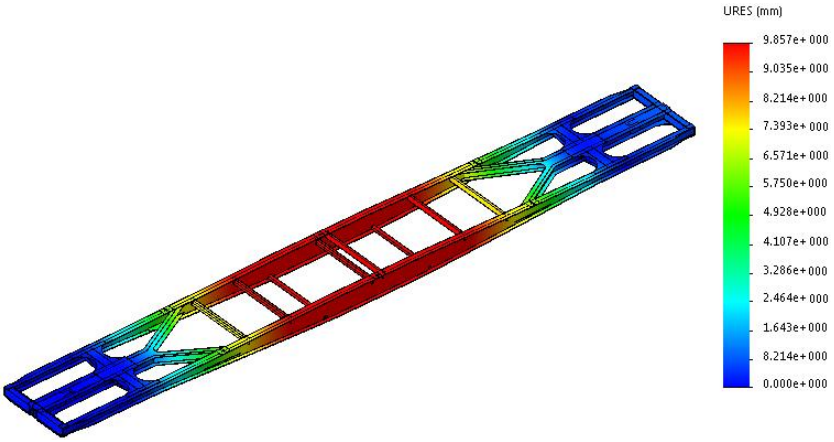

Figure 3.89 – Displacements in the bearing structure units of the flat wagon at design mode III (impact, compression)

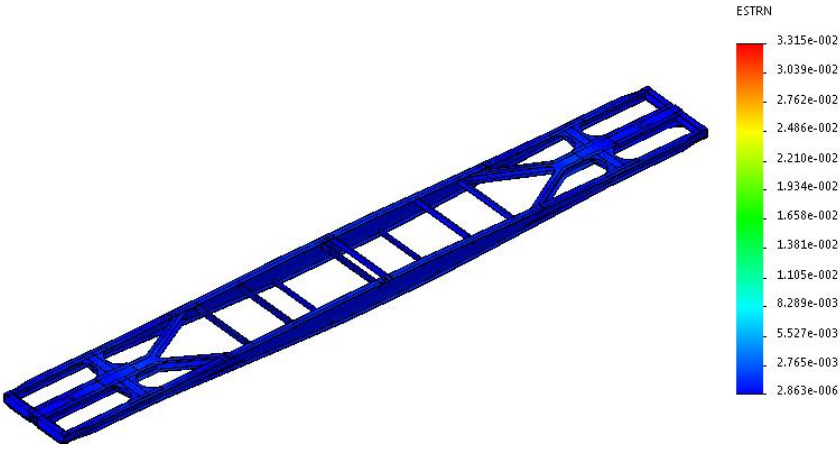

Figure 3.90 – Deformations of the bearing structure of the flat wagon at design mode III (impact, compression)

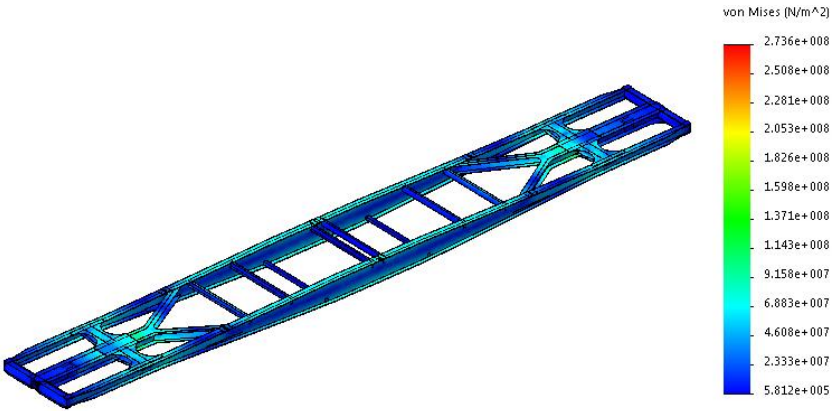

Figure 3.91 – Stress state of the bearing structure of the flat wagon at design mode III (tensile, jerk)

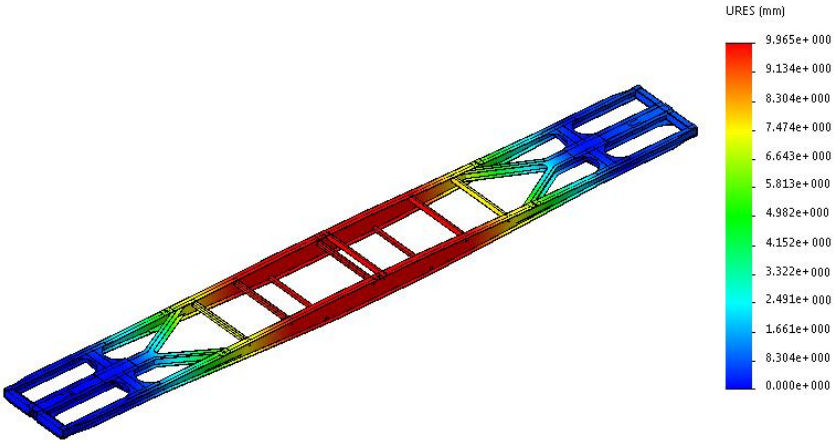

Figure 3.92 – Displacements in the bearing structure units of the flat wagon at design mode III (tension, jerk)

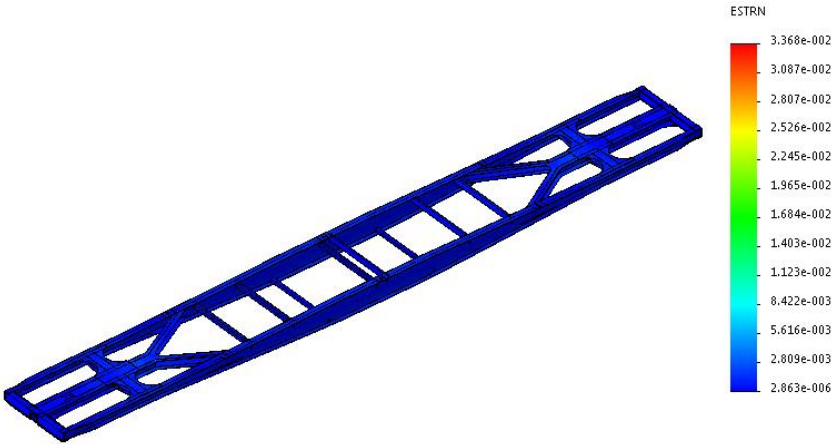

Figure 3.93 – Deformations of the bearing structure of the flat wagon at design mode III (tensile, jerk)

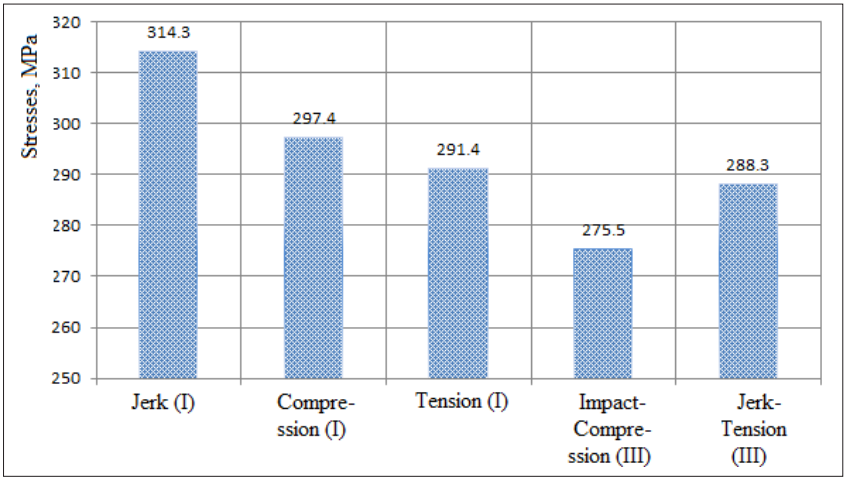

Figure 3.94 – Stresses arising in the bearing structure of the flat wagon under operating loads

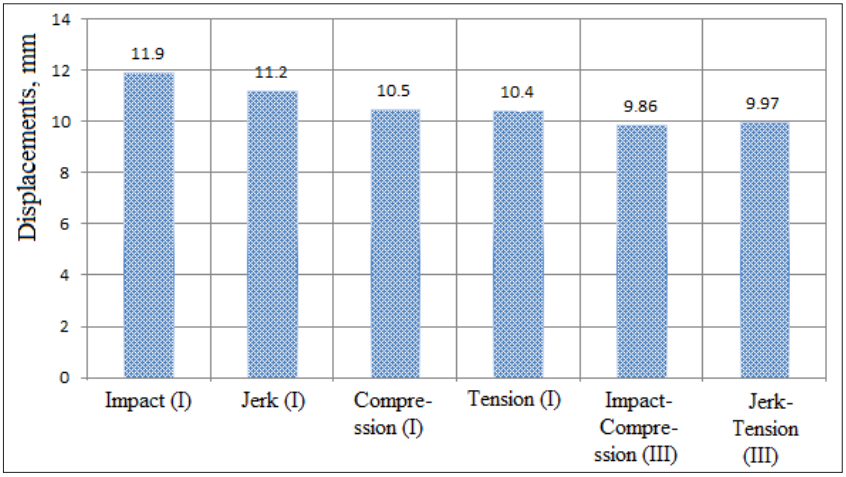

Figure 3.95 – Displacements in the bearing structure of the flat wagon under operating loads

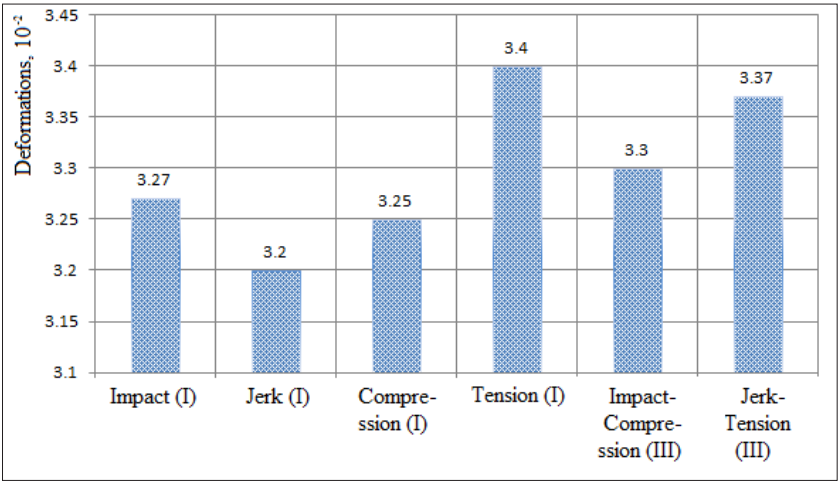

Figure 3.96 – Deformations of the bearing structure of the flat wagon under operating loads

These histograms show that the highest stress occurs at design mode I (impact) and is concentrated in the area of interaction between the bolster beam and the centre sill; it amounts to about 340 MPa, which is 1.5 % lower than the yield stress of the structural material [21, 22].

The maximum displacements in the structure occur in the middle part of the main longitudinal beams of the frame and are about 12 mm, the deformations in the structure are $3.27 \cdot 10^{-2}$.

To improve the operating efficiency of the flat wagon mod. 13-7024, it is proposed to create an articulated flat wagon on its basis by removing the centre plate arrangement on the side of support on the middle bogie and installing elastic side bearings on the cantilever parts of the bearing structures of the two flat wagons forming the platforms (Figure 3.97).

The peculiarity of the proposed articulated wagon design is that the original version can be regained, since the bolster beam, unlike that in typical articulated flat wagons, is not removed in the area where the platforms rest on the middle bogie.

The strength of the improved bearing structure of the flat wagon was studied using the finite element method.

The FEM of the flat wagon is shown in Figure 3.98. The number of mesh elements is 245,607, the number of nodes is 84,599. The maximum element size is 80 mm, the minimum element size is 16 mm, the maximum aspect ratio is 2,613.8, the percentage of elements with an aspect ratio of less than 3 is 11.5, and more than 10 is 14.8. The minimum number of elements in the circle is 11, and the ratio of element size increase is 1.9.

The design diagram of the improved bearing structure of the flat wagon is shown in Figure 3.99. The forces in the model are indicated the same way as those mentioned above for the calculation of a typical flat wagon structure.

The results of the strength calculation for design mode I (jerk) are shown in Figures 3.100–3.102.

The results of the strength calculation for design mode I (tension) are shown in Figures 3.103–3.105.

The results of the strength calculation for design mode I (compression) are shown in Figures 3.106–3.108.

a)

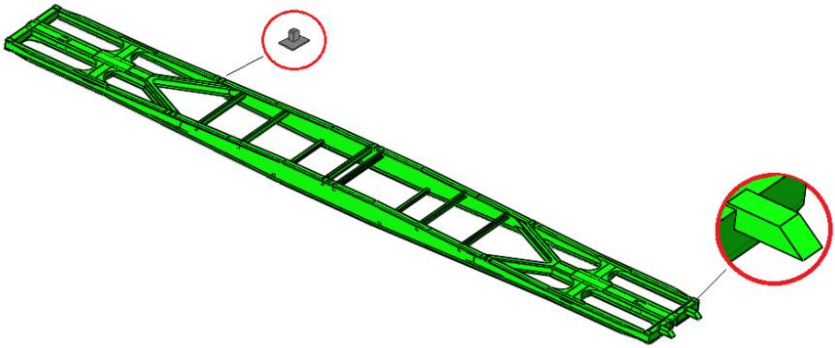

b)

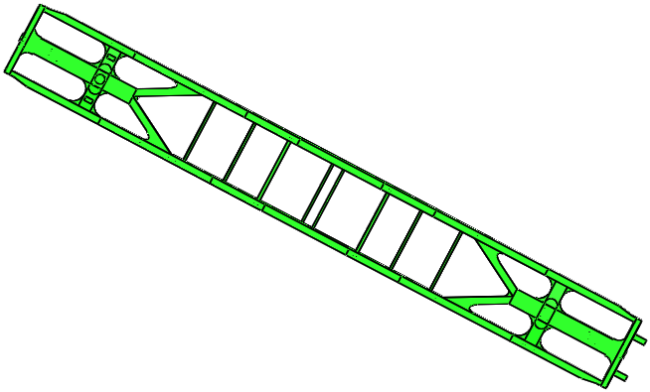

Figure 3.97 – Platform of an articulated flat wagon based on the existing structure
a) side view; b) bottom view

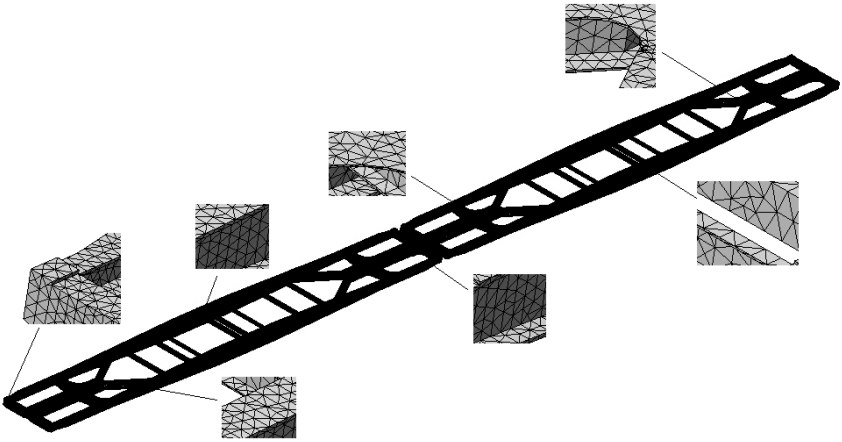

Figure 3.98 – FEM of the bearing structure of the articulated flat wagon

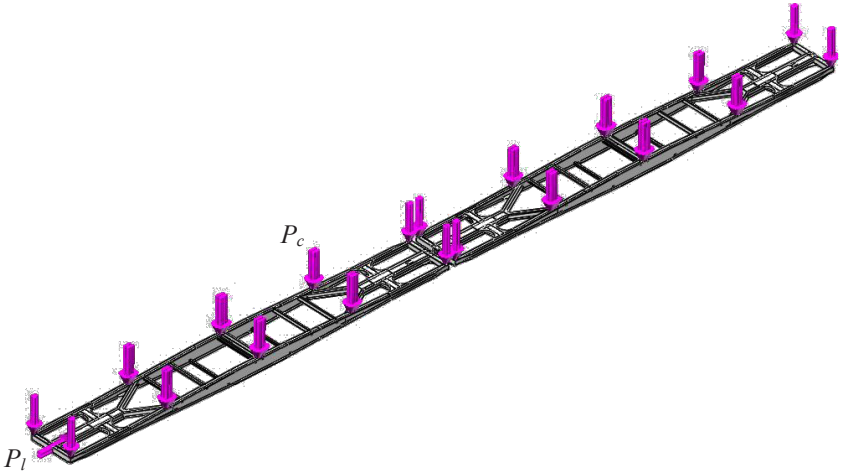

Figure 3.99 – Design diagram of the bearing structure of the articulated flat wagon

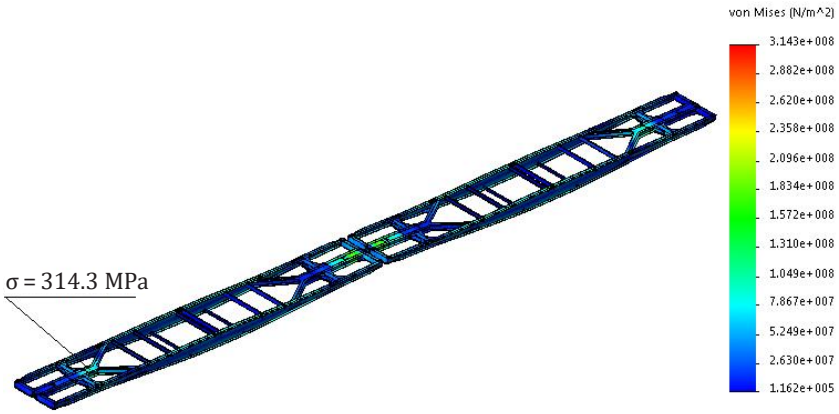

Figure 3.100 – Stress state of the bearing structure of an articulated flat wagon at design mode (jerk)

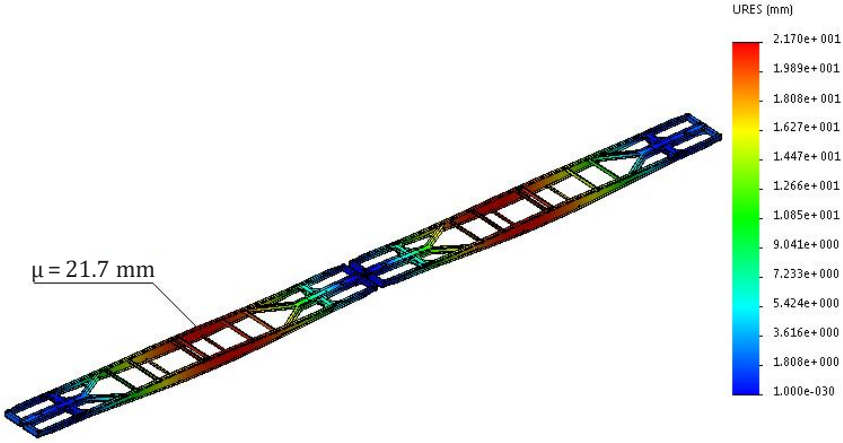

Figure 3.101 – Displacements in the bearing structure units of the articulated flat wagon at design mode I (jerk)

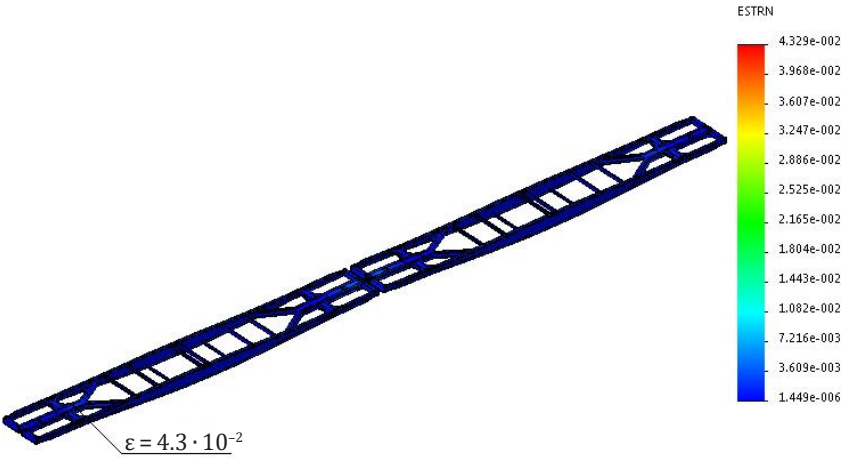

Figure 3.102 – Deformations of the bearing structure of the articulated flat wagon at design mode I (jerk)

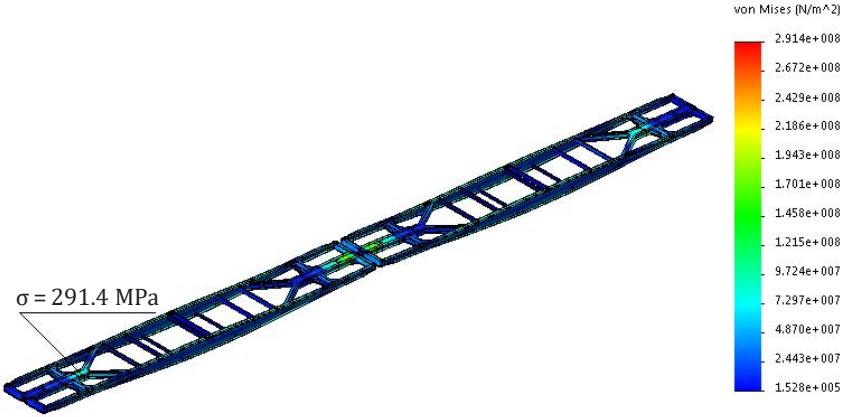

Figure 3.103 – Stress state of the bearing structure of the articulated flat wagon at design mode (tension)

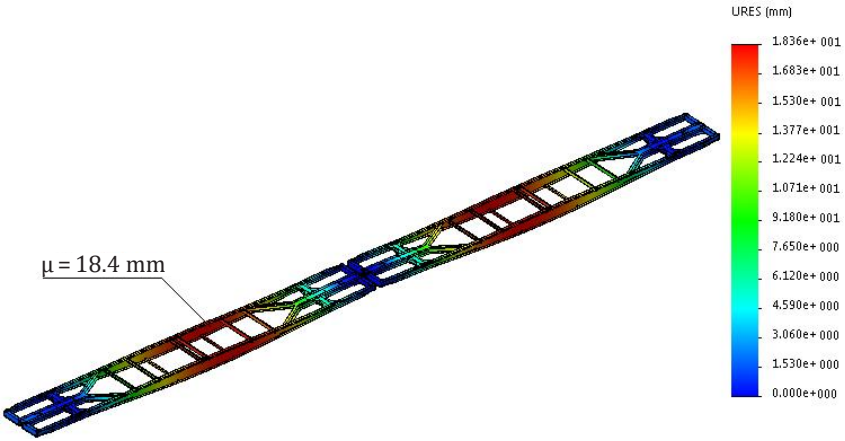

Figure 3.104 – Displacements in the bearing structure units of the articulated flat wagon at design mode I (jerk)

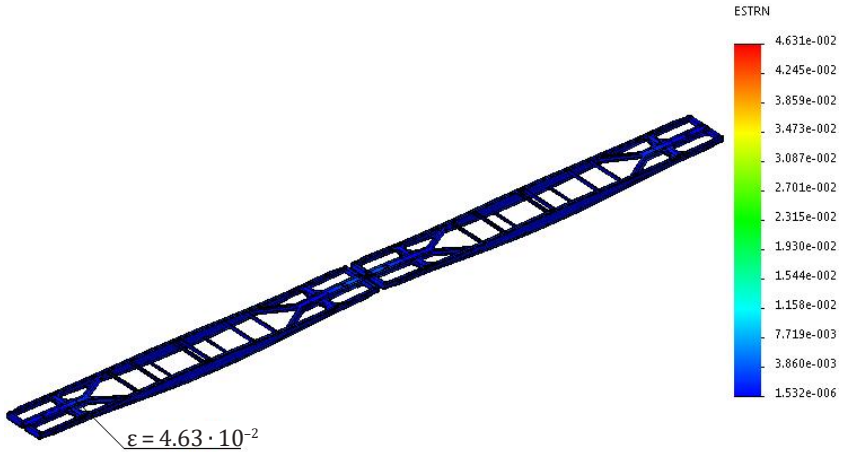

Figure 3.105 – Deformations of the bearing structure of the articulated flat wagon at design mode I (jerk)

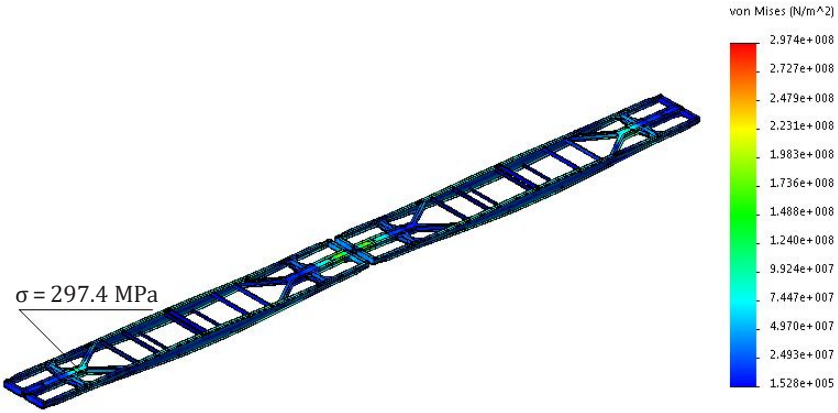

Figure 3.106 – Stress state of the bearing structure of the articulated flat wagon at design mode I (compression)

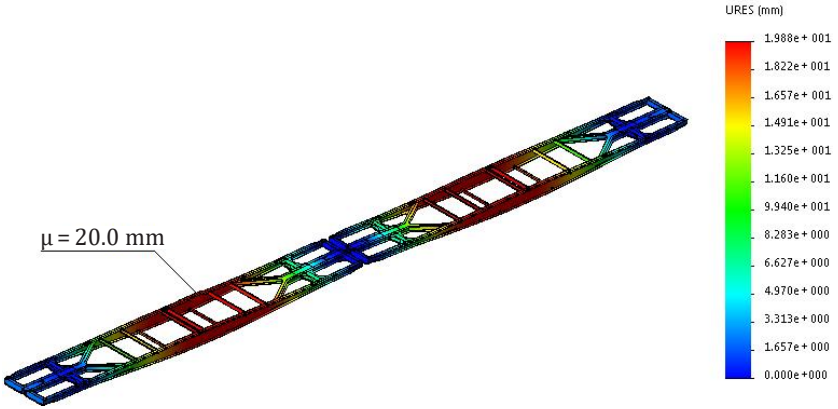

Figure 3.107 – Displacements in the bearing structure units of the articulated flat wagon at design mode I (compression)

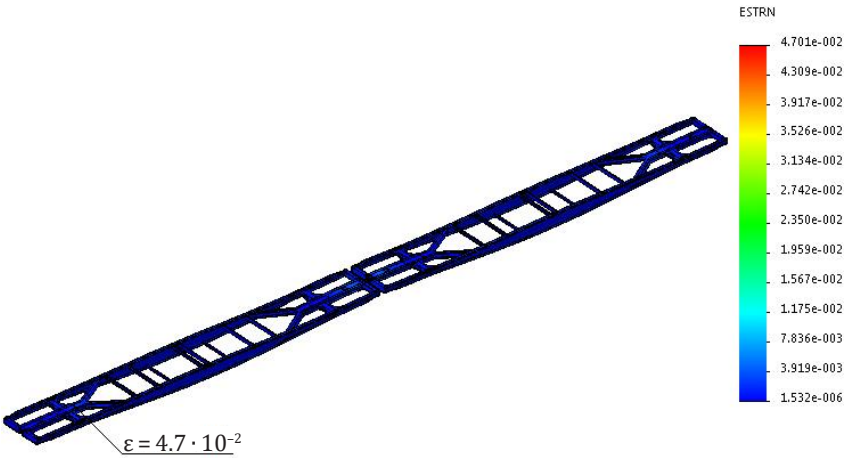

Figure 3.108 – Deformations of the bearing structure of the articulated flat wagon at design mode I (compression)

The results of the strength calculations for design mode III (impact/compression) are shown in Figures 3.109–3.111.

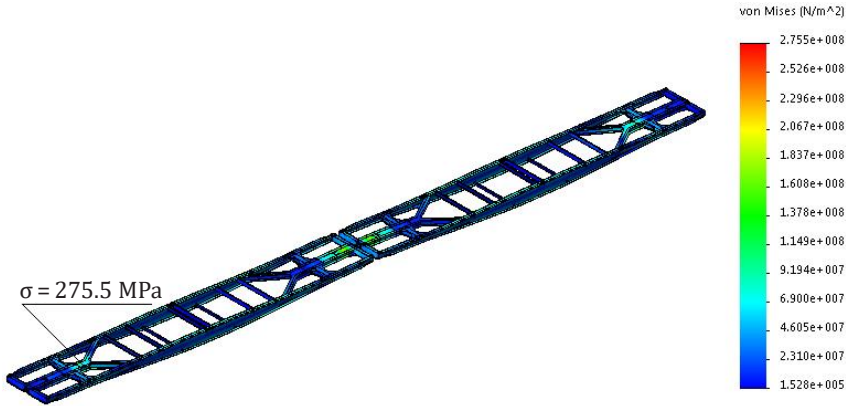

Figure 3.109 – Stress state of the bearing structure of the articulated flat wagon at design mode I (impact/compression)

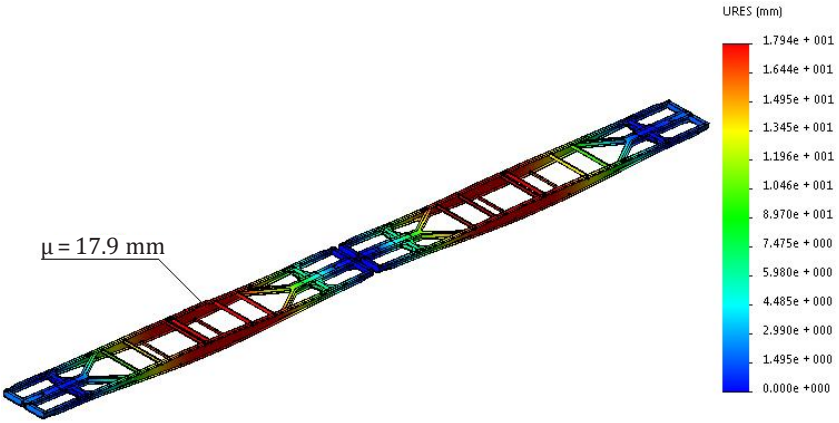

Figure 3.110 – Displacements in the bearing structure units of the articulated flat wagon at design mode I (impact/compression)

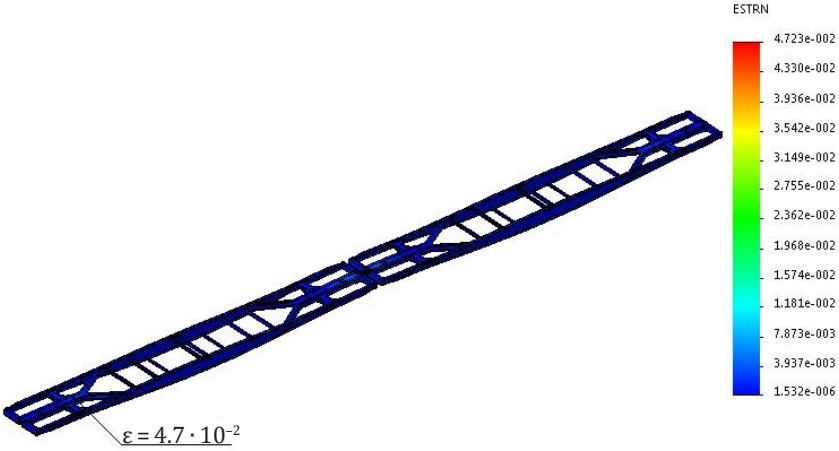

Figure 3.111 – Deformations of the bearing structure of the articulated flat wagon at design mode I (impact/compression)

The results of the strength calculations for design mode III (jerk/tension) are shown in Figure 3.112–3.114.

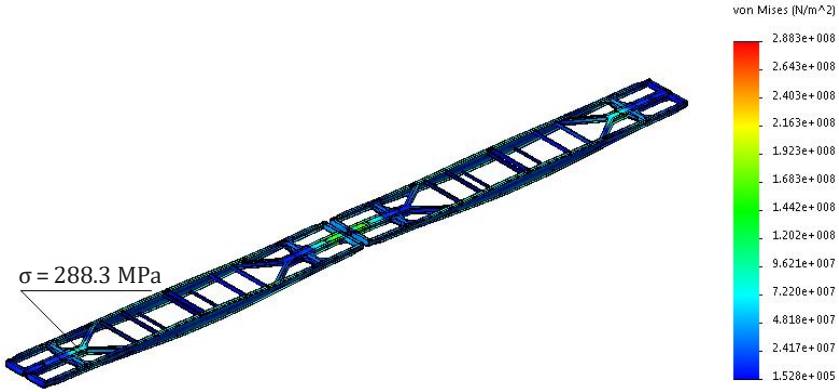

Figure 3.112 – Stress state of the bearing structure of the articulated flat wagon at design mode I (jerk/tension)

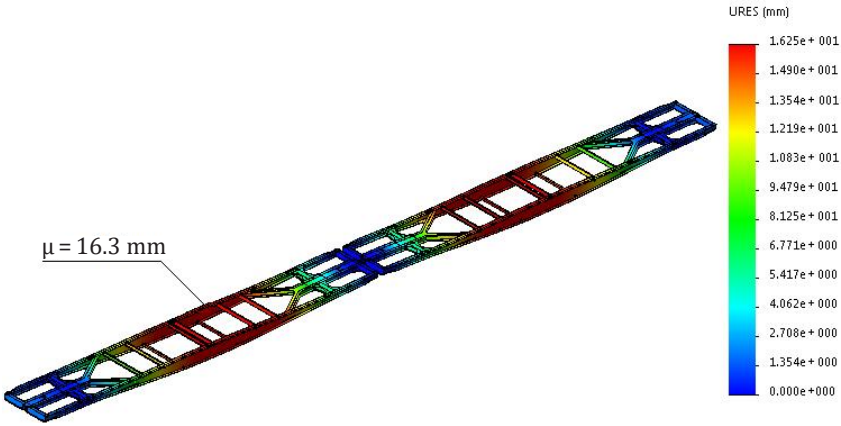

Figure 3.113 – Displacements in the bearing structure units of the articulated flat wagon at design mode I (jerk/compression)

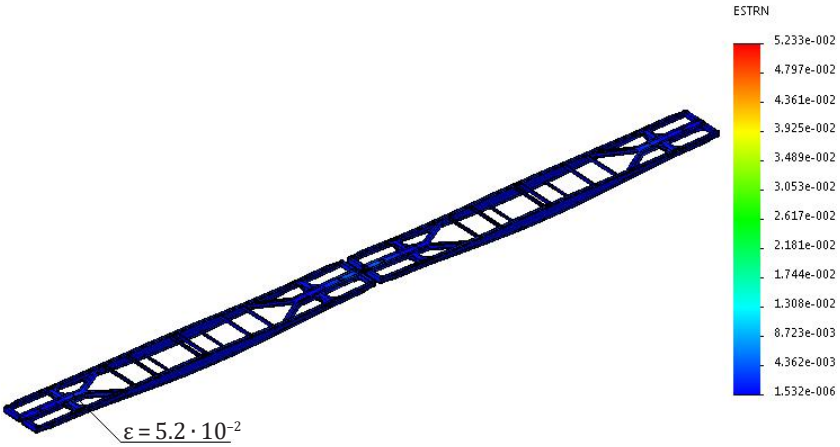

Figure 3.114 – Deformations of the bearing structure of the articulated flat wagon at design mode I (jerk/tension)

The strength indices of the bearing structure of the flat wagon were analysed through histograms (Figures 3.115–3.117).

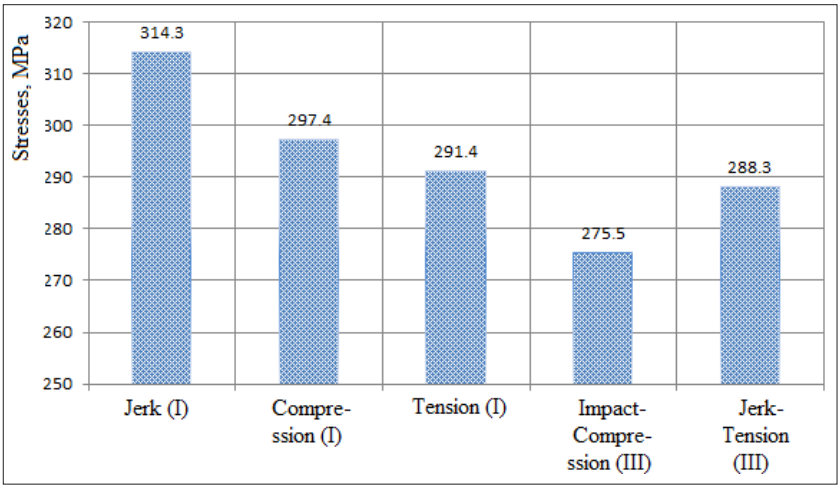

Figure 3.115 – Stresses arising in the bearing structure of the articulated flat wagon under the action of operating loads

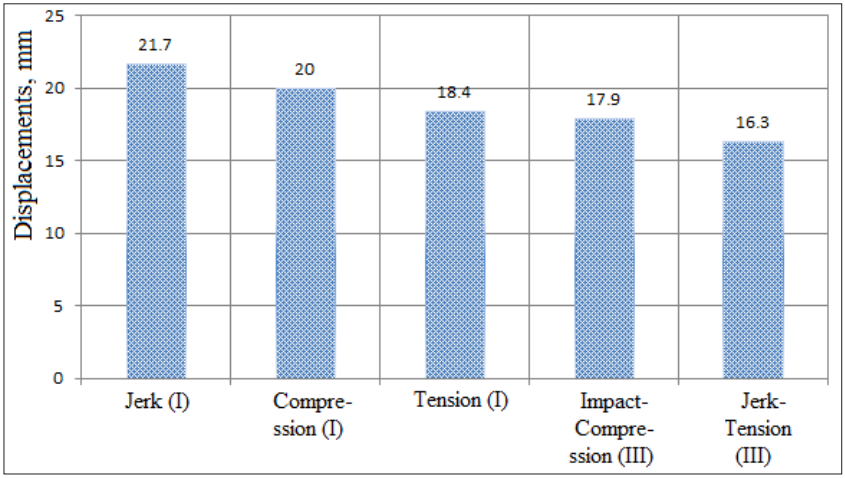

Figure 3.116 – Displacements in the bearing structure units of the articulated flat wagon under the action of operating loads

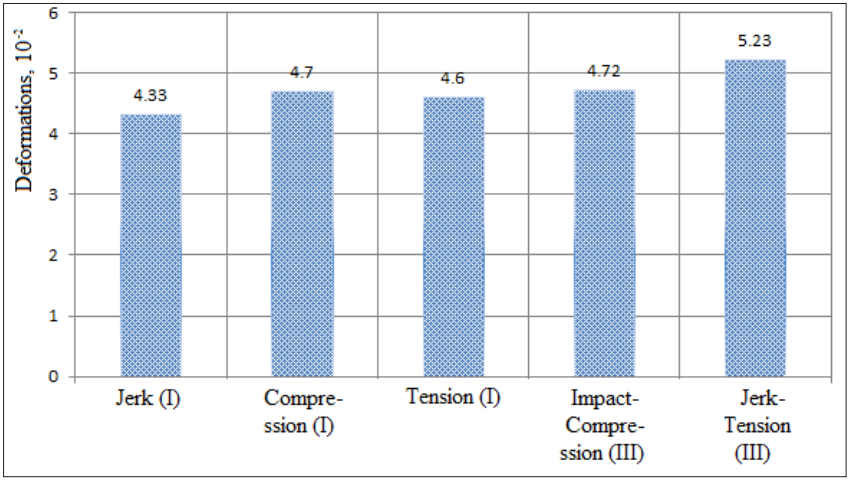

Figure 3.117 – Deformations of the bearing structure of the articulated flat wagon under the action of operating loads

The above histograms show that the highest stress occurs at design mode I (jerk) and is concentrated in the area of interaction between the bolster beam and the centre sill; it amounts to about 315 MPa and does not exceed the permissible values. The maximum displacements in the structure occur in the middle part of the main longitudinal beams of the frame and are 21.7 mm; deformations in the structure are $4.33 \cdot 10^{-2}$.

3.5 Improvements in the bearing structure of an articulated flat wagon by lowering its centre of gravity

The efficiency of rail transportation of freight including military equipment, if it complies with the established dimensions, can be improved by means of using articulated flat wagons with a lower centre of gravity (Figure 3.118) [59]. The bearing structure of such a flat wagon consists of two platforms supported by three bogies mod. 18-100.

The bearing structure is designed on the basis of the flat wagon mod. 13-401. Its bolster beam has the box-section; the centre sill and main longitudinal beams are made of I-beams. In the cantilever parts, the main longitudinal beams are reinforced with vertical sheets. In addition, in the cantilever parts of the platforms are installed braces that partially relieve the centre sill when receiving an impact load.

The bolster beam on the side where the platform rests on the middle bogie is replaced with an I-beam (Figure 3.119). The platforms are interconnected by means of a standard coupling system SAC-1.

The bearing structure of the flat wagon can be used for carrying large containers. For this purpose, the cantilever parts are equipped with folding fitting stops.

For carrying military equipment, the bearing structure of the flat wagon can be equipped with wheel stoppers and other reusable devices.

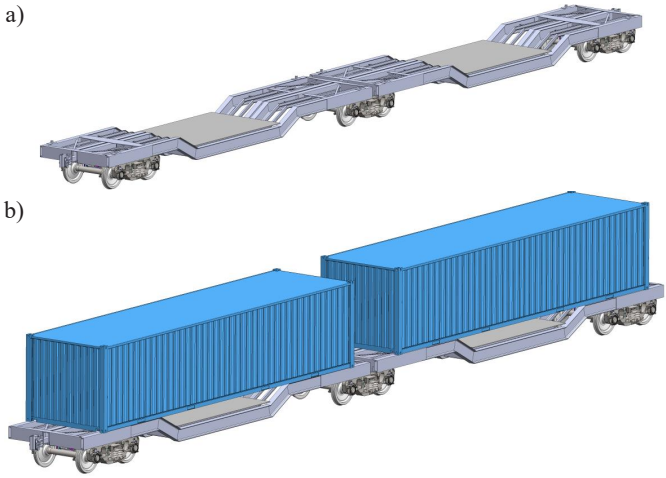

Figure 3.118 – Articulated flat wagon with lower centre of gravity
a) unloaded; b) loaded

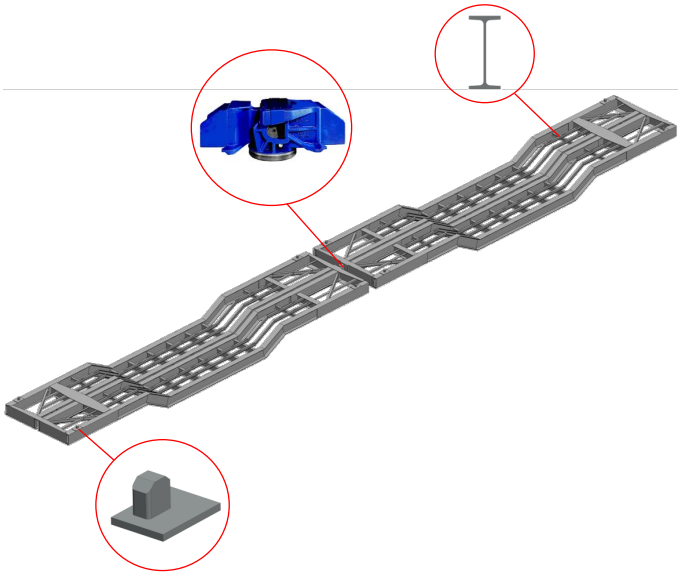

Figure 3.119 – Bearing structure of the articulated flat wagon with a lowered centre of gravity

The middle part of the platform has a sector from which the military equipment can fire while the flat wagon is moving. This flat wagon design is protected by a Ukrainian patent (Appendix A).

The possibility of transporting the flat wagon as part of a combined train by train ferry was checked by means of mathematical modelling [59].

$$\begin{cases} \left(\frac{D}{12\cdot g}(B^2+4z_g{}^2)\right)\ddot{q}_1+\left(\Lambda_\theta\cdot\frac{B}{2}\right)\dot{q}_1=p_b'\cdot\frac{h}{2}+\Lambda_\theta\cdot\frac{B}{2}\cdot\dot{F}(t), \\ I_W^\theta\cdot\ddot{q}_2=p_W'\cdot\frac{h_W}{2}+M_W^D+M_W^C, \\ I_C^\theta\cdot\ddot{q}_3=p_C'\cdot\frac{h_C}{2}+M_C^W, \end{cases} \tag{3.18}$$

where $q_1\approx\theta_F$ is the generalized coordinate, which corresponds to the angular displacement around the longitudinal axis of the train ferry; $q_2\approx\theta_W$ is the generalized coordinate, which corresponds to the angular displacement around the longitudinal axis of the flat wagon; $q_3\approx\theta_C$ is the generalized coordinate, which corresponds to the angular displacement around the longitudinal axis of the container. The origin of the coordinate system is located at the centre of mass of the train ferry.

For train ferry:

D is the weight water displacement; B is the width; h is the side height; Λ_θ is the coefficient of vibration resistance; z_g is the coordinate of the centre of gravity; p_b' is the wind load on the surface projection; $F(t)$ is the law of force that disturbs the movement of a train ferry with wagons on its decks.

For flat wagon with containers:

I_W^θ is the moment of inertia of the flat wagon; h_W is the height of the side of the flat wagon; p_W' is the wind load on the side surface of the flat wagon; M_W^D is the moment of forces that occurs between the flat wagon and the train ferry deck during angular displacements relative to the longitudinal axis; M_W^C is the moment

of forces that occurs between the flat wagon and the containers during angular displacements relative to the longitudinal axis; I_C^{θ} is the moment of inertia of the container; h_C is the height of the side surface of the container; p'_C is the wind load on the container side; M_C^W is the moment of forces that occurs between the container and the flat wagon during angular displacements relative to the longitudinal axis.

The model includes the oscillations of the train ferry relative to the longitudinal axis (roll). It is assumed that the roll is caused by the static effect of the wind on the surface projection of the train ferry [67].

$$\theta = arctg\frac{M_r}{D \cdot h}, \tag{3.19}$$

where D is the water displacement of the vessel; h is the transverse metacentric height; M_r is the roll moment.

The roll moment is determined by:

$$M_r = F\left(z_c + \frac{T}{2}\right), \tag{3.20}$$

where F is the wind pressure on the lateral above-water surface of the vessel; z_C is the distance from the centre of gravity of the above-water projection of the vessel to the actual waterline; T is the vessel draft.

The following formula was used to determine the transverse metacentric height [59, 67]:

$$h = z_m - z_g, \tag{3.21}$$

where z_m is the height of transverse metacentre.

The distance between the centre of gravity of the above-water surface and the actual waterline is calculated as follows:

$$z_c = \frac{S_1 z_1 + S_2 z_2 + ... + S_n z_n}{S_1 + S_2 + ... + S_n}, \tag{3.22}$$

where S_1,S_2,...S_n are the areas of the figures into which the lateral projection of the above-water surface is divided; z_1,z_2,...z_n are the

distances from the centres of gravity of the planes S to the actual waterline.

The wind pressure on the lateral projection of the above-water surface is determined by:

$$F = f \cdot S, \tag{3.23}$$

where f is the wind pressure per unit area of the above-water surface.

For the Black Sea, it can be taken as $f = 150$ kg/m^2 [68].

Taking into account the hydrometeorological characteristics of the Black Sea and the technical characteristics of the train ferry *Geroi Shipki*, the roll angle was 12.2°. The calculations included the deadweight capacity of the train ferry. It was also taken into account that each platform of the flat wagon is suitable for a 1AA container.

The calculation of the accelerations as components of the dynamic load acting on the wagon with containers included different angles of the sea wave in relation to the ship's hull:

$$\chi = \begin{cases} 0°; \\ 30°; \\ 45°; \\ 60°; \\ 120°; \\ 135°; \\ 150°; \\ 180°. \end{cases} \tag{3.24}$$

System of differential equations (3.18) was solved in MathCad. The initial displacements and velocities were assumed to be zero.

The calculation results are shown in Figures 3.120 and 3.121. The acceleration value is given without the horizontal component of the free fall acceleration. The total acceleration acting on the bearing structure of the flat wagon is 3.47 m/s^2, and on the container – 4.67 m/s^2.

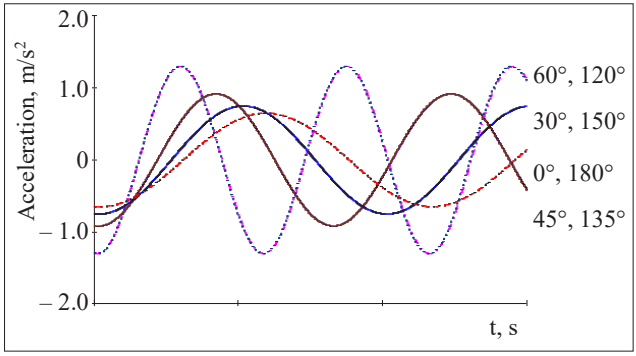

Figure 3.120 – Accelerations acting on the bearing structure of the flat wagon

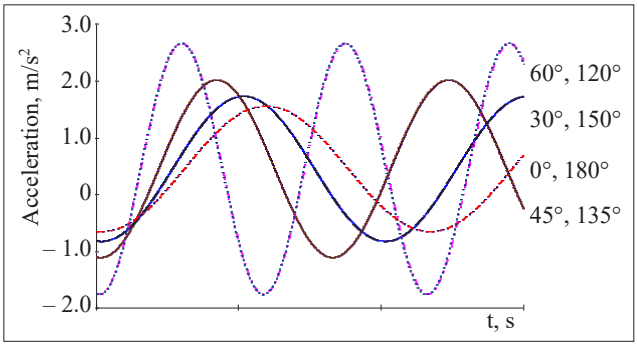

Figure 3.121 – Accelerations acting on the container

The resulting accelerations were taken into account when determining the stability of the container relative to the flat wagon frame.

The stability condition is as follows:

$$k_c = \frac{M_{rest}}{M_{over}} \geq 1, \tag{3.25}$$

where M_{rest} is the restoring moment; M_{over} is the overturning moment.

It is found that the stability of the container is ensured at roll angles of up to 25°.

Computer modelling was carried out to determine the acceleration distribution fields relative to the bearing structure of the flat wagon with containers. The calculation was performed using the finite element method in CosmosWorks.

Isoparametric tetrahedra were used in the FEM. The optimal number of elements was determined by the graphical analytical method. The number of mesh elements is 1,589,028, the number of nodes is 536,801. The maximum element size is 104.4 mm, the minimum – 20.8 mm. The maximum aspect ratio of the elements is 413.49. The percentage of elements with an aspect ratio of less than three is 33.1, and more than 10 is 19.8. The number of elements in a circle is 8. The ratio of element size increase is 1.6.

The design model of the bearing structure of the flat wagon is shown in Figure 3.122. It was taken into account that the vertical load from the gross weight of the containers and the load from the chain binders act on the bearing structure of the flat wagon R_{ch}. Since the chain binders are spatially distributed, the load transmitted through them to the bearing structure of the flat wagon breaks down into components. The container is subject to the vertical static load and the wind load P_w.

The model is fixed in the areas where it rests on the bogies and the working surfaces of the mechanical jacks. The structural material is Steel 09G2S.

The results of the calculations are shown in Figure 3.123.

It is found that the maximum accelerations of the container are concentrated in the upper corner parts behind the central axis of symmetry of the flat wagon and amount to about 4.8 m/s^2. The maximum accelerations of the bearing structure of the flat wagon occur in the cantilever parts of the platforms and are about 3.7 m/s^2.

The discrepancy between the results of mathematical and computer modelling of the dynamic load of the flat wagon with containers carried by a train ferry is shown in Figure 3.124.

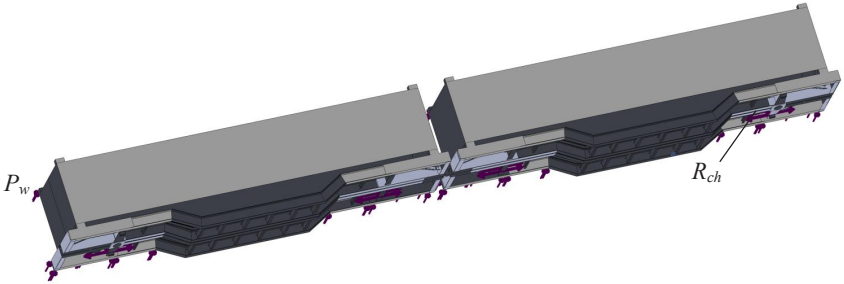

Figure 3.122 – Design model of the bearing structure of the flat wagon with containers

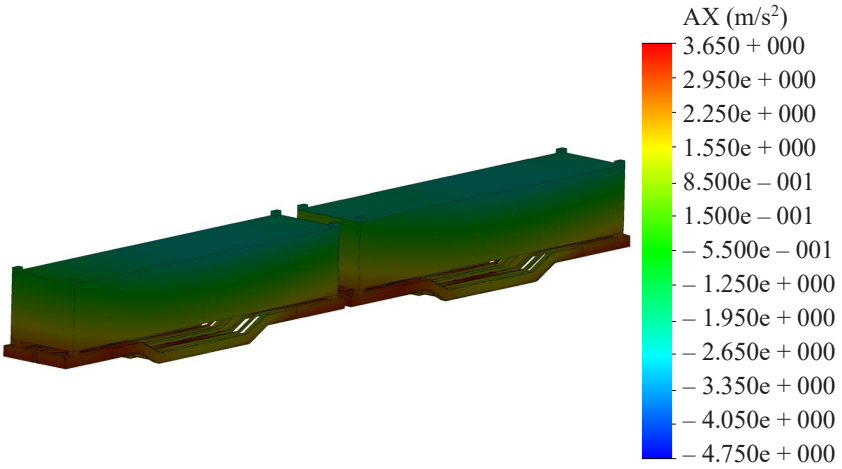

Figure 3.123 – Distribution of acceleration fields relative to the bearing structure of the flat wagon with containers

The calculations show that the maximum percentage of discrepancy between the results of mathematical and computer modelling does not exceed 11 %.

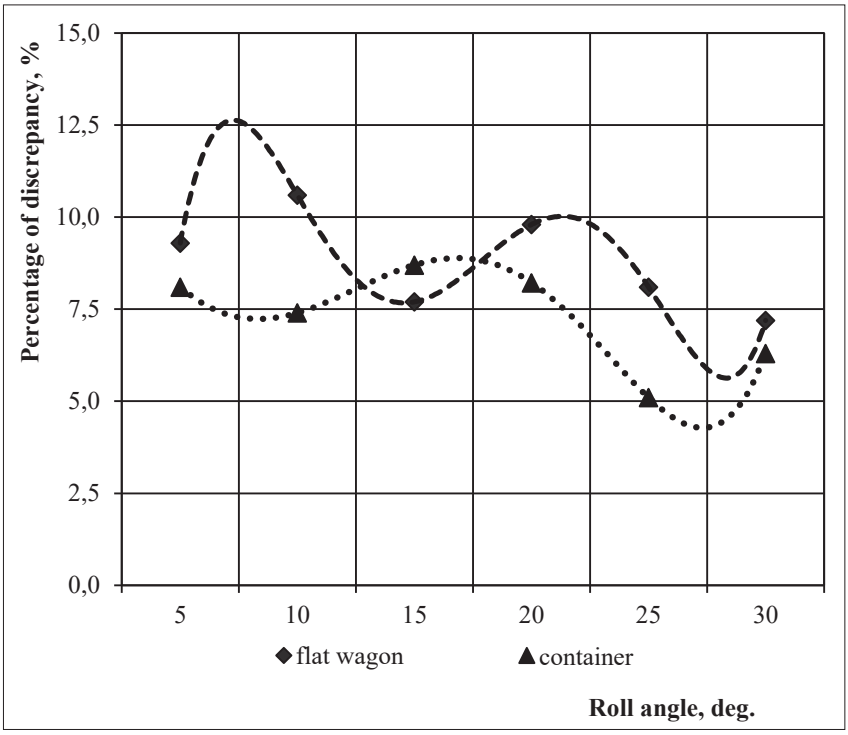

Figure 3.124 – Discrepancy between the results of mathematical and computer modelling of the dynamic load of the flat wagon

3.6 Improvements in the bearing structure of a flat wagon with higher efficiency for carrying various cargoes

It is proposed to improve the existing wagon structure so that to ensure its multiple functions and expand the range of cargoes transported. A special feature of this improvement in the wagons with the bearing structure presented by a frame is the use of an open-type boiler made of heat-resistant material (Figure 3.125) [65]. Such a boiler can be used on the frame of a tank wagon or a flat wagon. It is also possible to retrofit tank wagons by cutting off the upper part of the boiler and covering it with heat-resistant material.

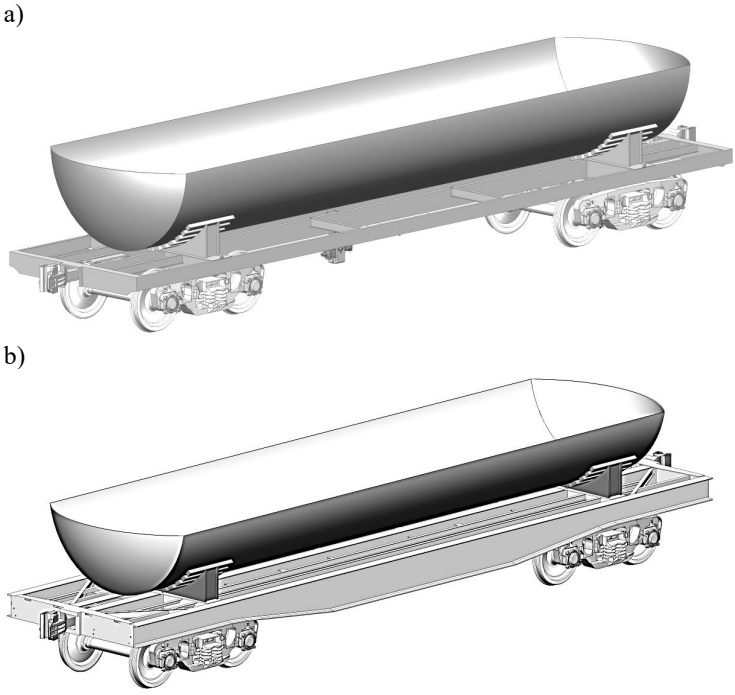

Figure 3.125 – Multipurpose wagon
a) based on a tank wagon; b) based on a flat wagon

It is proposed to use a removable cover (roof) attached to the top of the boiler to prevent from spillage of the liquid transported (Figure 3.126).

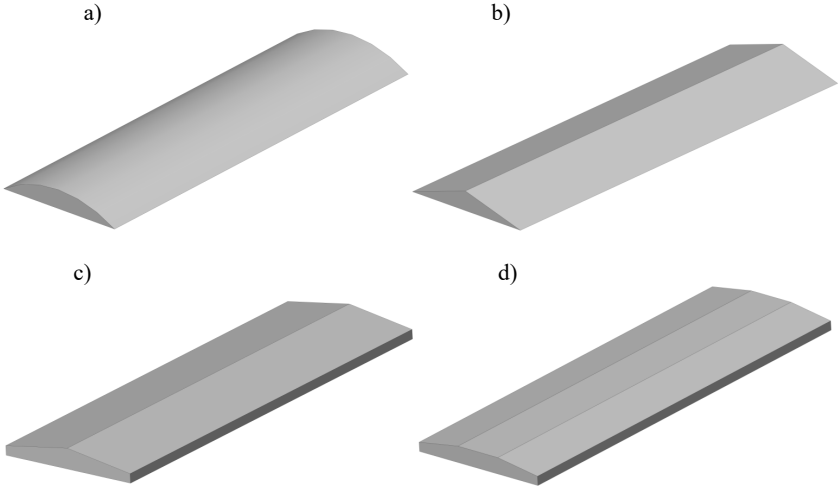

Figure 3.126 – Designs of removable covers
a) design 1; b) design 2; c) design 3; d) design 4

If required, the removable covers can be fitted with devices for maintenance and safety.

The wagon proposed can be used to carry liquid or bulk cargoes.

A spatial model of the multifunctional wagon was built in SolidWorks. The strength of the boiler was determined with the finite element method in SolidWorks Simulation using the criterion of maximum stresses.

It was taken into account that the boiler is made of a composite with linear elastic orthotropic properties. The main strength indices of the material are given in Table 3.6.

The composite can withstand the strength at a temperature of 700 °C. The number of layers assumed was two. The strength of the boiler was calculated for a thin-walled shell.

Table 3.6 – Main strength indices of the material

Parameter	Value
Modulus of elasticity, MPa	$2.42 \cdot 10^5$
Poisson's ratio	0.394
Shear modulus, MPa	318.9
Tensile strength in the longitudinal direction to the fibres, MPa	1,100–1,300
Tensile strength in the transverse direction to the fibres, MPa	650

The strength of the boiler under vertical loading was calculated with the liquid cargo transported (loading diagram I). The design diagram of the boiler is shown in Figure 3.127. It includes the vertical static load P_v^{st} at the payload capacity of the boiler and pressure of the freight P_a acting on the boiler. The calculation was carried out in static, so it did not include the dynamic load.

The pressure of the liquid cargo was calculated using the formula [65]:

$$P_{liq} = \rho \cdot g \cdot h, \tag{3.26}$$

where ρ is the liquid cargo density, kg/m^3; h is the height of cargo distributed in the boiler, m.

The model is fixed in the areas where the boiler rests on the supports. Since the model is rigidly fixed, the potential frictional forces between the wooden bars and the boiler are not taken into account. A linear thermal calculation was performed.

A spatial ten-node isoparametric tetrahedra were used in the finite element model, the number of them was calculated by the graphical analytical method. The method is based on a graphical (geometric) representation of acceptable solutions and the task of objective function. The number of mesh elements is 40,478, and the number of nodes is 20,573. The maximum mesh element size is 80 mm, the minimum – 16 mm.

The results of the calculation are shown in Figure 3.128. The maximum stresses occur in the middle part of the bottom and amount to 307.4 MPa; they do not exceed permissible stresses.

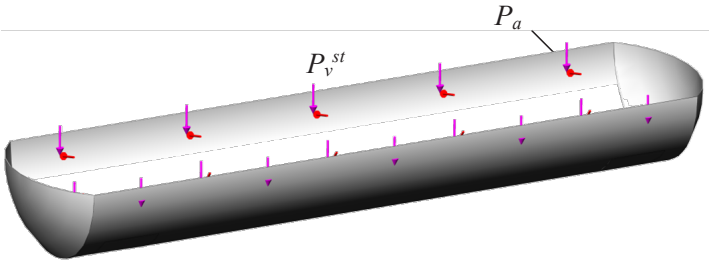

Figure 3.127 – Design diagram of the boiler (loading diagram I)

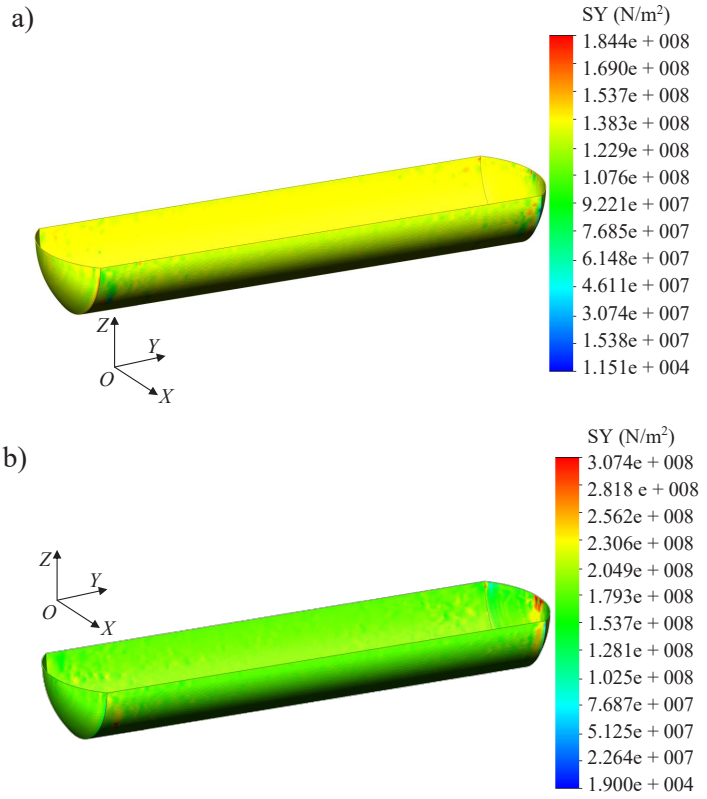

Figure 3.128 – Stress state of the boiler
a) (loading diagram I); b) (loading diagram II)

The maximum stresses are in the areas of interaction between the cylindrical part of the boiler and the bottoms, they amount to 184.4 MPa and do not exceed permissible limits.

The longitudinal load of the boiler (loading diagram II) was determined with the design diagram shown in Figure 3.129. The calculation was carried out in quasi-statics.

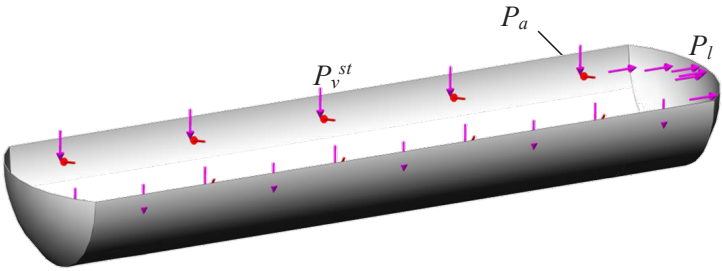

Figure 3.129 – Design diagram of the boiler (loading diagram II)

The maximum pressure from the hydraulic impact was determined by means of the ratio of the inertia force of the freight to the area of the vertical projection of the bottom [65]:

$$P_l = N \cdot \frac{m_w}{m_{gw}} \cdot \frac{1}{F}, \qquad (3.27)$$

where N is the impact force to the coupler, MN; m_w is the weight of freight in the boiler, kg; m_{gw} is the gross weight of the wagon, kg; F is the internal cross-sectional area of the boiler, m^2.

The next stage of the study included the investigation of the possibility of transporting high-temperature bulk freight in the boiler (loading diagram III). The design diagram of the boiler is identical to that shown in Figure 3.129. The pressure of the liquid cargo is replaced with the pressure of the bulk cargo. A temperature load P_T, which is equal to 700 °C, is also applied to the inner surface of the boiler (Fig. 3.130).

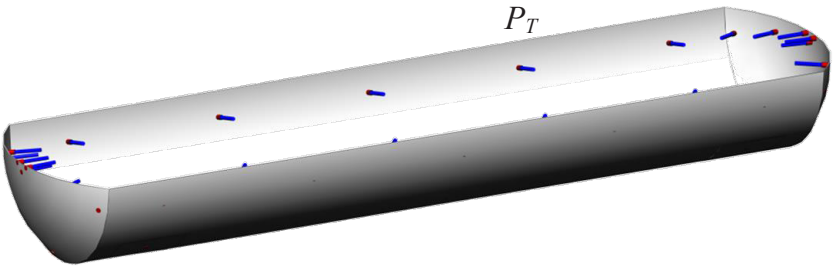

Figure 3.130 – Diagram with the temperature load to the boiler (loading diagram III)

The longitudinal dynamic load on the boiler can be determined with mathematical modelling using the mathematical model developed by Professor G. I. Bogomaz [69]. This model was improved and included in the determination of the load of the proposed wagon. The calculation was made for a shunting impact of the wagon with a load of 3.5 MN on the rear draft lug. It was assumed that the wagon was loaded to its full payload capacity with a conditional freight. The movement of the freight during an impact was not taken into account. The impact was considered as absolutely hard. The model included the frictional forces between the wooden bars and the boiler. The calculations also included that the wagon rested on bogies mod. 18-100 with the appropriate stiffness of the spring groups. The inertial coefficients were determined with the nominal parameters of the bearing structure components of the wagon.

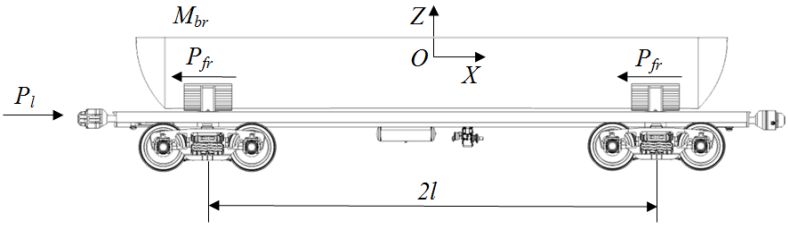

Figure 3.131 – Design diagram for determining the longitudinal load of the wagon

The design diagram for determining the longitudinal load of the wagon is shown in Figure 3.131.

The system of differential equations of motion for the wagon has the following form:

$$\begin{cases} M_{br} \cdot \ddot{x} + \left(M_W \cdot h\right) \cdot \ddot{\varphi} = P_l - 2P_{fr}, \\ I_W \cdot \ddot{\varphi} + \left(M_W \cdot h\right) \cdot \ddot{x} - g \cdot \varphi \cdot \left(M_W \cdot h\right) = l \cdot F_{FR} \left(sign\dot{\Delta}_1 - sign\dot{\Delta}_2\right) + \\ + l\left(k_1 \cdot \Delta_1 - k_2 \cdot \Delta_2\right), \\ M_W \cdot \ddot{z} = k_1 \cdot \Delta_1 + k_2 \cdot \Delta_2 - F_{FR} \left(sign\dot{\Delta}_1 - sign\dot{\Delta}_2\right), \end{cases} \quad (3.28)$$

herewith,

$$\Delta_1 = z - l \cdot \phi, \;\; \Delta_2 = z + l \cdot \phi,$$

where M_{br} is the gross weight of the wagon; M_W is the mass of the bearing structure of the wagon; I_W is the wagon's moment of inertia; P_l is the longitudinal force acting on the rear draft lug; P_{fr} is the frictional forces between the boiler and the wooden bars; l is the wagon base; F_{FR} is the dry frictional forces in spring suspension; k_1, k_2 are the stiffness of the suspension springs of the bogies; x, φ, z are the coordinates corresponding to the longitudinal displacement, the angular displacement around the transverse axis, and the vertical displacements of the wagon, respectively.

The results of the calculation show that the maximum acceleration acting on the boiler is 36.5 m/s^2, has a negative value and occurs at the moment of impact (Figure 3.132).

The resulting acceleration was taken into account in the strength calculations as a component of the dynamic load acting on the boiler during its longitudinal loading.

The calculation results are shown in Figure 3.133. The maximum stresses occur in the areas of interaction between the bottoms and the cylindrical parts of the boiler and amount to 314.5 MPa; they are within the permissible limits.

The dislocation fields of accelerations acting on the boiler and their numerical values were determined according to the design

diagram shown in Figure 3.132. The calculation was carried out using the options of SolidWorks Simulation. The calculation results are shown in Figure 3.134.

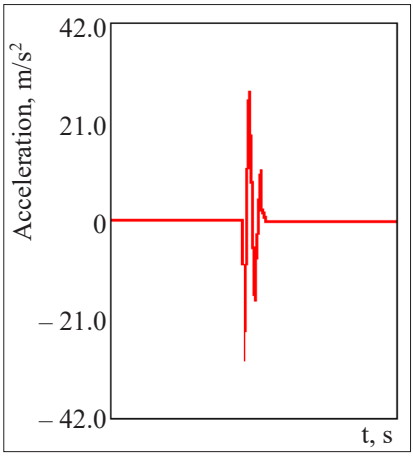

Figure 3.132 – Accelerations acting on the bearing structure of the wagon under longitudinal loads

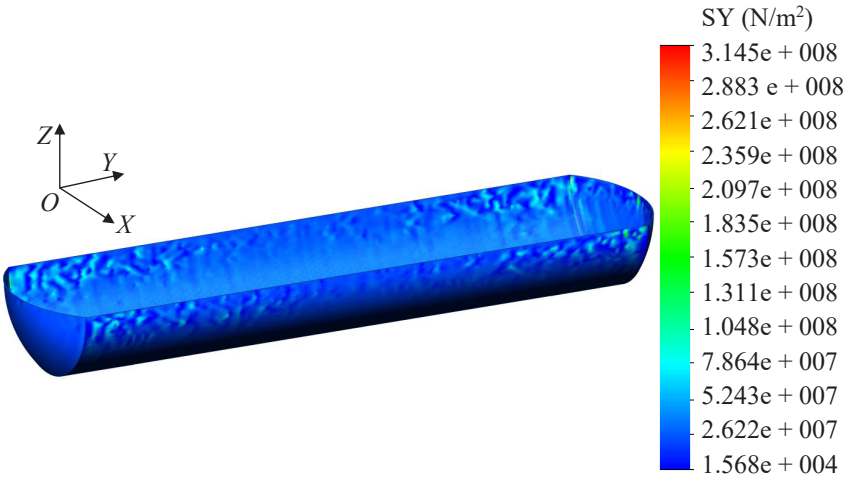

Figure 3.133 – Stress state of the boiler (loading diagram III)

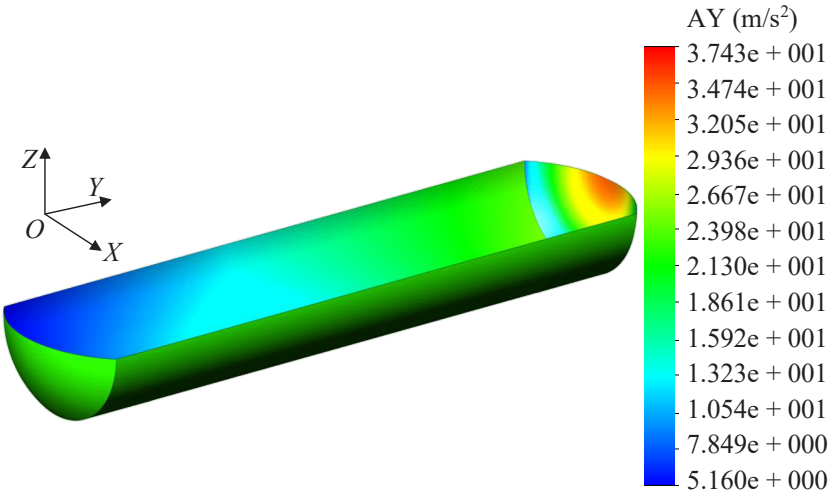

Figure 3.134 – Displacement fields of accelerations relative to the boiler

The maximum acceleration acting on the boiler is concentrated in the bottom and amounts to 37.4 m/s^2. In the cylindrical part of the boiler, the acceleration is in a range of 28.0–12 m/s^2.

The optimal number of experiments for the subsequent verification of the model was determined using Student's criterion:

$$n = \frac{t^2 \cdot \sigma^2}{\delta^2}, \tag{3.29}$$

where t is the tabular value of Student's criterion; σ is the root mean square deviation of a random variable; δ^2 is the absolute error of the measurement result.

The accelerations acting on the boiler at different impact forces to the wagon's coupler were obtained using variational calculations. The results are shown in Figure 3.135.

According to the data shown in Figure 3.135 and formula (3.29), it is established that the number of experiments conducted

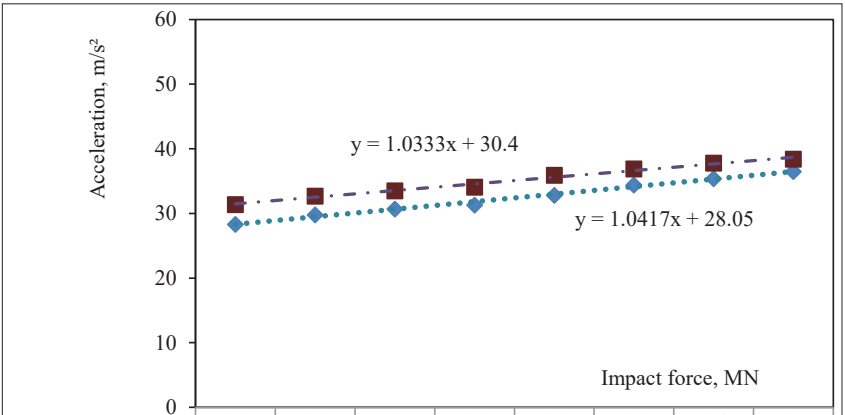

	2,8	2,9	3	3,1	3,2	3,3	3,4	3,5
mathematical model	28,3	29,8	30,7	31,3	32,8	34,4	35,4	36,5
computer model	31,4	32,7	33,5	34,1	35,9	36,9	37,8	38,4

Figure 3.135 – Results of modelling the dynamic load on the boiler

is sufficient to obtain an adequate result. The calculation error is 5.45 %.

The coefficient of variation for the sample obtained by mathematical modelling is 8.8 %, and that by the computer modelling is 7.2 %.

The results of the calculations shown in Figure 12 were used to verify the model of the dynamic load of the boiler according to the F-criterion by comparing the two dispersions [59]. This criterion was chosen as a determining factor because it is one of the most commonly used criteria in engineering calculations. Herewith,

$$F_p = \frac{S_{ad}^2}{S_{sq}^2}, \tag{3.30}$$

where S_{ad} is the dispersion of adequacy; S_{sq} is the error mean square.

The dispersion of adequacy was determined as:

$$S_{ad}^2 = \frac{\sum_{i=1}^{n}\left(y_i - y_i^p\right)}{\left(N-q\right)}, \tag{3.31}$$

where y_i^p is the calculated value obtained by modelling; y_i is the number of degrees of freedom; N is the number of experiments in the planning matrix; q is the number of equation coefficients.

The error mean square was calculated as:

$$S_{sq}^2 = \frac{1}{N}\sum_{i=1}^{n} S_i^2, \tag{3.32}$$

where S_i^2 is the dispersion in each row where parallel experiments were conducted.

It is found that with the variance of adequacy $S_{ad} = 8.23$ and the error mean square $S_{sq} = 6.44$, the actual value of the F-test $F_p = 1.27$, which is less than the tabular value $F_t = 3.58$ at the level of significance $\alpha = 0.05$. Thus, the adequacy hypothesis is not denied.

3.7 Improvements in the bearing structure of a long-wheelbase flat wagon for reducing the vertical loads in operation

One of the most promising types of flat wagons suitable for carrying containers on 1,520-mm gauge lines is the long-base flat wagon mod. 13-7024 [70].

Due to the variable profile height of the longitudinal beams of the frame, the fitting stops are placed on special foundations (Figure 3.136).

The dynamic load on the bearing structure of the flat wagon, and, therefore, the containers placed on it can be reduced by means of improved foundation designs (Figure 3.137). The improvement includes boot 2 with spring 4 in the middle of foundation 1. For bouncing oscillations when the vertical dynamic load P_v exceeds

the spring stiffness *C*, fitting stop plate 3 moves relative to boot 2. This reduces the dynamic load of the container due to frictional forces P_{fr}, which occurs between boot 2 and fitting baseplate 3.

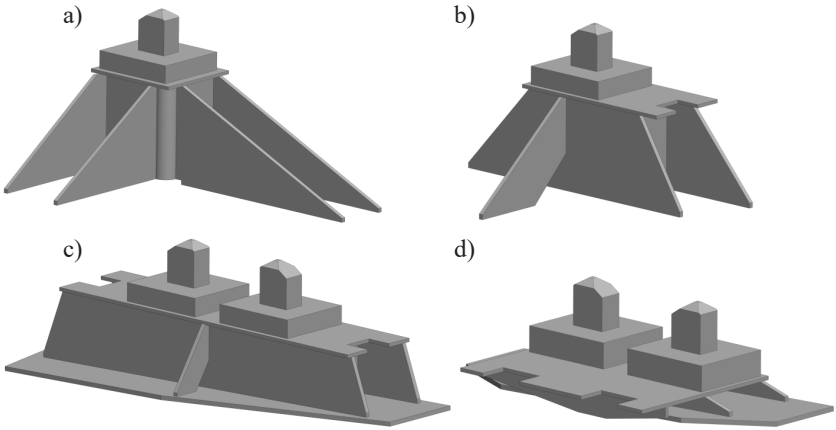

Figure 3.136 – Foundations for fitting stops on flat wagons
a) corner; b) second from the stub sill; c) third from the stub sill; d) central

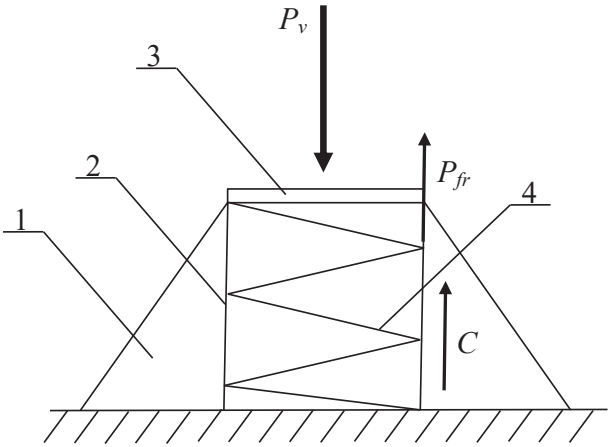

Figure 3.137 – Design diagram of the foundation for a fitting stop

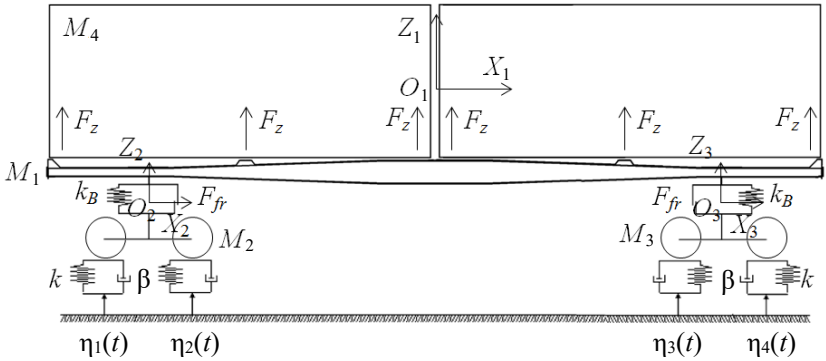

Figure 3.138 – Design diagram of the flat wagon

This flat wagon design is patented in Ukraine [62]; the description is given in Appendix A.

The proposed solution is substantiated using the mathematical model of the dynamic load of the flat wagon loaded with containers. The design diagram of the flat wagon is shown in Figure 3.138.

The system of differential equations of motion has the form:

$$\begin{cases} M_1 \cdot \ddot{q}_1 + C_{1,1} \cdot q_1 + C_{1,2} \cdot q_2 + C_{1,3} \cdot q_3 = \\ = -F_{fr} \cdot \left(sign\left(\dot{\delta}_1\right) + sign\left(\dot{\delta}_2\right)\right) - F_z, \\ M_2 \cdot \ddot{q}_2 + C_{2,1} \cdot q_1 + C_{2,2} \cdot q_2 + B_{2,2} \cdot \dot{q}_2 = \\ = F_{fr} \cdot sign\left(\dot{\delta}_1\right) + k\left(\eta_1 + \eta_2\right) + \beta\left(\dot{\eta}_1 + \dot{\eta}_2\right), \\ M_3 \cdot \ddot{q}_3 + C_{3,1} \cdot q_1 + C_{3,3} \cdot q_3 + B_{3,3} \cdot \dot{q}_3 = \\ = F_{fr} \cdot sign\left(\dot{\delta}_2\right) + k\left(\eta_3 + \eta_4\right) + \beta\left(\dot{\eta}_3 + \dot{\eta}_4\right), \\ M_4 \cdot \ddot{q}_4 = F_z - M_4 \cdot g - F_{fr}^c \cdot \left(sign\left(\dot{q}_1\right) + sign\left(\dot{q}_4\right)\right), \end{cases} \quad (3.33)$$

$$F_z = -k_k' \left(y_1 - y_4 \right), \quad (3.34)$$

where M_1 is the weight of the bearing structure of the flat wagon; M_2, M_3 are the weight of the first and second bogies, respectively; M_4 is the container weight; C_{ij} is the elasticity factors of the

elements of the oscillating system, determined according to the spring stiffness coefficients k_B; B_{ij} is the scattering function; β is the damping coefficient; F_{fr} is the frictional force in the bogie spring group; δ_i is the deformation of the elastic elements of the spring suspension; $\eta_i(t)$ is the track irregularity; F_{fr}^{c} is the frictional force that occurs between the fitting baseplate and the boot.

It is assumed in equations of motion (1)–(4) that

$Z_1 \sim q_1$ is the coordinate characterising the translational displacements of the bearing structure of the flat wagon relative to the vertical axis;

$Z_2 \sim q_2$ is the coordinate characterising the translational displacements of the first bogie relative to the vertical axis;

$Z_3 \sim q_3$ is the coordinate characterising the translational displacements of the second bogie relative to the vertical axis; and

$Z_4 \sim q_4$ is the coordinate characterising the translational displacements of the container relative to the vertical axis.

The input parameters of the model are the technical characteristics of the bearing structure of the flat wagon, spring suspension, containers, and disturbing action (Table 3.7).

Table 3.7 – Input parameters for modelling the dynamic load of the flat wagon

Parameter	Numeric Value
Weight of the bearing structure of the flat wagon, t	10.4
Container weight, t	24
Bogie weight, t	4.3
Stiffness of the spring suspension, kN/m	8.000
Relative friction coefficient	0.1
Track stiffness, kN/m	100.000
Damping coefficient	200
Stiffness of elastic elements in the foundations, kN/m	2.000

Mathematical model (3.34) was reduced to the normal Cauchy form, and then integrated using the Runge-Kutta method. The calculation results are shown in Figures 3.139 and 3.140.

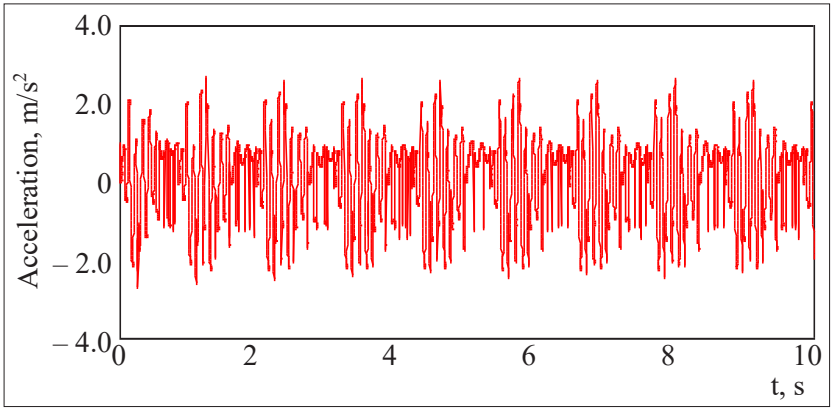

Figure 3.139 – Acceleration of the bearing structure of the flat wagon

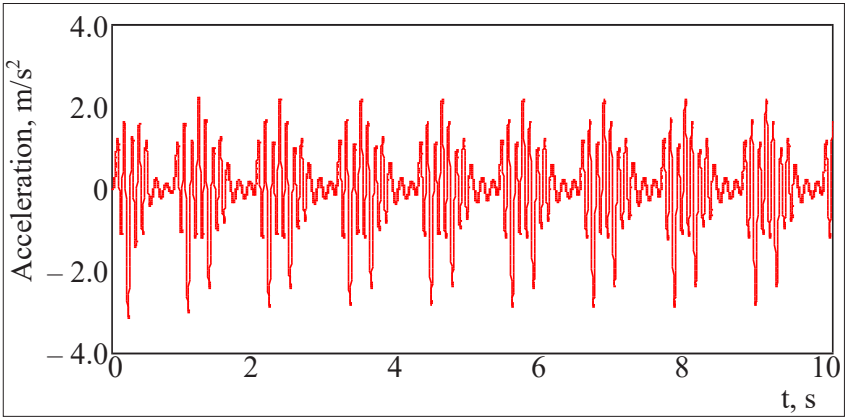

Figure 3.140 – Acceleration of the container on the flat wagon

Thus, the maximum acceleration acting on the flat wagon is 2.67 m/s^2, and on the container – 3.15 m/s^2. The resulting accelerations are 5.3 % and 6.2 % lower than those acting on the flat wagon and the container, respectively (if their typical interaction is taken into account).

The strength of the foundations for a fitting stop was determined with a spatial model. The calculation was based on the example of a corner foundation (Figure 3.141).

The design diagram includes the vertical load P_v with the acceleration obtained by solving mathematical model (3.33). The model also includes the frictional forces P_{fr} between the vertical parts of the boot and the baseplate (Figure 3.142).

Between the horizontal part of the fitting baseplate and the bottom of the boot are elastic connections with a stiffness of 2,000 kN/m. The model is fixed in the areas where it rests

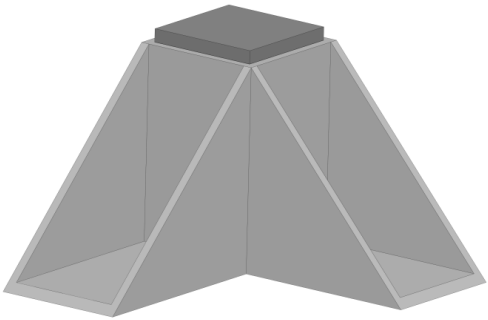

Figure 3.141 – Spatial model of the foundation for a fitting stop

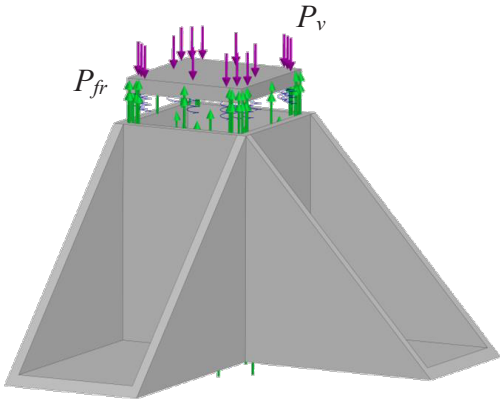

Figure 3.142 – Design diagram of the foundation for a fitting stop

on the flat wagon frame. The structural material is composite with orthotropic properties. The calculation was made for the superstructure with thin-walled shells.

The calculation results are shown in Figure 3.143.

The maximum stresses occur in the inclined parts of the foundation and amount to 113.6 MPa, which is significantly lower than permissible values.

It should be noted that the improved composite superstructure can reduce the tare weight of the flat wagon by 2.5 % compared to that of a typical design. The dynamic loading of the bearing structure of the flat wagon was modelled and the design diagram is shown in Figure 3.144.

The diagram's symbols are identical to those shown in Figure 3.138.

The results of the calculations are shown in Figures 3.145–3.147.

The results of the calculations of the dynamic load of the flat wagon demonstrate that the dynamics indices are within permissible limits. The motion of the flat wagon is 'good'. The maximum acceleration in the centre of mass of the bearing structure of the flat wagon is 5.9 m/s^2.

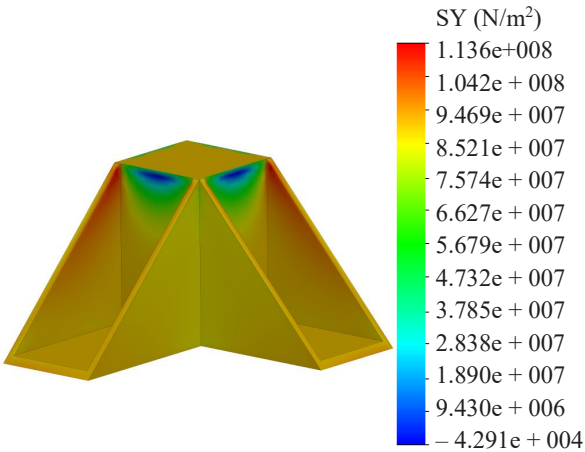

Figure 3.143 – Stress state of the foundation for a fitting stop

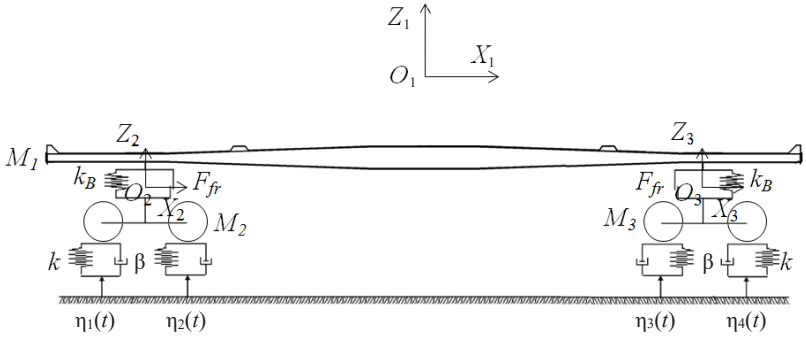

Figure 3.144 – Design diagram of the flat wagon

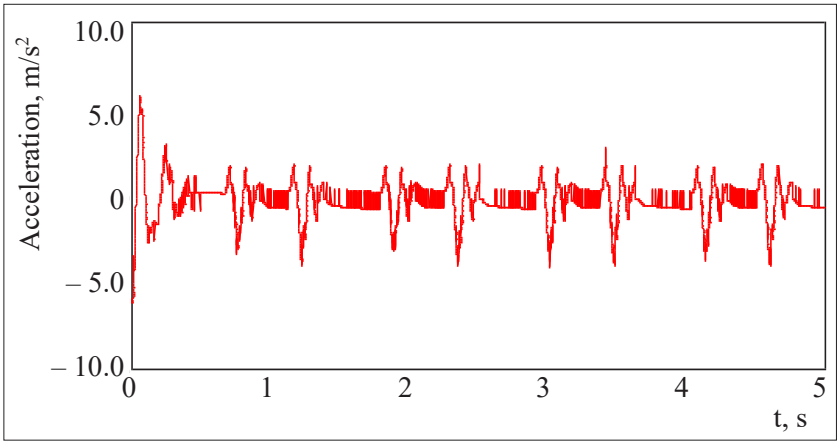

Figure 3.145 – Accelerations in the centre of mass of the bearing structure of the flat wagon

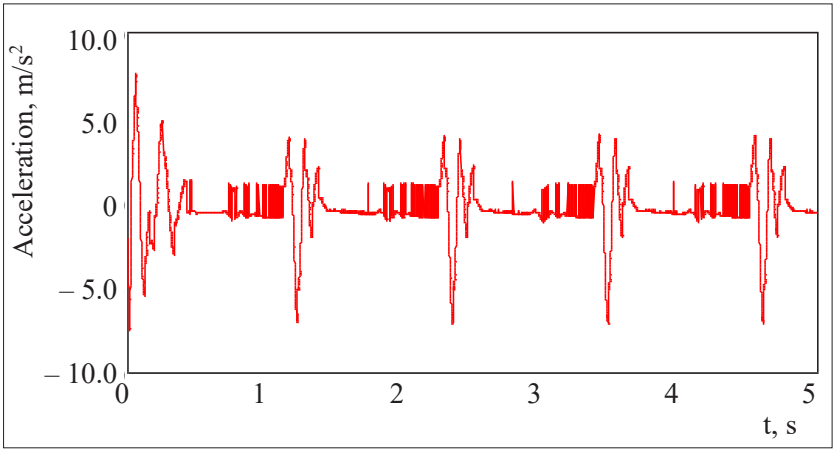

Figure 3.146 – Accelerations in the areas where the bearing structure rests on the bogies

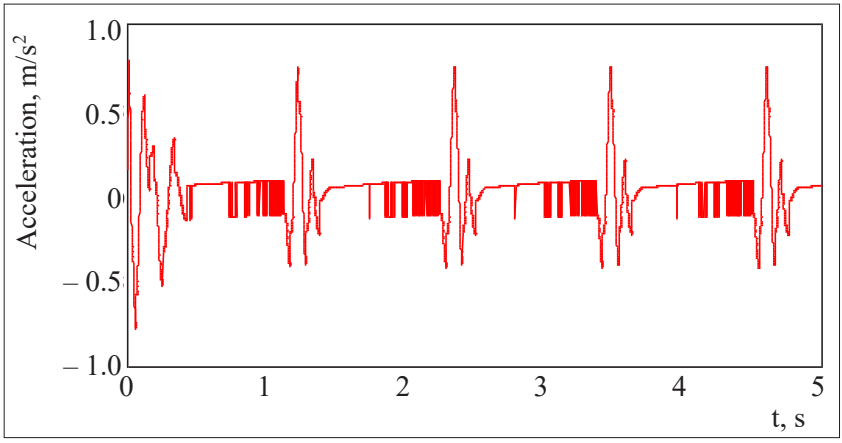

Figure 3.147 – Coefficient of vertical dynamics

The acceleration in the areas where the bearing structure of the flat wagon rests on the bogies is 7.4 m/s^2. The coefficient of vertical dynamics is 0.75.

In addition, the study included the calculation of the fatigue resistance coefficient of the bearing structure of the flat wagon. It was calculated with the safety factor according to the following formula [70]:

$$n = \frac{\sigma_{-1D}}{\sigma_{a,e}} \geq [n], \tag{3.35}$$

where $\sigma_{a,e}$ is the design dynamic stress amplitude of a conditional symmetrical cycle reduced to the base N_0 and equivalent (regarding the damaging effect) to the amplitudes of the real operating mode for random stresses over the design service life, MPa; [n] is the allowable fatigue resistance factor.

The equivalent reduced amplitude of dynamic stresses for calculating the fatigue $\sigma_{a,e}$ in the case of a continuous stress amplitude distribution function is determined as [70]:

$$\sigma_{a,e} = \sqrt[m]{\frac{N_c}{N_0} \sum_{i=1}^{k} P_{vi} f_e \sum_{i=1}^{k} \sigma_{ai}^m P_i}, \tag{3.36}$$

where N_c is the total number of dynamic stress cycles over the design service life; p_{vi} is proportion of time spent on operating the wagon at the speed v_i; σ_{ai} is the stress amplitude level, MPa; m is indicator of the degree of fatigue curve; f_e is effective frequency of dynamic stresses, Hz.

The results of the calculation show that if the probability of stresses has the level σ_i, which is 0.95, then $\sigma_{a,e}$ = 51.3 MPa. Hence, the fatigue resistance factor is 4.6. Due to the lack of experimental data, the permissible value of the fatigue resistance factor is assumed to be 2.2. Therefore, condition (3.35) is fulfilled and the fatigue strength of the bearing structure of the flat wagon is ensured. Importantly that if the proposed diagram of interaction between the container and the flat wagon is taken into account, the fatigue resistance coefficient of the bearing structure of the flat wagon can be increased by 8 % compared to that of a typical diagram.

3.8 Improvements in the bearing structure of a flat wagon with sandwich panels

The impact of dynamic loads on the bearing structure of the flat wagon can be reduced and the safety of the freight transported can be increased by using sandwich panels for the flooring [71]. The peculiarity of a sandwich panel is that it consists of two metal sheets with an energy-absorbing viscous material in-between (Figure 3.148). The sandwich panel, while acting as an intermediate adapter between the wagon frame and the freight, can absorb the dynamic loads arising from bounce oscillations and reduce their impact on the freight.

The solution was substantiated by means of a mathematical model of the dynamic load of an open wagon in the vertical plane. The model includes bouncing oscillations as one of the most common types in operation.

The design diagram of the flat wagon is shown in Figure 3.149. The flat wagon mod. 13-401 was chosen as a prototype. The flat wagon was considered as a four-body system: a frame, two bogies (mod. 18-100) and freight placed on the frame. The freight was considered as conditional and the full payload capacity of the flat wagon was taken into account.

It was assumed that the wagon moved along a jointed rail track with elastic characteristics [31, 71].

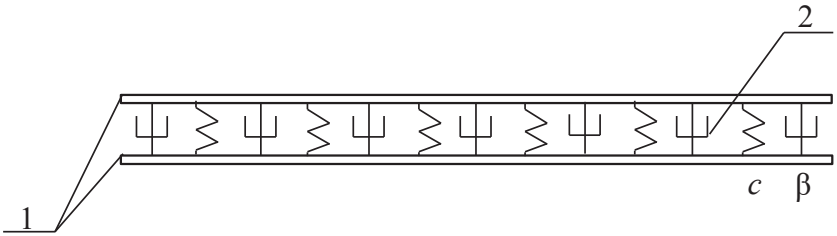

Figure 3.148 – Structural diagram of a sandwich panel
1 – metal sheets; 2 – energy-absorbing material

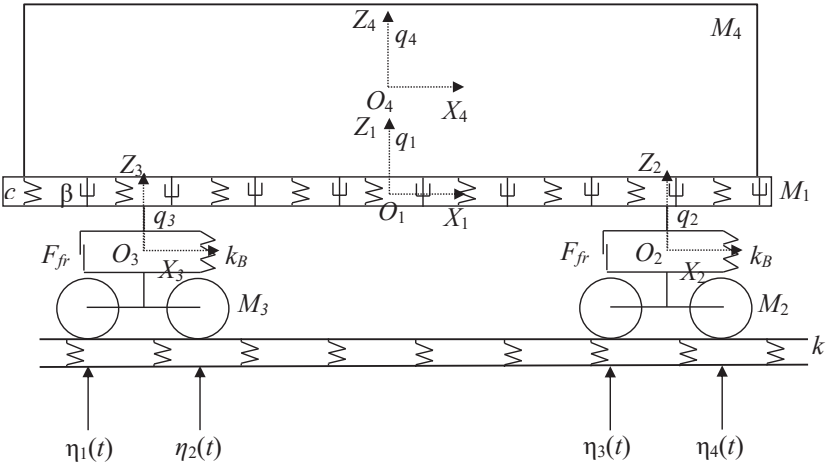

Figure 3.149 – Design diagram of the flat wagon

The system of differential equations of motion of the flat wagon has the following form:

$$\begin{cases} M_1 \cdot \ddot{q}_1 + C_{1,1} \cdot q_1 + C_{1,2} \cdot q_2 + C_{1,3} \cdot q_3 = -F_{fr} \cdot \left(sign\left(\dot{\delta}_1\right) + sign\left(\dot{\delta}_2\right)\right) - F_z, \\ M_2 \cdot \ddot{q}_2 + C_{2,1} \cdot q_1 + C_{2,2} \cdot q_2 + B_{2,2} \cdot \dot{q}_2 = F_{fr} \cdot sign\left(\dot{\delta}_1\right) + k\left(\eta_1 + \eta_2\right), \\ M_3 \cdot \ddot{q}_3 + C_{3,1} \cdot q_1 + C_{3,3} \cdot q_3 + B_{3,3} \cdot \dot{q}_3 = F_{fr} \cdot sign\left(\dot{\delta}_2\right) + k\left(\eta_3 + \eta_4\right), \\ M_4 \cdot \ddot{q}_4 = M_4 \cdot g - F_z, \end{cases} \quad (3.37)$$

where M_1 is the weight of the bearing structure of the flat wagon; M_2, M_3 are the weight of the first and second bogies, respectively; C_{ij} is the elasticity characteristics of the oscillating system elements determined by the stiffness coefficients of the spring suspension k_B; k is the track stiffness; B_{ij} is the dissipative coefficients; F_{FR} is the frictional force in the bogie's spring group; δ_i is the deformations of elastic elements of the spring suspension; η_i is the track irregularity; F_z is the force arising from the displacements of the freight relative to the flat wagon frame.

Herewith,

$$F_z = c \cdot (q_1 - q_4) + \beta \cdot (\dot{q}_1 - \dot{q}_4), \tag{3.38}$$

where c is the stiffness coefficient of the energy-absorbing material; β is the coefficient of viscous resistance of the energy-absorbing material.

The track irregularity was described by a periodic function of the following form [31, 70]:

$$\eta(t) = A \cdot (1 - \cos \omega t), \tag{3.39}$$

where A is the irregularity amplitude; ω is the frequency of oscillations.

System of differential equations of motion (3.37) was solved in MathCad and reduced to the Cauchy equations written in the normal form with subsequent integration using the Runge-Kutta method of stepwise iteration.

The initial conditions for solving the mathematical model were set to zero.

The resulting main indicators of the dynamics of the loaded flat wagon when moving over a track irregularity are shown in Figures 3.150–3.152.

It is found that the maximum accelerations acting in the centre of mass of the bearing structure of the flat wagon occur when it passes a track irregularity (joint) and are equal to 3.8 m/s^2 (Figure 3.150). During the subsequent oscillatory process, the acceleration decreases to 2.5 m/s^2. Thus, taking into account the proposed solution, the accelerations acting on the bearing structure of the flat wagon are reduced by 8.4 % compared to those in the typical wagon.

The accelerations acting on the first and second bogies facing the engine are shown in Figure 3.151. The numerical acceleration is about 9.4 m/s^2.

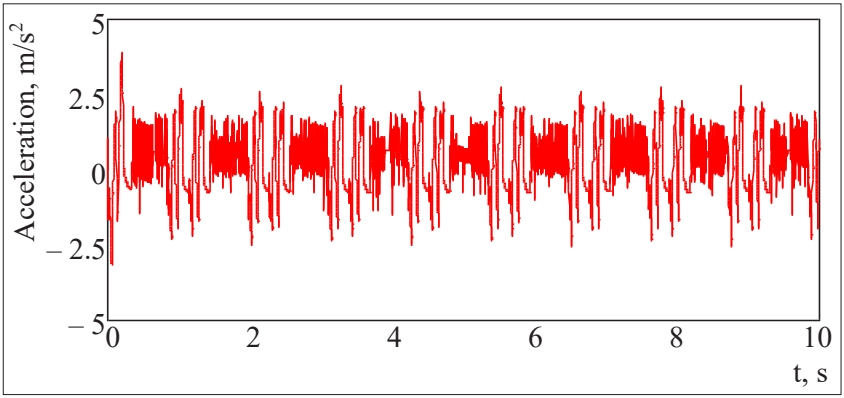

Figure 3.150 – Accelerations of the flat wagon in the centre of mass

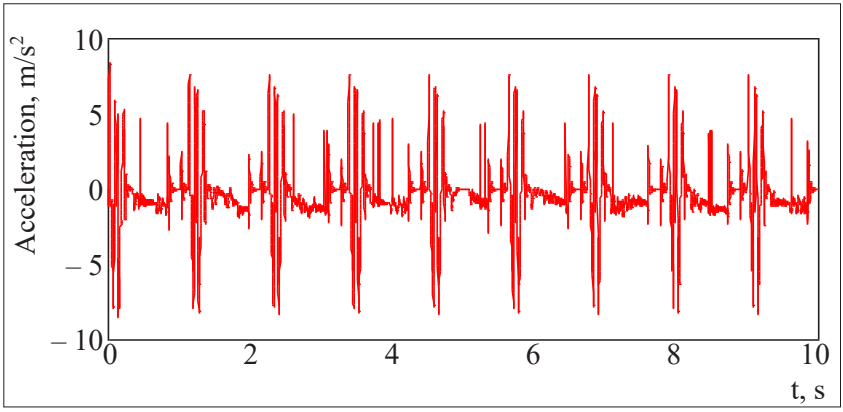

Figure 3.151 – Acceleration acting on the bogies

The acceleration acting on the freight placed on the flat wagon frame is 2.8 m/s² (Figure 3.152).

The resulting acceleration is 11.7 % lower than the acceleration acting on the freight according to a typical loading diagram.

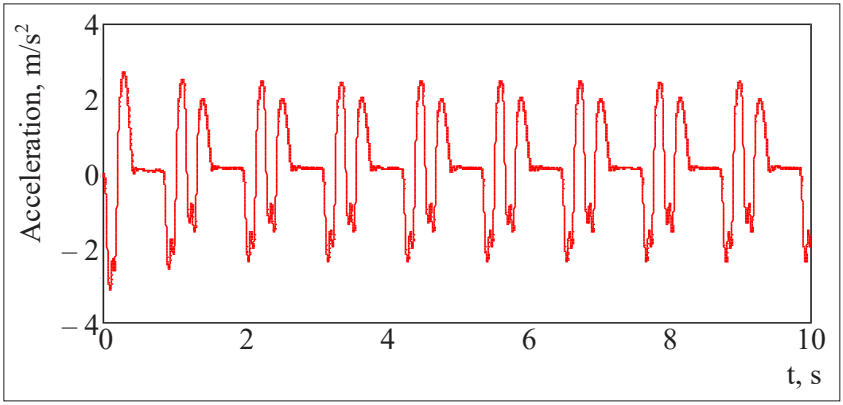

Figure 3.152 – Acceleration acting on the freight

The next stage of the study included the determination of the thickness of the sheets forming a sandwich panel that was considered as a slab with the width *a* and the height *b*. The sheet is fixed along the perimeter. The uniformly distributed load *P* is applied to the horizontal plane of the sandwich panel (Figure 3.153). The Bubnov – Galerkin method [71] was used to determine the thickness of the sheet forming the sandwich panel.

According to this method, the stresses acting in the slab are determined by the formula:

$$\sigma_X = P \cdot \frac{96}{\pi^4} \cdot \frac{(b^2 + \mu \cdot a^2) \cdot a^2 \cdot b^2}{\left(a^2 + b^2\right)^2 \cdot \delta^2}, \tag{3.40}$$

$$\sigma_Y = P \cdot \frac{96}{\pi^4} \cdot \frac{(a^2 + \mu \cdot b^2) \cdot a^2 \cdot b^2}{\left(a^2 + b^2\right)^2 \cdot \delta^2}. \tag{3.41}$$

If the thickness of the slab is determined by the stresses relative to the axis *X*, then:

$$\delta = \sqrt{\frac{P \cdot \frac{96}{\pi^4} \cdot (b^2 + \mu \cdot a^2) \cdot a^2 \cdot b^2}{\sigma_X \cdot \left(a^2 + b^2\right)^2}}. \tag{3.42}$$

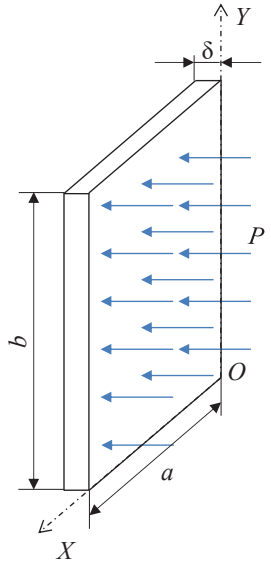

Figure 3.153 – Design diagram of a sandwich panel

If the thickness of the slab is determined using the stresses relative to the Y-axis, then formula (3.41) takes the form:

$$\delta = \sqrt{\frac{P \cdot \frac{96}{\pi^4} \cdot (a^2 + \mu \cdot b^2) \cdot a^2 \cdot b^2}{\sigma_Y \cdot \left(a^2 + b^2\right)^2}}. \quad (3.43)$$

It is assumed that the slab has a width of a = 1.914 m (seven sandwich panels are used on the frame) and a height of b = 3.0 m.

The sandwich panels are made of Steel 09G2S. When the flat wagon is loaded to the full payload capacity, the force acting on one panel is P = 98.1 kN.

Based on the calculations in accordance with formulae (3.42) and (3.43), the thickness of the panel is 6 mm.

Based on the values of sheet thicknesses, a spatial model of the sandwich panel was built (Figure 3.154) and strength was calculated. The graphic work was carried out in SolidWorks.

Aluminium foam is used as an energy-absorbing material. The modelled sandwich panels are laid on the floor of the frame (Figure 3.155).

The strength calculation was carried out using the finite element method in SolidWorks Simulation.

The strength of sandwich panels placed on the frame of the flat wagon was determined with a design diagram (Figure 3.156), which includes the vertical load P_v caused by vertical static and dynamic loads.

The model of the bearing structure of the flat wagon is fixed to the horizontal surfaces of the centre plates. Tetrahedra are used

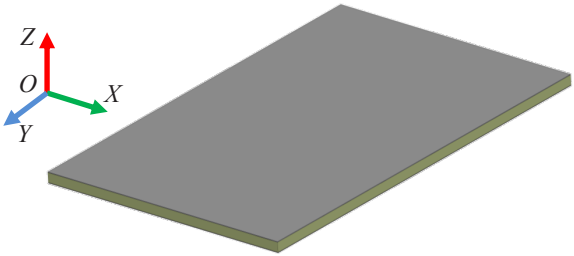

Figure 3.154 – Spatial model of the sandwich panel

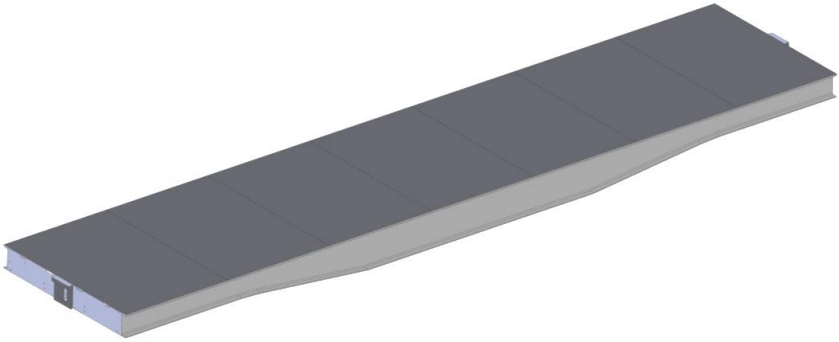

Figure 3.155 – Sandwich panels on the flat wagon frame

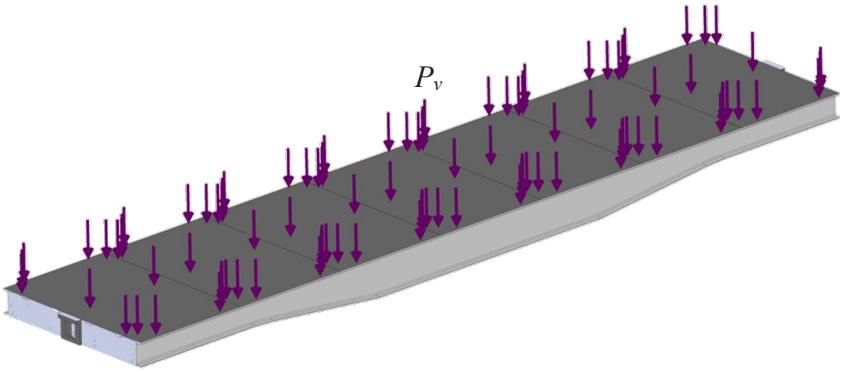

Figure 3.156 – Design diagram of the flat wagon

for the finite element model. The model has 373,651 elements and 127,073 nodes. The maximum size of the element is 180 mm and the minimum size is 36 mm. The bearing structure is made of Steel 09G2S that is typical in the manufacture of bearing structures of wagons.

The results of the strength calculation show that the maximum stresses in the frame of the flat wagon are 131.7 MPa (Figure 3.157). These stresses occur in the areas of the centre sill, where it interacts with the bolster beam due to the fixation of the model at the centre plate. The maximum stresses in the sandwich panels are about 94.5 MPa, which is almost twice lower than permissible stresses. A stress of 210 MPa is taken permissible in accordance with [21, 22].

The maximum displacements occur in the middle part of the flat wagon frame and amount to 4.35 mm (Figure 3.158).

The research reveals that the use of sandwich panels for the bearing structure of a flat wagon is reasonable.

As far as the use of sandwich panels increases the tare weight of a flat wagon by 12 %, the study also included the determination of main dynamic indicators of an unloaded wagon in motion. The design diagram of the flat wagon is shown in Figure 3.160.

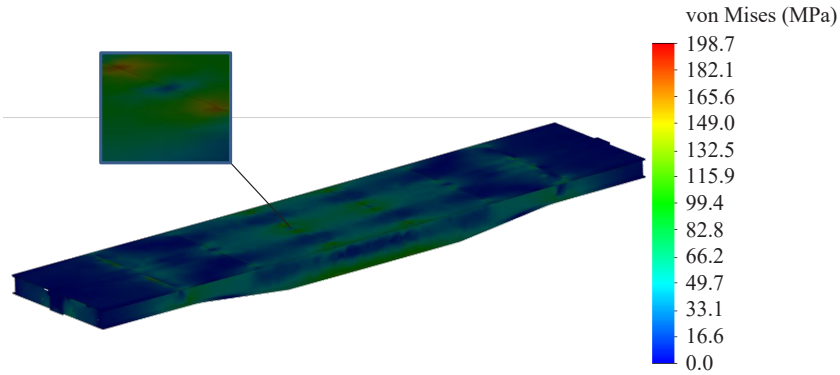

Figure 3.157 – Stress state of the bearing structure of the flat wagon

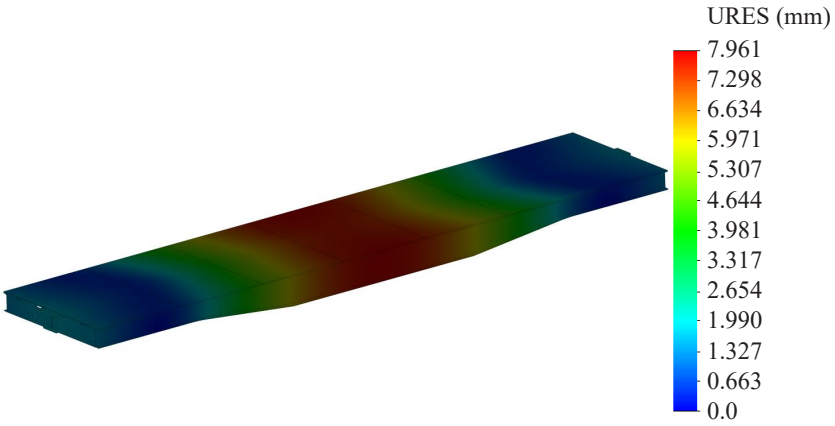

Figure 3.158 – Displacements in the bearing structure of the flat wagon

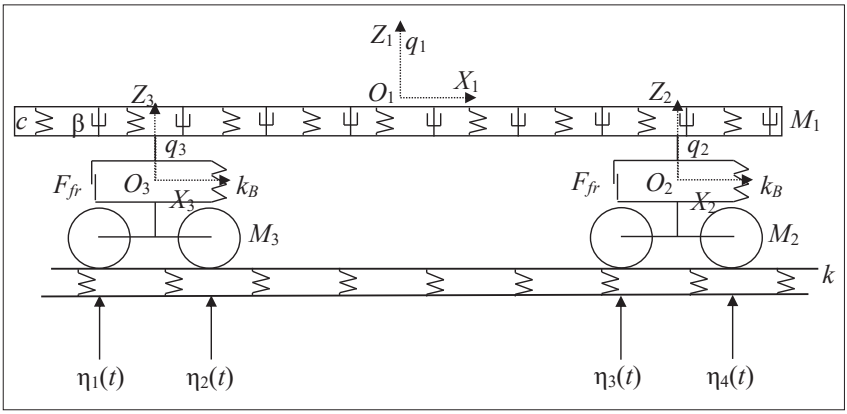

Figure 3.159 – Design diagram of an unloaded flat wagon moving over a track irregularity

The mathematical model that describes the movement of the flat wagon:

$$\begin{cases} M_1 \cdot \ddot{q}_1 + C_{1,1} \cdot q_1 + C_{1,2} \cdot q_2 + C_{1,3} \cdot q_3 = -F_{fr} \cdot \left(sign\left(\dot{\delta}_1\right) + sign\left(\dot{\delta}_2\right)\right), \\ M_2 \cdot \ddot{q}_2 + C_{2,1} \cdot q_1 + C_{2,2} \cdot q_2 + B_{2,2} \cdot \dot{q}_2 = F_{fr} \cdot sign\left(\dot{\delta}_1\right) + k\left(\eta_1 + \eta_2\right), \\ M_3 \cdot \ddot{q}_3 + C_{3,1} \cdot q_1 + C_{3,3} \cdot q_3 + B_{3,3} \cdot \dot{q}_3 = F_{fr} \cdot sign\left(\dot{\delta}_2\right) + k\left(\eta_3 + \eta_4\right). \end{cases} \quad (3.44)$$

All components included in this mathematical model are identical to those used in model (3.38).

The results of the calculations are shown in Figures 3.160 and 3.161.

The maximum acceleration of the flat wagon in the centre of mass is about 6 m/s^2 (0.6 g), and the acceleration of the bogies is about 8.5 m/s^2. The dynamics indicators obtained correspond to a 'good' motion of the wagon.

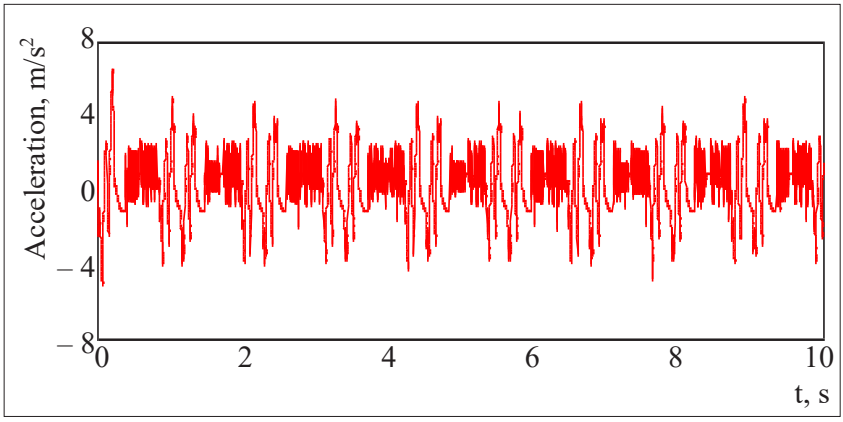

Figure 3.160 – Acceleration of the flat wagon in the centre of mass

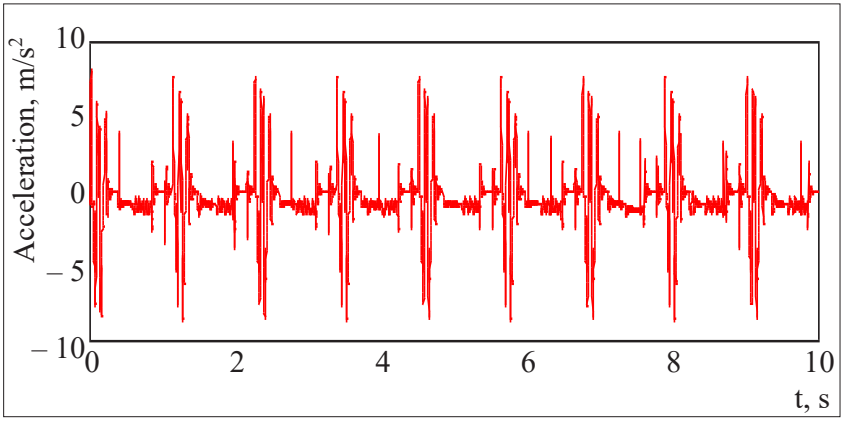

Figure 3.161 – Acceleration applied to the bogies

3.9 Adaptation of the bearing structure of a flat wagon for carrying liquid cargoes

It is proposed to install a boiler module on a universal flat wagon so that to use its bearing structure for carrying liquid cargoes (Figure 3.162) [72].

The boiler rests on the frame of the flat wagon using wooden bars mounted on metal supports. Thus, the support diagram used is identical to that of tank wagons. The boiler can be fixed with tie-down clamps or other lashing devices. It is proposed to use composite materials in the production of boilers, which will reduce the total tare weight of the wagon compared to that of a metal structure by 3.7 %.

This solution can facilitate the creation of multimodular wagons suitable for carrying swap bodies and other vehicles.

It is important to note that this solution is feasible for the existing wagons and can be used for modernisations or repairs. The proposed solution can also be used for developing new multifunctional wagon designs.

The load of the improved flat wagon was determined by modelling its dynamics under a shunting impact, as the case of the highest load of the structure in operation.

Mathematical model (3.28) was used for this purpose. The calculation results show that the acceleration acting on the bearing structure of the flat wagon is 0.38 g, which is within the permissible limits [21]. The resulting acceleration value was included in the strength calculations of the bearing structure of the flat wagon.

The strength of the bearing structure of the flat wagon was calculated for a shunting impact using the finite element method in SolidWorks Simulation. The finite element model of the bearing structure of a flat wagon is shown in Figure 3.163. Isoparametric tetrahedra were used in this model. The optimal number of finite elements was calculated using the graphical analytical method. The number of mesh elements was 2,521,451, and the number of nodes was 809,251. The maximum mesh element size is 45.0 mm, the minimum element size is 9.0 mm, the maximum aspect ratio is 145.69, the percentage of elements with an aspect ratio of less than three is 52.1, and more than ten is 2.59. The minimum number of elements in the circle is 13, and the ratio of the element size increase is 1.9.

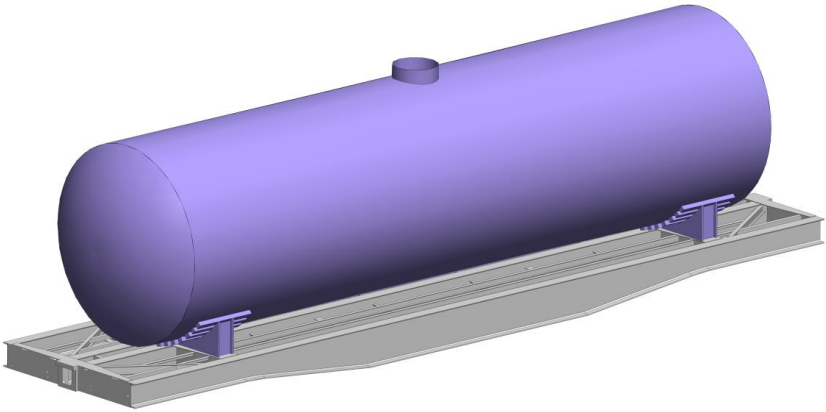

Figure 3.162 – Spatial model of the flat wagon

The design model includes the condition that the improved bearing structure of the flat wagon is subjected to the vertical static load P_v^{st} and the longitudinal load P_l (Figure 3.164). The boiler is subject to the excessive vapour pressure P_p, the pressure on the bottom caused by the movement of the liquid cargo (water-hammer effect) P_{lc}, as well as the hydrostatic pressure P_h.

The maximum pressure from the water-hammer effect was determined by formula (3.27).

The model was secured in the areas where the bearing structure of the flat wagon rests on the bogies. The bearing structure of the flat wagon is made of Steel 09G2S, and the boiler is made of composite with a titanium matrix reinforced with boron, borsic, silicon carbide, beryllium, and molybdenum fibres. The model also includes wooden bars and their characteristics.

The results of the strength calculation are shown in Figures 3.165 and 3.166.

The maximum equivalent stresses occur in the area of interaction between the centre sill and the bolster beam and amount to about 340 MPa; the maximum displacements are 8.6 mm. Thus, the resulting stresses do not exceed the yield strength of the structural material [21].

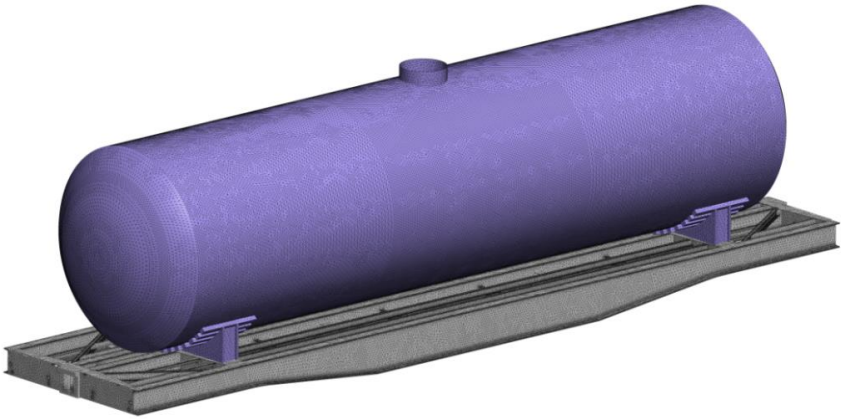

Figure 3.163 – FEM of the bearing structure of the flat wagon

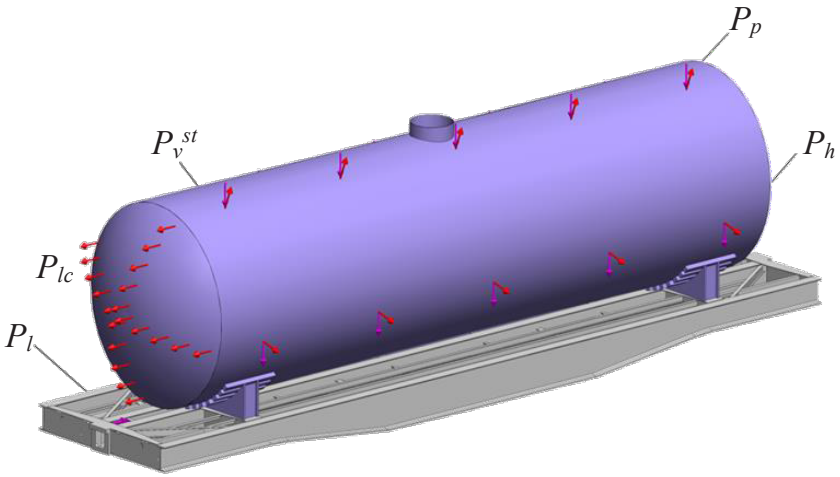

Figure 3.164 – Design diagram of the bearing structure of the flat wagon

The frequencies and shapes of natural oscillations of the bearing structure of the flat wagon were determined with a modal analysis using options of SolidWorks Simulation. The calculation was based on the design diagram shown in Figure 3.165. Some forms of oscillations of the bearing structure of the flat wagon are shown in Figure 3.167.

The numerical values of natural oscillation frequencies are given in Table 3.8.

Table 3.8 – Natural oscillation frequencies of the bearing structure of the flat wagon

Oscillation shape	Frequency, Hz	Oscillation shape	Frequency, Hz
1	11.38	6	17.46
2	12.19	7	17.48
3	17.3	8	17.54
4	17.31	9	17.62
5	17.45	10	17.86

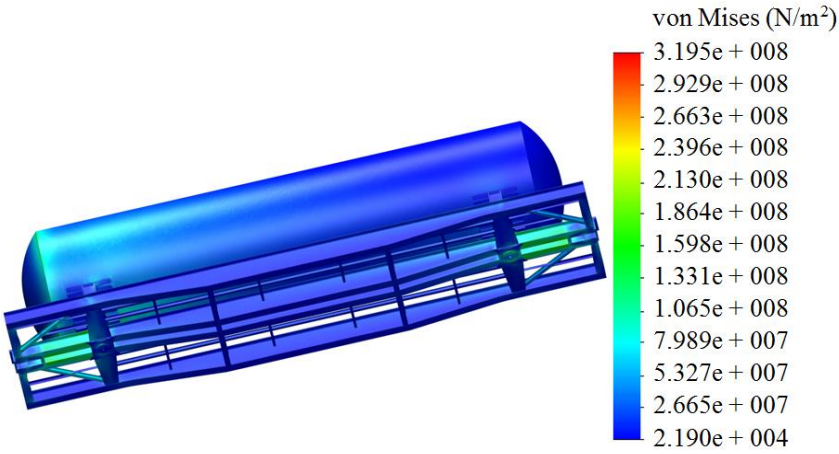

Figure 3.165 – Stress state of the bearing structure of the flat wagon

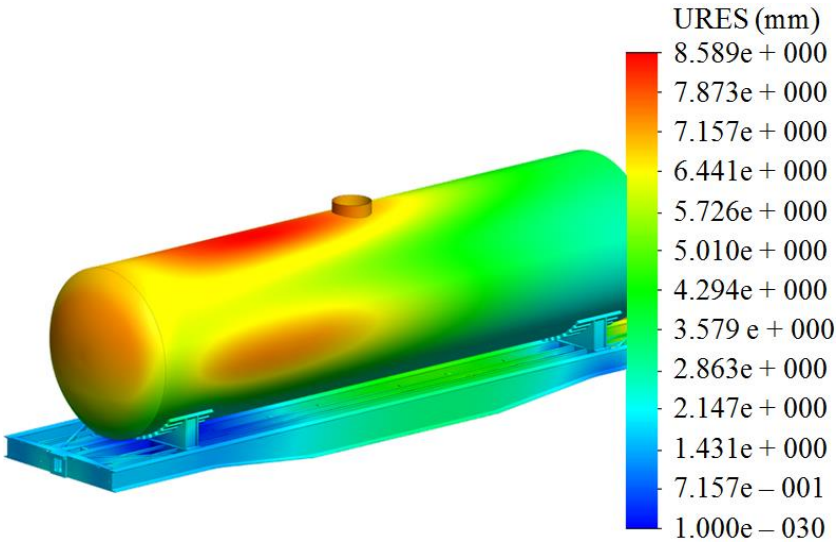

Figure 3.166 – Displacements in the bearing structure of the flat wagon

As known, the traffic safety of a wagon can be ensured when the first natural frequency of bending oscillations of the bearing structure in the vertical plane is not lower than 8 Hz [21]. The calculation results show that the natural oscillation frequencies are within the permissible limits.

This flat wagon design is patented in Ukraine [73]; the description is given in Appendix A.

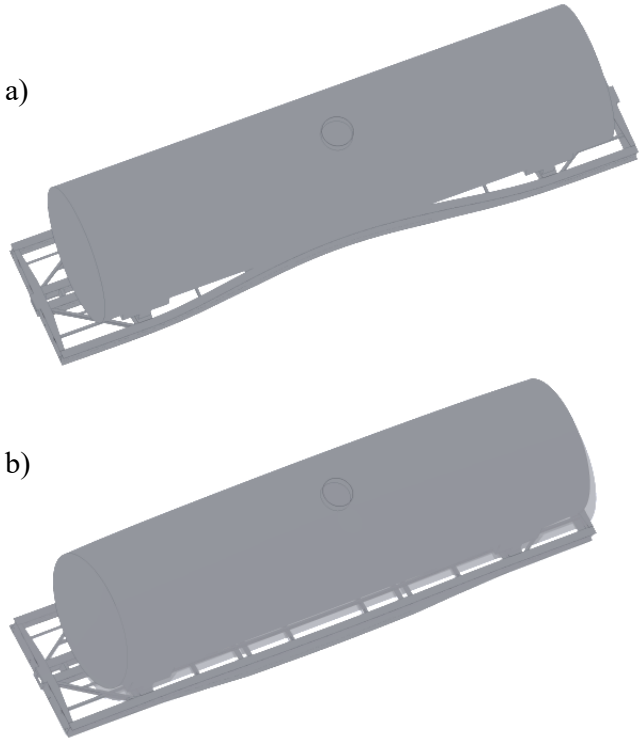

Figure 3.167 – Some oscillations of the bearing structure of the flat wagon (deformation scale 20:1)
a) mode 1; b) mode 2

3.10 Situational adaptation of a flat wagon mod. 13-7024 for carrying strategic freight

The bearing structure of the flat wagon mod. 13-7024 consists of the frame with two subframes placed in the cantilever parts (Figure 3.168). The frame design also includes two sidewalls of welded cross-sectional structure with variable stiffness. These sidewalls consist of 22-mm thick bottom and top sheets and 8-mm thick vertical sheets. The flat wagon frame has two end beams, six intermediate beams, and two additional intermediate beams. Four diagonal T-section braces installed transfer the longitudinal loads from the centre sills of the underframes to the sidewalls (TU U 35.2-05763814-062:2005).

It is proposed to use a removable module on the flat wagon for carrying strategic freight including military equipment, agricultural machinery, etc. (Figure 3.169).

The removable module is presented by a frame structure (Figure 3.170) covered with a metal sheet on top. Fitting stops are installed in the corners of the removable module. The stops on the cantilever part of the flat wagon are higher than those on the opposite side of the module. This solution makes it possible to create a straight horizontal plane for the freight.

The profiles for the frame were determined with the epures of internal forces arising in the loaded module. The module was considered as a rod system on four supports (Figure 3.171).

The calculation was performed in LIRA-CAD using built-in options.

The results obtained were substantiated with the strength calculation of the removable module when it was subjected to a vertical load. The graphic works were carried out in SolidWorks. The finite element method was used as a calculation method. It was implemented in SolidWorks Simulation. The design diagram of the module is shown in Figure 3.172.

It is taken into account that the module bears the vertical load P_v using its full payload capacity. The module is fixed at fittings.

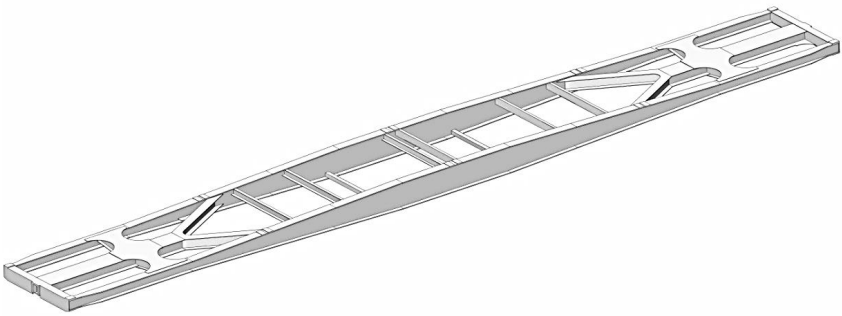

Figure 3.168 – Bearing structure of the flat wagon mod. 13-7024

a)

b)

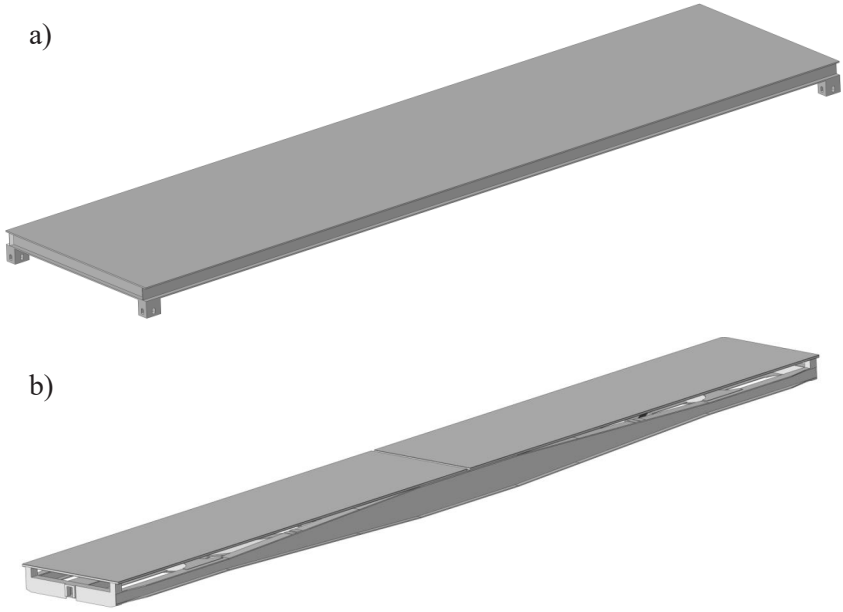

Figure 3.169 – Removable module
a) general view; b) placed on the flat wagon

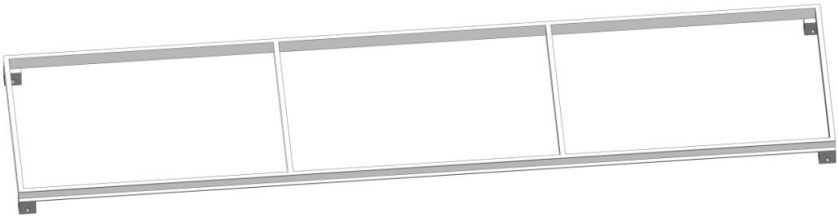

Figure 3.170 – Removable module frame

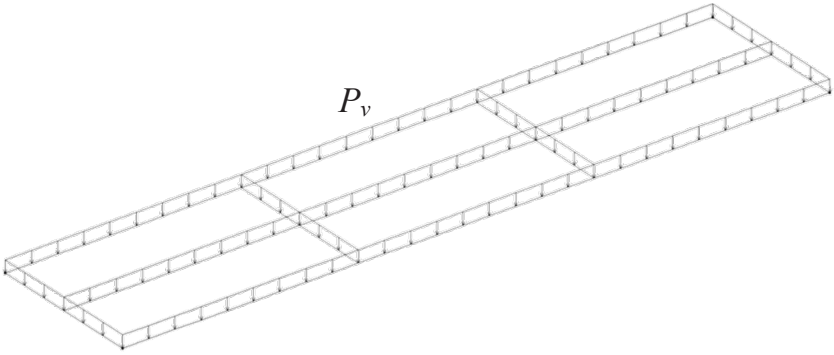

Figure 3.171 – Design diagram of the removable module

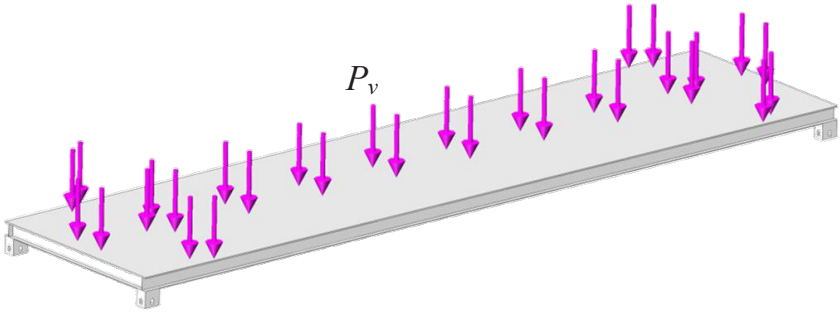

Figure 3.172 – Design diagram of the removable module

The finite element model of the module is formed by isoparametric tetrahedra. Their optimal value was determined with the graphical analytical method. The finite element model has 38,893 elements and 12,561 nodes. The maximum element size is 120 mm, and the minimum element size is 24 mm.

The dynamic load of the removable module was determined using the relevant calculations. Two load diagrams of the removable module were taken into account:

– the vertical loads to the removable module; and
– the longitudinal loads to the removable module.

The removable module was calculated when it was subjected to vertical loads in accordance with the diagram shown in Figure 3.173.

The study of the longitudinal load of the removable module included the vertical load P_v from the freight, as well as the longitudinal load P_l (Figure 3.173).

The longitudinal load P_l is applied to the fitting stops facing the engine.

The design diagram shown in Figure 3.173 was used to obtain the values of the bending moments that occur at the cross-section of the removable module (Figure 3.174). The 'tension' is marked in orange, and the 'compression' was indicated in blue.

The maximum bending moment occurs in the corners of the removable module and amounts to 126 kN·m. The bending moment in the rods of the middle span of the detachable module is 60.3 kN·m.

The maximum bending moment value was used to determine the profile of the removable module. The calculation was based on a known relationship:

$$W = \frac{M}{[\sigma]}, \tag{3.45}$$

where M is the bending moment acting in the section of the removable module; [σ] is the permissible stresses of the material of the removable module.

Based on the calculations and provided that the removable module was made of Steel 09G2S, it was obtained that

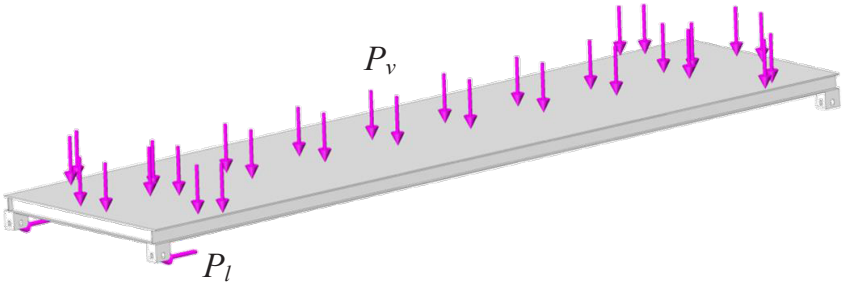

Figure 3.173 – Design diagram of the removable module

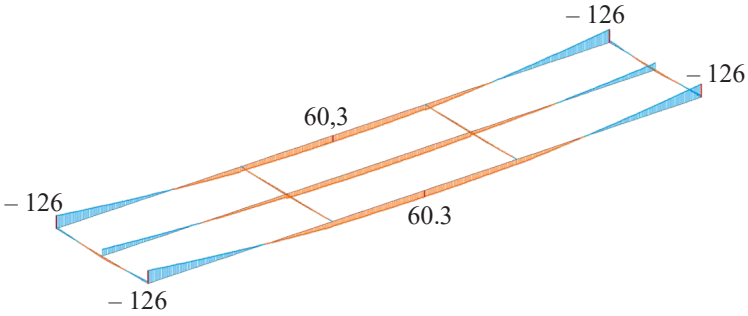

Figure 3.174 – Diagram of bending moments in the cross-section of the removable module (kN · m)

$W \approx 400$ cm^3. Based on the obtained moment of resistance, channel No. 30 was selected as the frame profile.

The classical Bubnov-Galerkin method was used to determine the thickness of the sheets that form the module. Based on the calculations and physical and mechanical properties of low-alloy Steel 09G2S, a sheet thickness of 5.25 mm was obtained. The calculation also included the maximum potential load of the removable module. Thus, if two modules are placed on the flat wagon, the load on one module is equal to half the load capacity of the flat wagon.

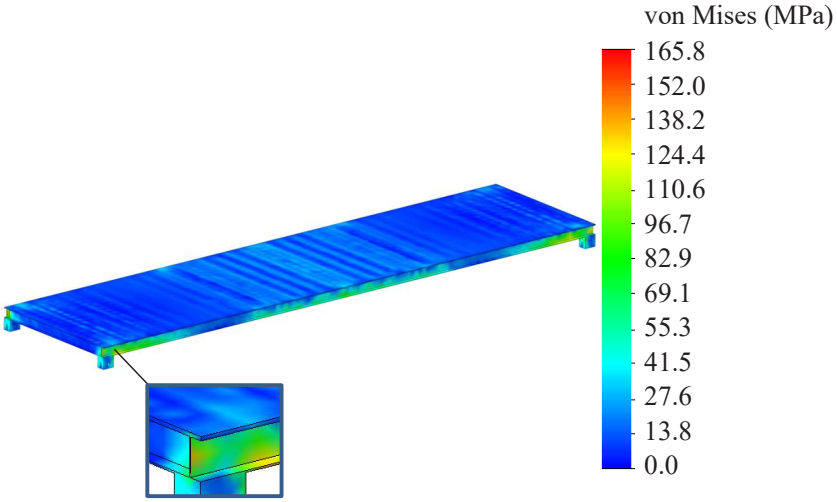

Figure 3.175 – Stress state of the removable module

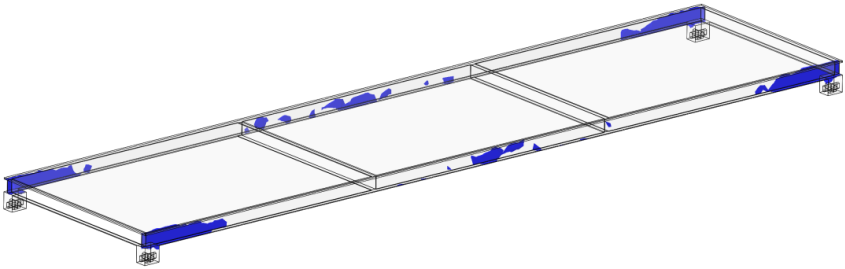

Figure 3.176 – Most loaded areas of the removable module

Taking into account the obtained parameters of the structural components of the removable module, its strength under static load was calculated.

The results of the calculation are shown in Figures 3.175–3.177. It is found that the maximum stresses occur in the corner parts of the removable module and amount to 165.8 MPa (Figure 3.176). These stresses are 21 % lower than the permissible limits. The permissible stress was taken equal to 210 MPa.

The most heavily loaded areas of the removable module are its corners and the middle areas of the longitudinal beams of the frame (Figure 3.176). The maximum displacements occur in the middle part of the removable module and are equal to 8.66 mm (Figure 3.177).

Since the removable module is fixed to the fittings and the load is applied to the horizontal surface, the displacement fields are distributed relative to its structure.

The vertical load on the removable module was studied with mathematical modelling. It was taken into account that two removable modules are placed on the flat wagon moving over a track irregularity. The removable modules are loaded with a conditional freight using their full payload capacity. It was also taken into account that the dynamic system is formed by three bodies: the bearing structure of the flat wagon with two removable loaded modules and two bogies. The design diagram is shown in Figure 3.178.

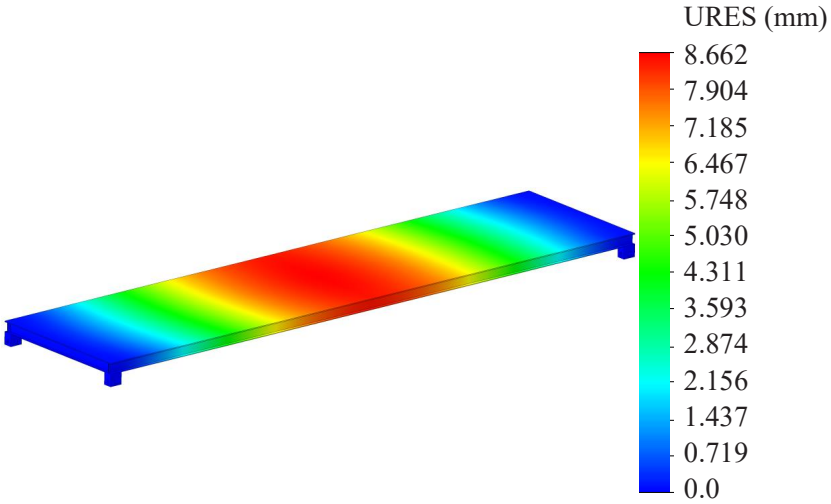

Figure 3.177 – Displacements in the removable module units

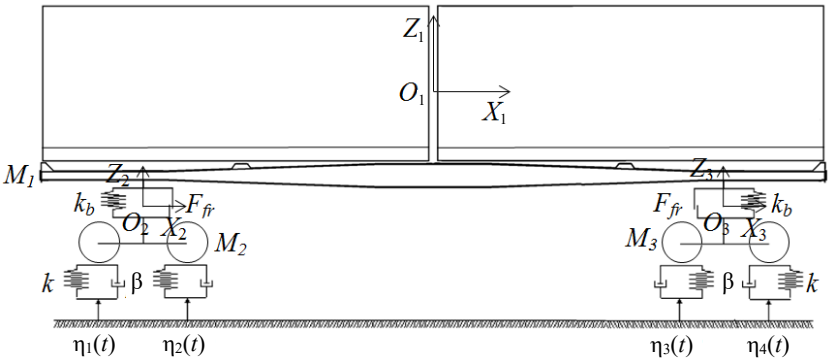

Figure 3.178 – Design diagram of the loaded flat wagon

It was assumed that the flat wagon moved over an irregularity of the elastic-dissipative track.

The reactions of the track are proportional to its deformations and the speed of these deformations. It was also assumed in the calculations that the bearing structure of the flat wagon is supported by bogies mod. 18-100.

The system of differential equations of the movement for the flat wagon has the form [12]:

$$\begin{cases} M_1 \cdot \ddot{q}_1 + C_{1,1} \cdot q_1 + C_{1,2} \cdot q_2 + C_{1,3} \cdot q_3 = -F_{fr} \cdot \left(sign\left(\dot{\delta}_1\right) + sign\left(\dot{\delta}_2\right) \right), \\ M_2 \cdot \ddot{q}_2 + C_{2,1} \cdot q_1 + C_{2,2} \cdot q_2 + B_{2,2} \cdot \dot{q}_2 = F_{fr} \cdot sign\left(\dot{\delta}_1\right) + k\left(\eta_1 + \eta_2\right) + \beta\left(\dot{\eta}_1 + \dot{\eta}_2\right), \\ M_3 \cdot \ddot{q}_3 + C_{3,1} \cdot q_1 + C_{3,3} \cdot q_3 + B_{3,3} \cdot \dot{q}_3 = F_{fr} \cdot sign\left(\dot{\delta}_2\right) + k\left(\eta_3 + \eta_4\right) + \beta\left(\dot{\eta}_3 + \dot{\eta}_4\right), \end{cases} \quad (3.46)$$

where M_1 is the weight of the bearing structure of the flat wagon; M_2, M_3 are the weight of the first and second bogies, respectively; C_{ij} is the elasticity characteristics of the oscillation system elements determined by the spring stiffness coefficients k_b; B_{ij} is the scattering function; k is the track stiffness; β is the damping coefficient; F_{fr} is the frictional force in the bogie spring group; δ_i is the deformation of elastic elements of spring suspension; $\eta_i(t)$ is the track irregularity.

In (3.46), the coordinate q_1 characterizes the vertical displacements of the bearing structure of the flat wagon; q_2, q_3 are the displacements of bogies.

System of differential equations of motion (3.46) was solved in MathCad. The vector of initial conditions is as follows: the initial displacement of the loaded bearing structure is 0.004 m, the speed is 0; for bogies these values are 0.003 m and 0, respectively. The calculation results are shown in Figure 3.180.

Figure 3.179 shows that the maximum acceleration acting on the bearing structure of the loaded flat wagon is 1.46 m/s^2 (0.1 g), which corresponds to the 'excellent' motion of the flat wagon.

The resulting acceleration was included in the strength calculation of the removable module. The calculation results are shown in Figures 3.180 and 3.181. The maximum stresses occur in the corners of the removable module and amount to 179.3 MPa (Fig. 3.180), which is 14.6 % lower than the permissible stresses.

The maximum displacements are in the middle part of the removable module and amount to 8.9 mm (Figure 3.181).

The distribution of displacement fields relative to the structure of the removable module has the same explanation as that of its static load.

The longitudinal load of the removable module was studied using mathematical modelling at design mode III (jerk) provided that the wagon moves as part of a train. The design diagram of the flat wagon is shown in Figure 3.182.

Mathematical model (3.28) includes the initial conditions close to zero, and the maximum accelerations acting on the bearing structure of the flat wagon about 24 m/s^2 (0.24 g). These accelerations were included when determining the strength of the removable module under longitudinal loading.

The results of the calculation show that the maximum stresses occur in the corners of the removable module on the side of the longitudinal load and amount to 184.6 MPa (Figure 3.183). The resulting stresses are 12 % lower than permissible.

The maximum displacements occur in the middle part of the module and are 9.1 mm (Figure 3.184).

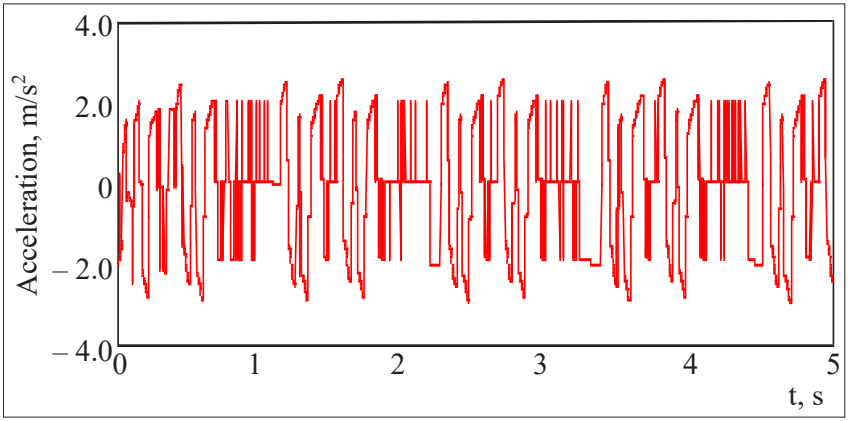

Figure 3.179 – Accelerations to the bearing structure of the loaded flat wagon

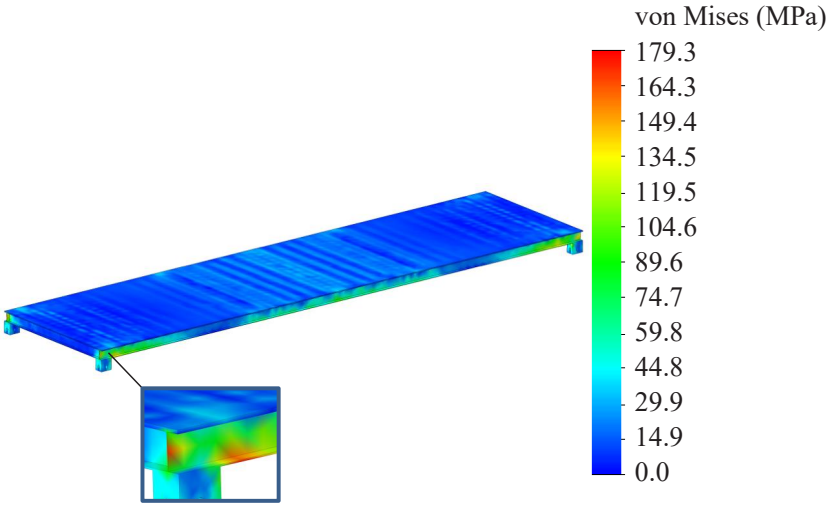

Figure 3.180 – Stress state of the removable module at its vertical loading

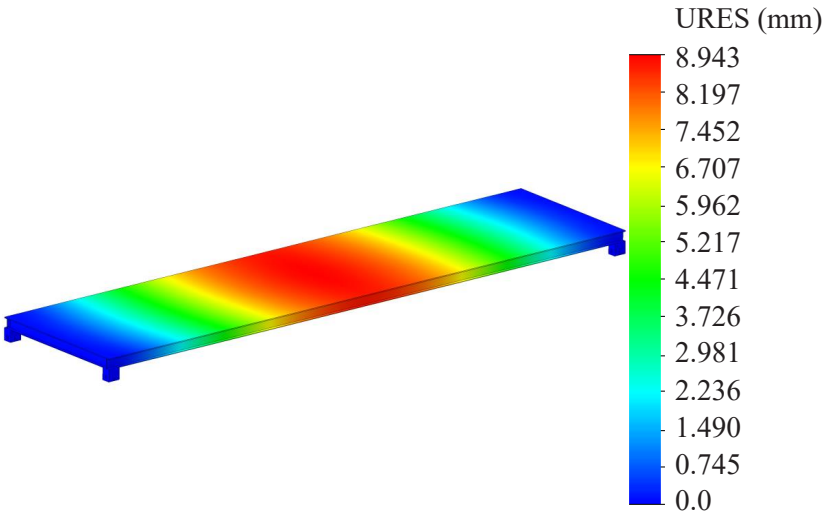

Figure 3.181 – Displacements in the removable module units at its vertical loading

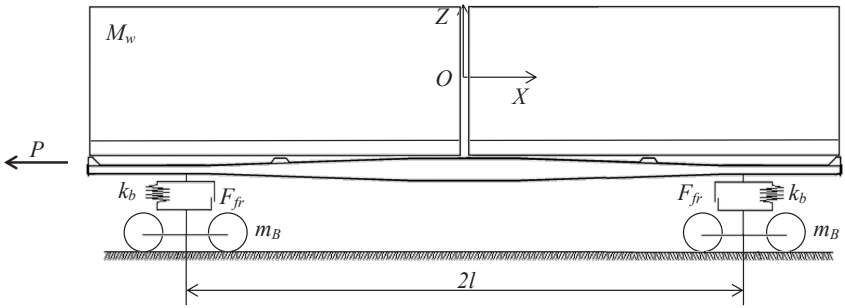

Figure 3.182 – Design diagram of the loaded flat wagon

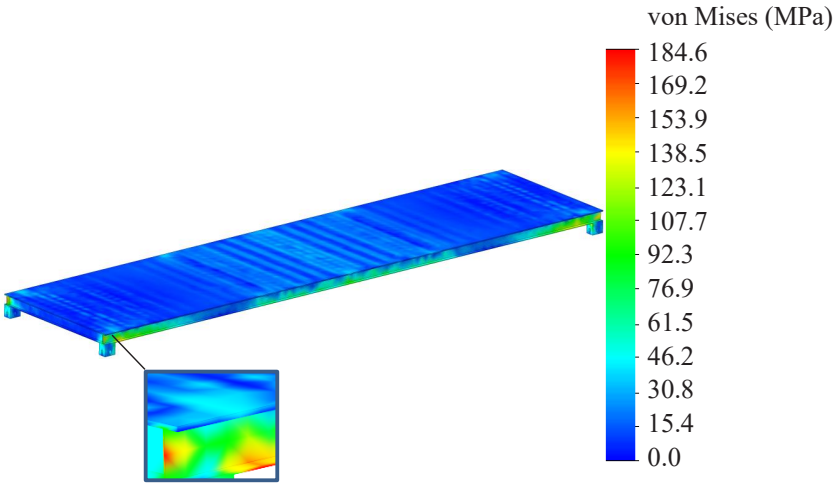

Figure 3.183 – Stress state of the removable module at longitudinal loading

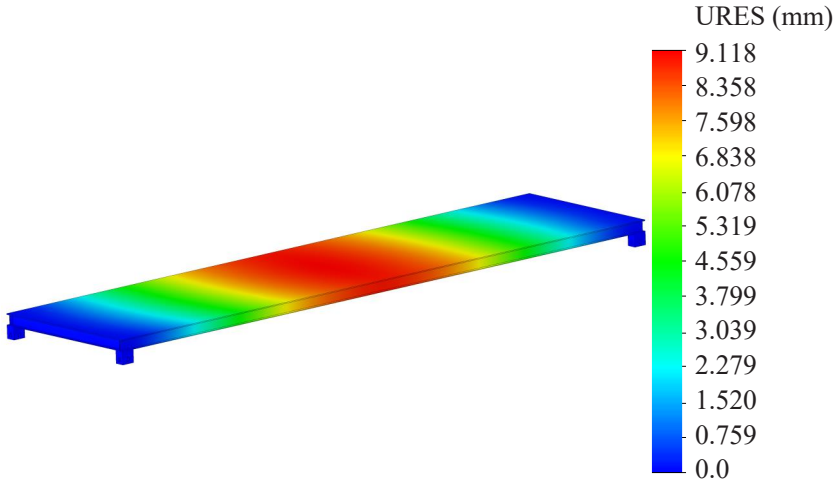

Figure 3.184 – Displacements in the removable module units at longitudinal loading

This distribution of displacement fields can also be explained by the fact that the middle part of the removable module is loaded and the freight is secured at the fittings. Therefore, the middle part of the module has the maximum compliance, and, thus, bear the largest displacements.

Conclusions to Part 3

1. Measures to improve the bearing structure of the flat wagon used for carrying containers are proposed. One of them is the installation of fixed or folding fitting stops on the main longitudinal beams of the frame. This solution was implemented by the Research and Development Centre 'Wagons' (Russia). The strength calculations conducted confirmed the possibility of this improvement.

It is also proposed to improve the bearing structure of the flat wagon mod. 13-401 to be used for carrying steel coils and timber bundles. The results of the strength calculation for the improved bearing structure are presented. The main strength indices are within the permissible limits. It is also proposed to equip the wagon with a removable roof for carrying industrial woodchips. The design features and the strength calculation of the removable roof under the main load diagrams are presented.

2. The possibility of improving the bearing structure of the flat wagon for military-strategic purposes was considered. It is proposed to install special D-rings to secure chain binders on the main longitudinal beams of the frame. The results of strength calculations of the improved bearing structure of the flat wagon are presented. It is found that the proposed improvement is appropriate.

3. Measures are also proposed to improve the bearing structure of the flat wagon for carrying containers. The solution deals with using channels reinforced with vertical metal plates for the main longitudinal beams of the frame, which can reduce the material

consumption of the bearing structure of the flat wagon compared to a typical one. The results of the strength calculation of the bearing structure of the flat wagon are presented. It is found that under the main operating loading modes, the strength of the bearing structure of the flat wagon is ensured.

4. Measures to create an articulated flat wagon based on the long-wheelbase wagon mod. 13-7024 for carrying containers are proposed. The solution requires removing the centre plate assembly on the side where the wagon rests on the middle bogie and installing elastic side bearings on the cantilever parts of the bearing structures of the two flat wagons forming the platforms. If needed, the proposed articulated flat wagon can be restored to the original design, since the bolster beam, unlike that in typical articulated flat wagons, is not removed in the area where the platforms rest on the middle bogie. The results of strength calculation of the bearing structure of the flat wagon under the main operating loading modes confirmed the feasibility of the proposed solutions.

5. The bearing structure of a low deck articulated flat wagon is proposed. This two-platformed wagon is supported by three bogies. The lowered middle section makes it possible to carry oversized freight on the flat wagon in compliance with the established dimensions. The cantilever parts of this flat wagon are equipped with folding fitting stops for fastening containers. Military equipment can be secured using wheel stoppers and other reusable devices mounted on the bearing structure of the flat wagon.

The study included mathematical modelling of the dynamic load of the bearing structure of the articulated flat wagon when transported by a train ferry. The maximum acceleration acting on the bearing structure of the flat wagon is 3.47 m/s^2, and that on the container is 4.67 m/s^2. The stability of the container transported was investigated. It is found that its stability is ensured at roll angles of up to 25°.

The study also included computer modelling of the dynamic load on the bearing structure of the articulated flat wagon when transported by a train ferry. The acceleration values and their

distribution fields relative to the bearing structure of the flat wagon and the container are determined. The maximum accelerations of the container are concentrated in the upper corner parts behind the central axis of symmetry of the flat wagon and amount to about 4.8 m/s^2. The maximum accelerations of the bearing structure of the flat wagon occur in the cantilevered parts of the platforms and are about 3.7 m/s^2.

It is found that the maximum percentage of discrepancy between the results of mathematical and computer modelling does not exceed 11 %.

6. It is proposed to improve the bearing structure of the flat wagon to increase its efficiency so that to carry a wide range of cargoes.

The strength of a boiler for carrying high-temperature, liquid or bulk cargoes under operating conditions is determined. The calculation included the vertical load of the boiler with the liquid cargo (diagram I), longitudinal load (diagram II), as well as the effect of temperature load (diagram III). Under diagram I, the maximum stresses are in the areas of interaction between the cylindrical part of the boiler and the bottoms; they amount to 184.4 MPa. At diagram II, the maximum stresses occur in the middle part of the bottom and amount to 307.4 MPa. At diagram III, the maximum stresses occur in the areas of interaction between the bottoms and the cylindrical parts of the boiler and amount to 314.5 MPa. Thus, under all the loading diagrams considered, the maximum stresses are within the permissible limits.

The dynamic load of the boiler for carrying high-temperature, liquid or bulk cargoes is determined. The results of mathematical modelling of dynamic load show that the maximum acceleration acting on the boiler is 36.5 m/s^2.

The results of computer modelling of the dynamic load of the boiler show that maximum axial acceleration is concentrated in the bottom and is 37.4 m/s^2. In the cylindrical part of the boiler, the acceleration is in a range of 28.0–12 m/s^2.

The dynamic load models of the boiler for carrying high-temperature liquid or bulk cargoes were verified. The calculation

was carried out according to the F-criterion. It is found, that when the variance of adequacy $S_{ad} = 8.23$ and the error mean square $S_y = 6.44$, the actual F-criterion is $F_p = 1.27$, which is less than the tabular value $F_t = 3.58$ at the significance level $\alpha = 0.05$. Therefore, the hypothesis of adequacy is confirmed.

7. An improvement of the bearing structure of a long-wheelbase flat wagon is proposed to reduce its vertical load in operation.

The dynamic load of the bearing structure of the flat wagon was determined taking into account a new diagram of interaction with containers. The maximum acceleration acting on the flat wagon is 2.67 m/s^2, and that on the container is 3.15 m/s^2. The resulting acceleration values are 5.3 % and 6.2 % lower than those for a flat wagon and a container, respectively, if taking into account the typical diagram of interaction.

The strength of the foundation for container fitting stops was determined. The method of maximum normal stresses was used as a calculation method. The maximum stresses occur in the inclined parts of the foundation and amount to 113.6 MPa, which is significantly lower than permissible limits.

The dynamic load of the improved unloaded flat wagon was determined. The results of the calculations made it possible to find that the dynamics indicators are within the permissible limits, and the motion of the flat wagon is 'good'. The maximum acceleration in the centre of mass of the bearing structure of the flat wagon is 5.9 m/s^2. The acceleration in the areas where the bearing structure of the flat wagon rests on the bogies is 7.4 m/s^2. The coefficient of vertical dynamics is 0.75.

It is found that, taking into account the proposed diagram of interaction between the container and the flat wagon, it becomes possible to increase the fatigue resistance coefficient of the bearing structure of the flat wagon by 8 % compared to that for the typical diagram.

8. It is proposed to improve the bearing structure of the flat wagon by using sandwich panels.

The dynamic load of the loaded flat wagon with sandwich-panel flooring is determined. The maximum accelerations acting in the

centre of mass of the bearing structure of the flat wagon occur when it passes a track irregularity and are equal to 3.8 m/s^2. During the subsequent oscillatory process, the acceleration decreases to 2.5 m/s^2. Thus, taking into account the proposed solution, the accelerations acting on the bearing structure of the flat wagon are reduced by 8.4 % compared to those for the typical diagram. The acceleration acting on the freight placed on the flat wagon is 2.8 m/s^2, which is 11.7 % lower than that acting on the freight if taking into account the typical loading diagram.

The strength of the sandwich panels used for the flat wagon flooring was investigated. The maximum stresses in sandwich panels are about 94.5 MPa, which is almost twice lower than the permissible stresses. A stress of 210 MPa was accepted as permissible. The maximum displacements occur in the middle part of the flat wagon frame and amount to 4.35 mm.

The dynamic load of an unloaded flat wagon with a sandwich panel floor was determined. The maximum acceleration of the bearing structure of a flat wagon in the centre of mass is about 6 m/s^2 (0.6 g). The acceleration of the bogies is about 8.5 m/s^2. The obtained dynamics indicators correspond to a 'good' motion of the wagon.

The proposed flat wagon designs are patented in Ukraine and descriptions are presented in Appendix A.

The research will contribute to the development of recommendations for modern railway vehicle designs and improve the efficiency of the transport industry.

9. Measures are proposed to adapt the flat wagon to the transportation of liquid cargoes by installing the boiler module that rests on the frame of the flat wagon through wooden bars mounted on metal supports. It is proposed to make the boiler of composites, which will reduce the total tare weight of the wagon by 3.7 % compared to that made of metal.

The dynamic load of the improved flat wagon under a shunting impact, as the case of the highest load to the structure in operation, was determined. The results of the calculation show that the acceleration acting on the bearing structure of the flat wagon is 0.38 g.

The main strength indices of the improved flat wagon were determined. The maximum equivalent stresses occur in the area of interaction between the centre sill and the bolster beam; they amount to about 340 MPa and do not exceed the permissible limits. The maximum displacements are 8.6 mm and concentrated in the area of the hatches.

The modal analysis of the improved design of the flat wagon was carried out. The shapes and natural frequencies of oscillations of the bearing structure of the improved flat wagon were determined. It is found that the first natural frequency of oscillations is greater than 8 Hz. Therefore, the safety of the wagon in operation is ensured.

The research will help to improve the efficiency of railway transport operations and gather the database of developments of innovative railway vehicle designs.

10. Measures for the situational adaptation of the flat wagon mod. 13-7024 for carrying strategic freight by using a removable module are proposed. The parameters of the structural components of the removable module are determined. Channel No. 30 is chosen as the profile for the frame of the removable module. The thickness of the sheet forming the loading area, is 5.25 mm. The strength calculation of the removable module under static load shows that the maximum stresses occur in its corner parts and amount to 165.8 MPa, but they are 21 % lower than the permissible ones. The maximum displacements occur in the middle part of the removable module and are 8.66 mm.

The dynamic load and strength of the removable module when it is subjected to vertical loads are investigated. It is found that the maximum acceleration acting on the removable module placed on the flat wagon when it moves along the track irregularity is 1.46 m/s^2 (0.1 g). This acceleration value corresponds to an 'excellent' motion of the flat wagon. The strength calculation of the removable module shows that the maximum stresses occur in its corners and amount to 179.3 MPa. The resulting stresses are 14.6 % lower than permissible. The maximum movements are in the middle part of the removable module and amount to 8.9 mm.

The dynamic load and strength of the removable module under longitudinal loads are investigated. The maximum longitudinal accelerations acting on the bearing structure of the removable module placed on the flat wagon are about 24 m/s^2 (0.24 g). The results of the strength calculation of the removable module show that the maximum stresses occur in the corners of the removable module on the side of the longitudinal load and amount to 184.6 MPa. Importantly that the resulting stresses are 12 % lower than the permissible values. The maximum displacements occur in the middle part of the module and are 9.1 mm.